

# GUIDE TO PERMAFROST AND QUATERNARY GEOLOGY OF THE FAIRBANKS AREA, ALASKA

*Edited by De Anne S. P. Stevens*

Guidebook 11



Published by

STATE OF ALASKA  
DEPARTMENT OF NATURAL RESOURCES  
DIVISION OF GEOLOGICAL & GEOPHYSICAL SURVEYS



2023



---

# GUIDE TO PERMAFROST AND QUATERNARY GEOLOGY OF THE FAIRBANKS AREA, ALASKA

*Edited by De Anne S. P. Stevens*

With contributions by Jason Addison, Danielle L. Ayers, James E. Begét, Jeffrey Benowitz, Kevin L. Bjella, Matthew T. Bray, Laura Brosius, Patricia Burns, Charles M. Collins, Thomas A. Douglas, Dennis Filler, Daniel Fortier, Hugh M. French, Doug Goering, Karen S. Henry, Larry Hinzman, Elden Johnson, Torre Jorgenson, Mikhail Z. Kanevskiy, Paul Layer, Michael R. Lilly, Vladimir Romanovsky, Yuri L. Shur, De Anne S.P. Stevens, David Stone, Les Viereck, Katey Walter, and Kenji Yoshikawa

---

Division of Geological &  
Geophysical Surveys

Guidebook 11

Prepared for  
Ninth International Conference on Permafrost  
June 29 – July 3, 2008  
University of Alaska Fairbanks  
De Anne S.P. Stevens, Trip Leader

This report was originally prepared for the Ninth International Conference on Permafrost and distributed in draft form to conference attendees in 2008 and subsequently published in 2023 in the original format. Any links in this report were current in 2008 but may not be active at the time at publication.

*Cover photo: Massive ice in permafrost exposed in cut near Fox, Alaska. Photo taken September 2, 2006, by Vladimir Romanovsky.*





**STATE OF ALASKA**

Mike Dunleavy, *Governor*

**DEPARTMENT OF NATURAL RESOURCES**

John Boyle, *Commissioner*

**DIVISION OF GEOLOGICAL & GEOPHYSICAL SURVEYS**

David LePain, *State Geologist and Director*

Publications produced by the Division of Geological & Geophysical Surveys (DGGS) are available to download from the DGGS website ([www.dggs.alaska.gov](http://www.dggs.alaska.gov)). Publications on hard-copy or digital media can be examined or purchased in the Fairbanks office:

**Alaska Division of Geological & Geophysical Surveys**

**3354 College Rd., Fairbanks, Alaska 99709-3707**

**Phone: (907) 451-5010 Fax (907) 451-5050**

[dggspubs@alaska.gov](mailto:dggspubs@alaska.gov)

[www.dggs.alaska.gov](http://www.dggs.alaska.gov)

Alaska State Library  
State Office Building, 8th Floor  
333 Willoughby Avenue  
Juneau, Alaska 99811-0571

Alaska Resource Library & Information  
Services (ARLIS)  
3150 C Street, Suite 100  
Anchorage, Alaska 99503-3982



## INTRODUCTION

### General Statement

by

*Larry Hinzman*

*Director, International Arctic Research Center—University of Alaska Fairbanks*

*Program Chair, NICOP U.S. National Committee*

This field guide was prepared to accompany the Ninth International Conference on Permafrost (NICOP) convened in Fairbanks, Alaska, June 29 through July 3, 2008. We anticipate this report will be useful for many years to come for those who have more than a casual interest in permafrost. Field site visits have always been a major component of the International Conferences on Permafrost and present the opportunity for scientists, engineers, and land managers from around the world to observe the processes and challenges inherent in living with permafrost. We attempted to design these field trips to appeal to a broad range of interests, with individual trips focused on engineering applications, ecological interactions, hydrology, and periglacial processes. Fairbanks is an ideal setting to view many permafrost features first-hand. Many aspects of our landscape, our ecology, and our culture are dominated by the presence or absence of permafrost. Living in the zone of warm, discontinuous and ice-rich permafrost, local residents had to adapt or develop innovative building techniques to protect permafrost from thawing. This guide includes discussions of construction techniques that minimize thermal and mechanical disturbance to the underlying permafrost as well as an examination of the role played by permafrost in the boreal forest ecosystem. As a small city with a less-than-century-long history, it is still quite easy to find undisturbed permafrost features, including relict ice wedges and polygonal ground. We hope the reader finds this guide useful in developing a better appreciation for the challenges of living with permafrost in a warming climate.

## ORGANIZATION

This guidebook includes updated information relating to some of the sites originally described in the 1965 “Central and South-central Alaska Guidebook F” (Péwé; reprinted 1977) for the Seventh International Quaternary Association (INQUA) Conference and the 1983 “Guidebook to Permafrost and Quaternary Geology along the Richardson and Glenn Highways between Fairbanks and Anchorage, Alaska” (Péwé and Reger) for the Fourth International Conference on Permafrost. It also includes descriptions of many new sites in the Fairbanks area. Authors are drawn from a wide spectrum of disciplines, including engineering, geology, hydrology, and ecology, making this guidebook a truly interdisciplinary overview of the landscape of the Fairbanks area.

The guidebook is organized into two sections. The first section, “Part I: Field Guide to Permafrost, Periglacial, and Quaternary History Sites near Fairbanks, Alaska,” describes individual sites that were designed to be visited in various combinations and sequences by multiple groups attending the NICOP local field trips. These site descriptions are thus discrete entities and can be used as stand-alone field trip destinations. The site numbers for Part I are essentially random and do not imply any particular order. The second section of the guidebook, “Part II: Field Guide for Permafrost Features in Caribou–Poker Creeks Research Watershed (CPCRW) and Environs of Fairbanks, Alaska,” is a fully realized field trip, and the site numbers are presented in the sequence visited during the official field trip.

## ACKNOWLEDGMENTS

The authors and editors appreciate the efficient publication support provided by Joni Robinson (DGGS). Without her assistance, this guidebook would not have been possible. Field trip logistics and scheduling were ably provided by Deb Bennett (Water and Environmental Research Center) and Elizabeth Lilly (Geo-Watersheds Scientific), whose tireless efforts in support of all the NICOP field trips are greatly appreciated.

## REFERENCES CITED

- Péwé, T.L., ed., 1977, 1965 INQUA Conference guidebook to central Alaska: Alaska Division of Geological & Geophysical Surveys Miscellaneous Publication 4, 141 p.
- Péwé, T.L., and Reger, R.D., eds., 1983, Guidebook to Permafrost and Quaternary Geology along the Richardson and Glenn Highways between Fairbanks and Anchorage, Alaska: Alaska Division of Geological & Geophysical Surveys Guidebook 1, 263 p., 1 sheet, scale 1:250,000.

## Sites in Guidebook Part 1

1: Thompson Drive (64.851, -147.841)

2: Farmers Loop (64.884, -147.668)

3: Trans-Alaska Pipeline (64.930, -147.627)

4: Cold Climate Housing Research Center (64.930, -147.627)

5: Sunnyside House (64.884, -147.785)

6: O'Connor Creek Pingos (64.902, -147.907)

7: Murphy Dome (64.953, -148.360)

8: Gold Hill (64.855, -147.921)

9: Goldstream Thermokarst (64.912, -147.934)

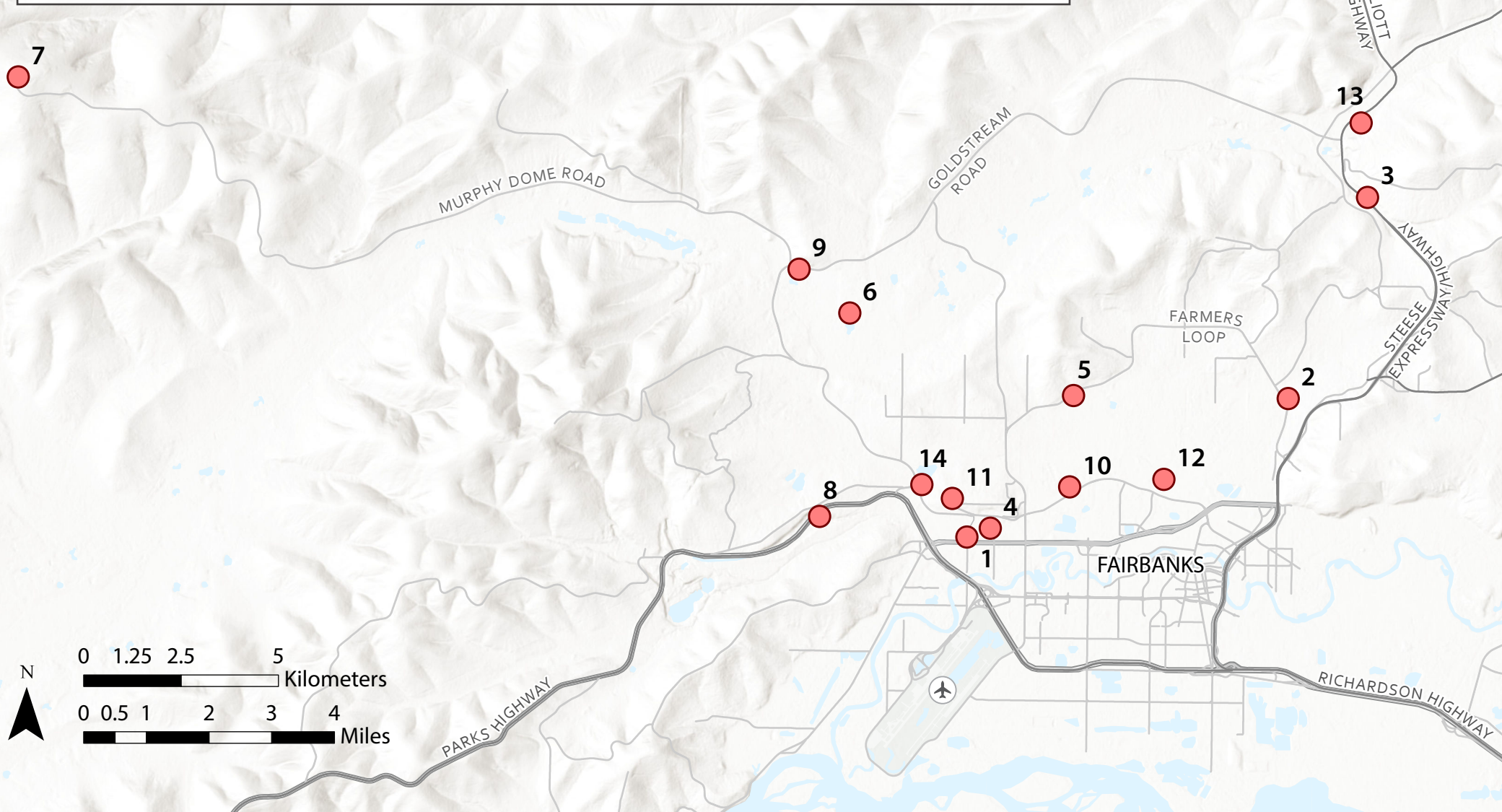
10: Great Northwest Peat Mine (64.863, -147.786)

11: International Arctic Research Center (64.863, -147.850)

12: Creamers Field (64.865, -147.735)

13: Permafrost Tunnel (64.947, -147.630)

14: Sheep Creek Thermokarst Pond (64.863, -147.866)





## **PART I**

---

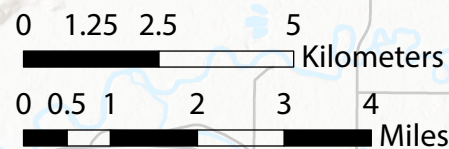
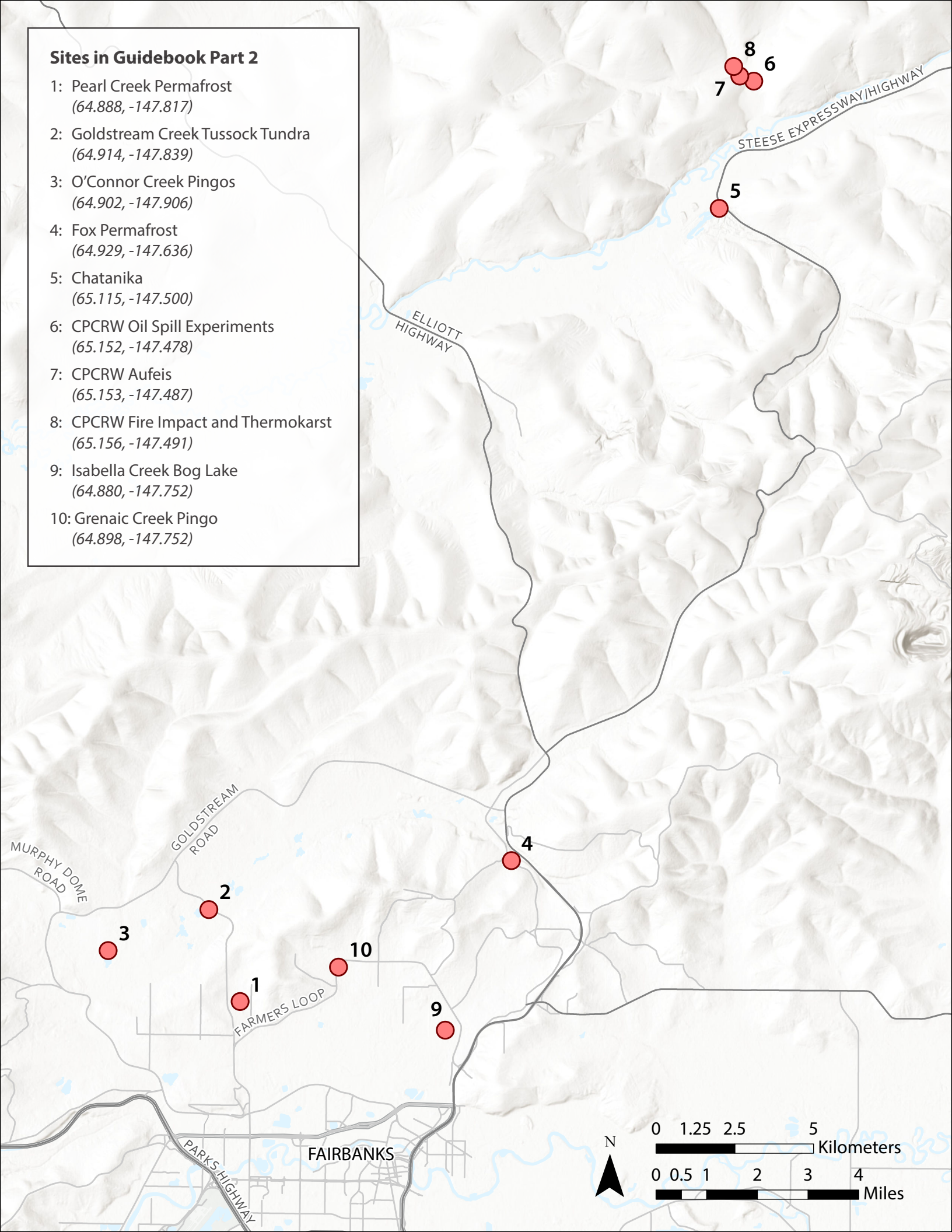
### **Field Guide to Permafrost, Periglacial, and Quaternary History Sites near Fairbanks Alaska**

#### **CONTENTS**

- 1 Site 1: Thompson Drive
- 5 Site 2: The Fairbanks Permafrost Experiment Station, Alaska-Historical Highlights
- 11 Site 3: Trans Alaska Pipeline and Permafrost
- 13 Site 4: Studying the Effectiveness of an Underground, Adjustable Foundation for Alleviating the Problems Associated with Building on Permafrost
- 17 Site 5: Sunnyside House Building on Permafrost: Failures and Solutions
- 19 Site 6: O'Connor Creek Pingos
- 23 Site 7: Murphy Dome
- 29 Site 8: Gold Hill (Péwé Climatic Change Permafrost Reserve)
- 35 Site 9: Thermokarst Pits and Fens in Goldstream Valley
- 37 Site 10: College Peat Ice Wedges
- 39 Site 11: GeoData Center – Map Office – Alaska Satellite Facility User Services Office
- 41 Site 12: Thermokarst and Drunken Forest
- 45 Site 13: Late-Pleistocene Syngenetic Permafrost in the CRREL Permafrost Tunnell, Fox Alaska
- 67 Site 14: Sheep Creek Thaw Pond: Thermokarst Lakes and Methane Emissions
- 71 Permafrost Features in Caribou–Poker Creeks Research Watershed (CPCRW) and Environs of Fairbanks, Alaska

## Sites in Guidebook Part 2

- 1: Pearl Creek Permafrost  
(64.888, -147.817)
- 2: Goldstream Creek Tussock Tundra  
(64.914, -147.839)
- 3: O'Connor Creek Pingos  
(64.902, -147.906)
- 4: Fox Permafrost  
(64.929, -147.636)
- 5: Chatanika  
(65.115, -147.500)
- 6: CPRW Oil Spill Experiments  
(65.152, -147.478)
- 7: CPRW Aufeis  
(65.153, -147.487)
- 8: CPRW Fire Impact and Thermokarst  
(65.156, -147.491)
- 9: Isabella Creek Bog Lake  
(64.880, -147.752)
- 10: Grenaic Creek Pingo  
(64.898, -147.752)



## PART II

---

### Permafrost Features in Caribou-Poker Creeks Research Watershed (CPCRW) and Environs of Fairbanks Alaska

#### CONTENTS

71	Stop 1: ..... Pearl Creek Elementary School Permafrost/Active-Layer Monitoring Site
74	Stop 2: .....Goldstream Creek
77	Stop 3: .....O'Connor Creek pingo site
79	Stop 4: .....Fox gold mining site permafrost outcrop
81	Stop 5: ..... Chatanika
84	Stop 6: ..... Caribou–Poker Creeks Research Watershed (CPCRW)
91	Stop 7: .....Aufeis (Icing) and permafrost hydrology
96	Stop 8: ..... Isabella Creek



# **PART I**

---

## **Field Guide to Permafrost, Periglacial, and Quaternary History Sites near Fairbanks Alaska**







Figure 2. Shoulder installation.



Figure 3. Thermosyphon installation.



Figure 4. Insulation installation.

embankment, providing a cooling effect during winter. This cooling effect exists because of the instability of an air layer that is warmer on the bottom and cooler on top, which is the case for the air trapped in the embankment structure during winter. Wintertime instability causes the air to circulate, thus providing enhanced cooling of the permafrost foundation soil beneath. In the summer, cooler air at the bottom of the layer causes circulation to cease, eliminating enhanced warming due to air movement during the warm season.

A cross section of test section #2 is shown in figure 5, with the temperature measurement points shown by black dots. This test section is on the northern approach to the railroad bridge. As the road approaches the bridge concourse the embankment thickness increases to approximately 10 m. Ventilated shoulders are used on both sides of the embankment and a horizontal air-convection layer extends across the upper portion of the embankment.

Test section #1 (fig. 6) combines a ventilated shoulder on the right side of the embankment with hairpin thermosyphons. Thermosyphons have been used for many years for passive cooling of building foundations, and other structures in permafrost zones. Perhaps the best-known application of these devices was for chilling of the vertical support members used on the trans-Alaska oil pipeline. In the past, thermosyphons have nearly always used an air-cooled condenser and thus always had a finned section projecting up into the ambient air. For use in highway structures, however, there are disadvantages to this design due to safety and vandalism concerns. In addition, the finned sections required for air cooling are expensive to manufacture and increase thermosyphon costs significantly. In an effort to avoid some of these problems, a new type of thermosyphon configuration is being utilized in Thompson Drive. The new devices are referred to as hairpin thermosyphons due to their shape and do not require an above-ground air-cooled condenser. Instead, the condenser pipe is buried underground and insulation sheeting is used to thermally separate the evaporator and condenser. Figure 6 shows a cross-sectional view of test section #1 with the thermosyphon evaporator and condenser indicated by heavy lines and the temperature measurement points indicated by black dots. In this design, the thermosyphon condenser and evaporator are connected by soft copper tubing (visible in fig. 2) and charged in the field.

During operation, the thermosyphons transfer heat from the lower evaporator section to the upper condenser section. The net effect is removal of heat from the base of the embankment beneath the insulation sheet (the insulation is indicated by the horizontal line just beneath the condenser in fig. 6) and rejection of heat through the asphalt surface at the top of the embankment. In this way, the base of the embankment and underlying permafrost



are cooled and the permafrost is preserved. The test section shown in figure 6 also contains a ventilated shoulder, which in this case is designed specifically to avoid problems with shoulder rotation and resultant destruction of the sidewalk on the right side of the roadway.

Figure 7 shows mean annual temperature contours for December 2005–December 2006. The shaded zones in the figure indicate where the mean annual temperatures are  $-0.5^{\circ}\text{C}$  or colder. The cooling influence of both the ventilated shoulder and the thermosyphon is demonstrated by the low-temperature regions adjacent to the shoulder and thermosyphon evaporator. Comparison with data collected a year earlier indicates that these zones of the embankment foundation are currently cooling at the rate of about  $1^{\circ}\text{C}$  per year. Over time the low-temperature regions are expected to expand downward, helping to cool the relatively warm permafrost below.

## REFERENCES

- Goering, D.J., and Kumar, P., 1996, Wintertime convection in open-graded embankments: Cold Regions Science and Technology, v. 24, no. 1, p. 57.
- Saboundjian, Steve, and Goering, D.J., 2003, Air convection embankments for roadways—A field experimental study in Alaska: Journal of the Transportation Research Board, v. 1821, p.20.

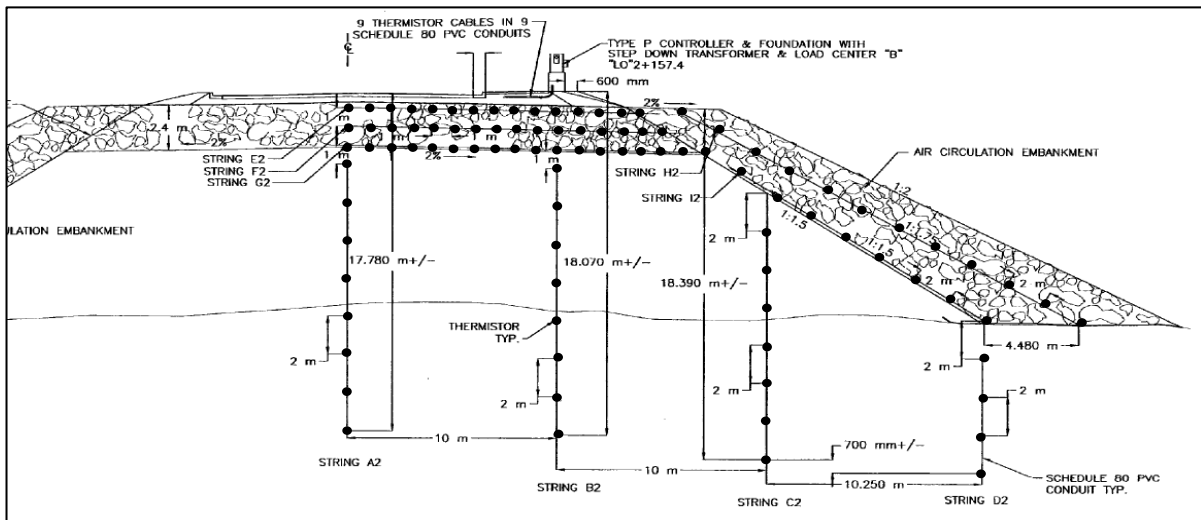


Figure 5. Cross-sectional view of test section #2, showing temperature measurement points (black dots).

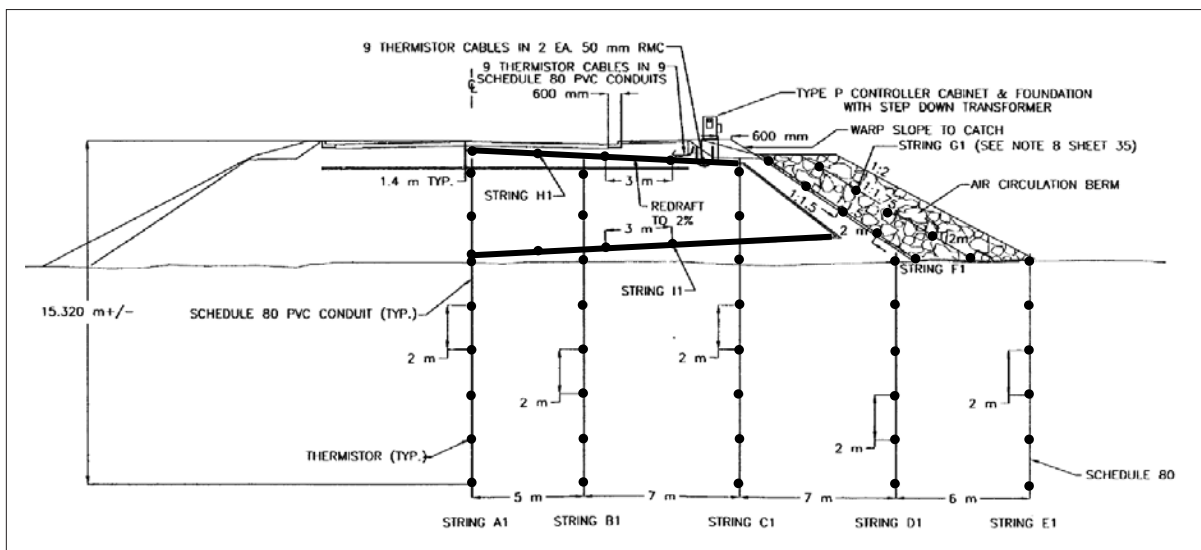


Figure 6. Cross-sectional view of test section #1, showing temperature measurement points (black dots). Hairpin thermosyphons were installed on alternate sides of the embankment at 2.5 m intervals.

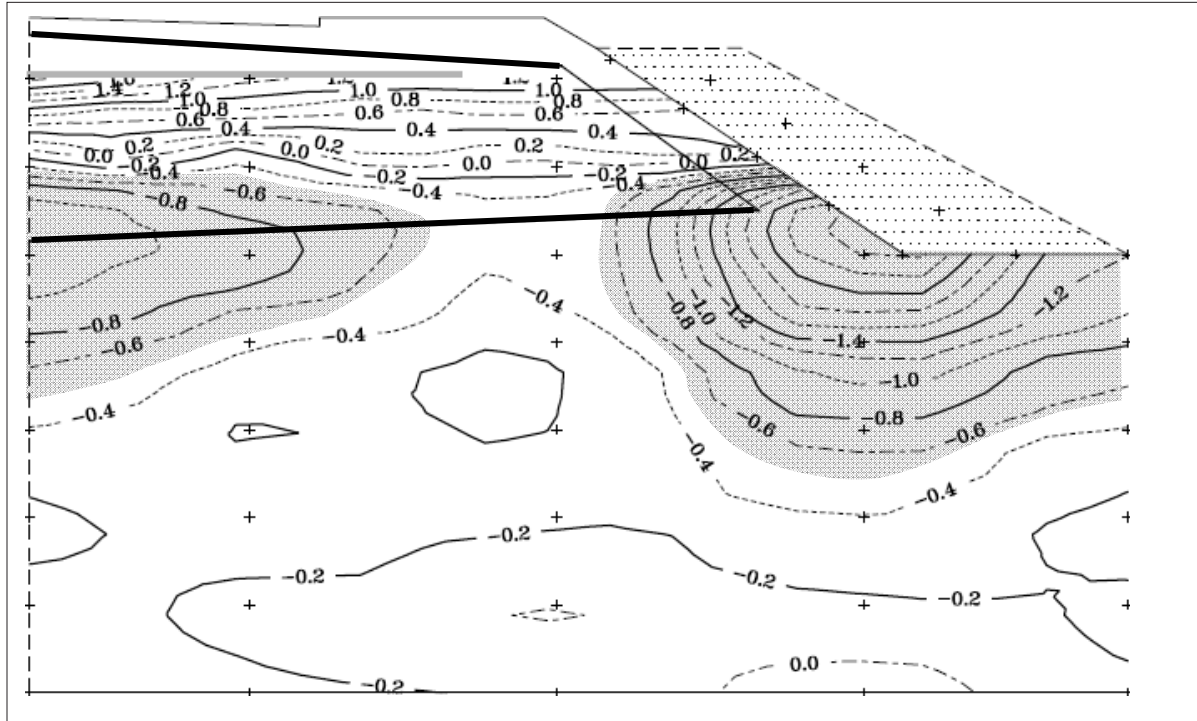


Figure 7. Mean annual temperature contours for test section #1 for the period December 16, 2005, to December 15, 2006.

## Site 2: The Fairbanks Permafrost Experiment Station, Alaska-Historical Highlights

Karen S. Henry<sup>1</sup>, Kevin Bjella<sup>2</sup>, and Thomas A. Douglas<sup>2</sup>

### INTRODUCTION

The Fairbanks Permafrost Experiment Station (64.877°N, 147.670°W) is a 54.6-hectares site established by the U.S. Army in 1945 to conduct geophysical and geotechnical engineering investigations on permafrost (fig. 1). Past research projects at this site that can be reviewed include the impact of vegetation removal on the ground thermal regime, pile foundations, the impact of pavement color on the thermal regime beneath pavement, and frost-jacking of survey markers. In addition, it is a Circumpolar Active Layer Monitoring (CALM) site; hence, monitoring of permafrost temperatures is ongoing, and future studies at the site are projected to address climate change impacts on permafrost and infrastructure located on permafrost.

The entrance to the station is gated and locked; permissions and access can be obtained by calling the Cold Regions Research and Engineering Laboratory in Fairbanks, Alaska (907-361-5149). Access to the Farmer's Loop Road site is from the north side of Farmer's Loop Road and ample parking is available.

The establishment of the Fairbanks Permafrost Experiment Station (FPES) was related to the construction in 1942 of the Alaska–Canada (ALCAN) Highway that linked the contiguous (“lower”) 48 states to Alaska via a route through Canada. The ALCAN Highway, considered a military necessity after the bombing of Pearl Harbor in 1941 due to possible invasion of Alaska by Japan, was constructed in just 8 months—from March through October 1942. The ALCAN immediately suffered considerable damage as the underlying permafrost responded to disturbance from construction. The difficulties of construction and maintenance of the ALCAN Highway because of the permafrost led to the establishment of FPES.

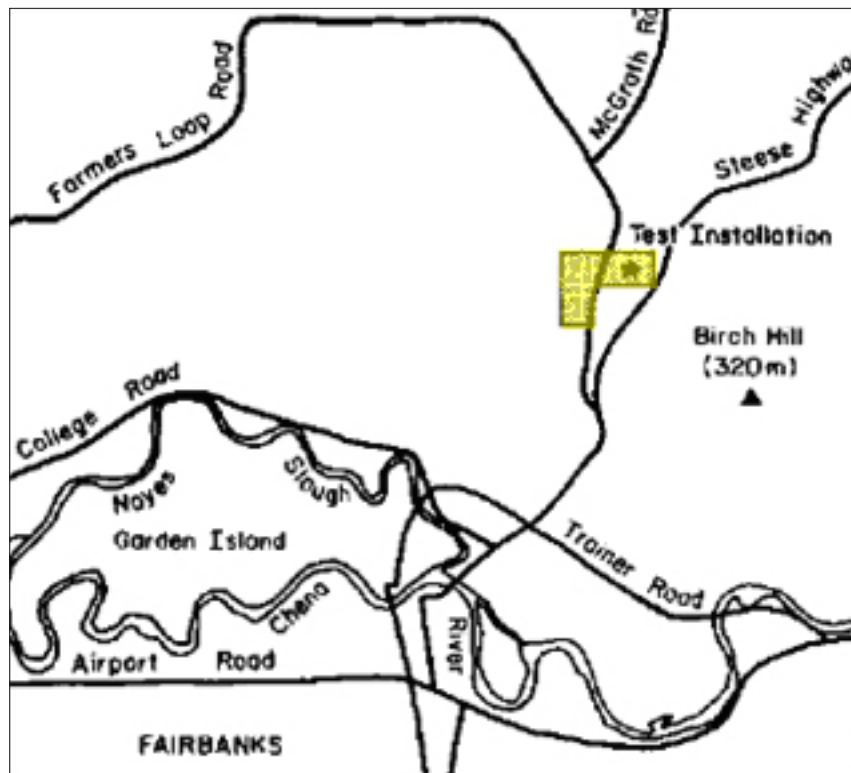


Figure 1. Map showing the location of the Fairbanks Permafrost Experiment Station site.

<sup>1</sup>HQ USAFA/DFCE, 2354 Fairchild Dr. Suite 6H-177, USAF Academy, Colorado 80840-6232; [karen.henry@usfa.edu](mailto:karen.henry@usfa.edu)

<sup>2</sup>U.S. Army Cold Regions Research and Engineering Laboratory Fairbanks, Alaska

Design of research projects and construction of support infrastructure were initiated in 1946 by the Alaska Department of the U.S. Army Corps of Engineers for the Permafrost Field Office of the Saint Paul District. In 1953, this 'Permafrost Field Office' joined the Arctic Construction Frost Effects Laboratory, or ACFEL (Boston, Massachusetts), which then operated the site under the name 'Alaska Field Station.' Responsibility for the 'Fairbanks Permafrost Experiment Station' (FPES) was assumed in 1961 by the Cold Regions Research and Engineering Laboratory (CRREL), where it remains. The FPES was designated a National Geotechnical Experimentation Site in 2003.

The ice-rich permafrost soil of FPES and its location in a discontinuous (warm) permafrost zone make it an ideal 'worst-case-scenario' for testing construction techniques, road and airfield designs, and piling and other foundations. Projects have included the long-term influence of vegetation removal on permafrost stability, experimental road surfaces, insulation of roads, experimental foundations, the measurement of frost-heave forces on piles, thawing of permafrost by passive solar means, the detection of permafrost by geophysical techniques, and bioremediation.

In light of recent Arctic climate warming, all historical records of ground temperatures and/or depths and thickness of permafrost in Arctic regions are of potential interest because they can be compared to the present temperatures and state of permafrost. Ground temperatures and thermal state of the ground were often documented in detail for studies conducted at FPES from the 1940s through the 1970s. For example, one study included a 'control' plot of land that has been left undisturbed, yet ground temperatures and depth to permafrost were monitored over a period of 26 years, from 1946 through 1972 (Linell, 1973).

## SITE DESCRIPTION

The Fairbanks Permafrost Experiment Station slopes to the west at a grade of about 3 percent, has good drainage except for the lowest elevations (fig. 2), and is located on the lower colluvial slopes of Birch Hill (to the southeast) and partly on valley fill. The natural soils are primarily silts to depths of 15–45 m, with many peat and ice-lens inclusions (Linell, 1973). A thick layer of silts, silty sand, and sand-gravel mixtures underlies the top layer of silt to bedrock at an approximate depth of 75 m. The site's relatively warm and discontinuous permafrost with frost-susceptible soil contributes to considerable frost-heave each winter, thaw settlement in the spring, and sensitivity to permafrost degradation. In 1946, the top of permafrost was about 1 m deep and the lower boundary was deeper



*Figure 2. An aerial view of the Fairbanks Permafrost Experiment Station taken in July 1958. The buildings in the photograph are no longer at the site because ground thawing caused settlement and distortion of the buildings. The cleared 'Linell plots' can be seen in the upper right center of the photograph, and an experimental runway can be seen behind the building in the upper left portion of the photo.*

than 49 m; the water table fluctuated between 0 and 2 m during thaw season (Lobacz and Quinn, 1966). Yearly thaw depths measured at the site for the past 3 years have ranged from 35 to 80 cm.

### Past permafrost research conducted at FPES

Past permafrost research at FPES falls into three categories: (1) Impact of vegetation removal and construction on the thermal state of the ground, (2) Frost-heave research (including frost-jacking of piles), and (3) Exploring means of maintaining frozen ground beneath roads and airfields. The earliest studies examined the influence of ground cover and removal, building foundations, types of pavement bases, insulated pavements, and various pavement surfaces on the thermal state of the ground (U.S. Army Corps of Engineers, 1950; Henry and Bjella, 2006).

### Past and present research evident at the site

The following descriptions of work are related to projects for which evidence of work can be observed during a site visit. Refer to figure 3 for the locations.

#### CIRCUMPOLAR ACTIVE LAYER MONITORING SITE ON HISTORICAL ‘LINELL PLOTS’

In 1946, three square plots measuring 61 m per side (3,721 m<sup>2</sup>)—now referred to as the ‘Linell Plots’—were established to investigate the influence of vegetation removal on permafrost (Linell, 1973). One of the plots was left undisturbed to preserve the subarctic taiga forest of white and black spruce. Vegetation was removed from two study plots—one plot was stripped of trees by hand but the roots and organic mat were left intact; the other plot was stripped of all surface vegetation and the organic mat. Linell (1973) described permafrost degradation at the two disturbed sites after 35 years.

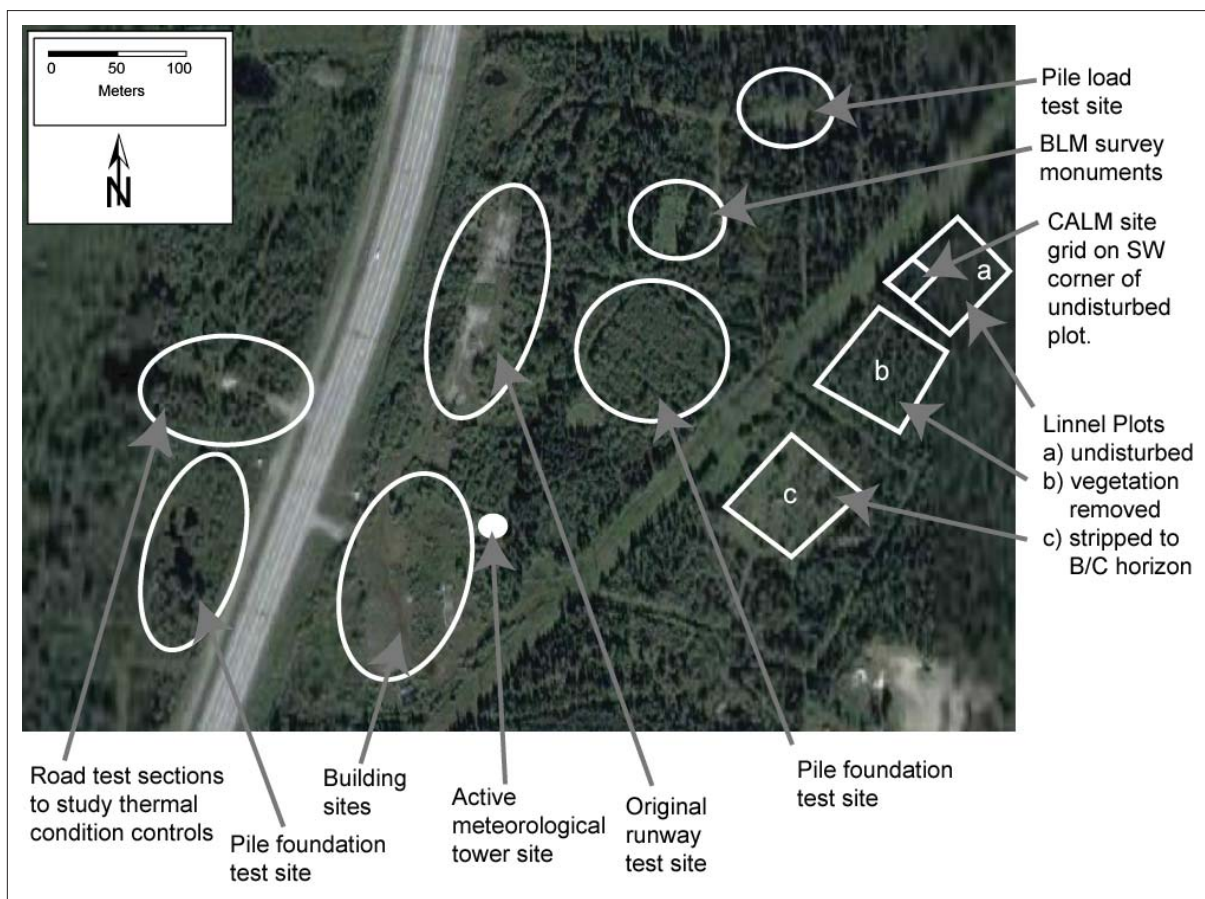


Figure 3. A recent aerial photograph of the Fairbanks Permafrost Experiment Station, showing the main research site locations.

*Table 1. Summary of the summer average temperatures, active layer depth, and moss thickness for 121 points at the undisturbed Linell plot (CALM site) for 2005–2007.*

<b>Year</b>	<b>May–October mean air temperature (°C)<sup>1</sup></b>	<b>Mean thaw depth with moss (cm)</b>	<b>Mean moss thickness (cm)</b>
2005	13.7	57.5	13.0
2006	12.6	53.5	13.5
2007	13.8	57.3	13.6
2008	12.5	57.1	N/A

<sup>1</sup>Meteorological information from the Alaska Climate Research Center (<http://climate.gi.alaska.edu/>).

In 2005, a Circumpolar Active Layer Monitoring Network (CALM) site was established in the undisturbed Linell plot. Thaw depths are measured in early October at 121 locations on a 10-by-10-m grid with 3-m spacing. The moss thickness and total thaw depth are measured and recorded at each probe location (table 1). In addition, in the summer of 2007, a 3-m-deep borehole was drilled and a thermistor string installed to measure ground temperatures at 10 depths; measurements continue.

Direct current resistivity measurements were obtained across the three Linell plots during the summer of 2007 to delineate the current state of permafrost. The results indicate that permafrost degradation following vegetation disturbance is ongoing 61 years later.

#### BUREAU OF LAND MANAGEMENT SURVEY MONUMENTS

In 1987, the Bureau of Land Management initiated a study of various types of survey monuments installed in this frost-prone area. In August 1987, 43 monuments were installed and were monitored through 1991 (via survey) for frost jacking. The monuments varied considerably in overall design from shallow rods, for example, 0.76 m deep, to rods more than 6.4 m long. Some were installed flush with the surface and others had between 100 mm and 0.9 m of ‘stick up,’ or portion of the monument above the ground surface. The rods used are of varying diameters and are made of a variety of metals. Some short rod monuments were anchored with 100- or 127-mm-diameter anchor plates. The installation techniques included driven to refusal, driven to refusal with finned rod at the top, driven to refusal with finned rod at the bottom, driven to refusal with 0.9 m of ‘stick up,’ driven short of refusal, driven short of refusal with a 76-, 100-, or 127-mm-diameter anchor plate. An August 1991 survey indicated that the maximum uplift experienced was 0.15 m, by a copper-weld rod. Some galvanized iron pipe monuments were experiencing corrosion, and pipe monuments where the vegetation had been carefully replaced around the base of the monument heaved less than other pipe monuments. A few monuments had actually sunk into the ground.

#### PAINTED PAVEMENT TEST SECTIONS

Berg and Aitken (1973) described the construction of a road test section in 1965 at FPES to investigate several means of controlling thermal conditions beneath the road. The entire road section was 100 m long, and comprised five test sections—from east to west they were (1) gravel base with white-painted asphalt concrete surface, (2) gravel base with asphalt concrete surface, (3) compressed peat beneath asphalt concrete surface, (4) dark gravel surface, and (5) gravel surface. The remnants of these test sections indicate the outstanding performance of the easternmost test section—that of the gravel base with white-painted asphalt concrete surface.

#### PILE LOAD TEST SITE FOR PILE FOUNDATIONS IN PERMAFROST

According to Crory (1966), pile load testing was initiated by the U.S. Army Corps of Engineers at the FPES in 1957 (pile installation techniques were studied earlier). The load tests were designed to study the factors that affect load capacity of the piles, including installation method, soil type, pile type, length, shape, whether point bearing, permafrost temperature, and rate of loading (Crory, 1966).

## REFERENCES

- Berg, R.L., and Aitken, G., 1973, Some passive methods of controlling geocryological conditions in roadway construction, in Proceedings, Second International Conference on Permafrost—North American contribution: Washington, DC, National Academy of Sciences, p. 581–596.
- Crory, F.E., 1966, Pile foundations in permafrost, in Proceedings, International Conference on Permafrost: Purdue University, Indiana, National Academy of Sciences: Washington, DC, National Research Council, Publication 1287, p. 467–476.
- Henry, K.S., and Bjella, K., 2006, History of the Fairbanks Permafrost Experiment Station, Alaska, in Proceedings, 13th International Symposium on Cold Regions Engineering, Cold Regions Engineering 2006—Current Practices in Cold Regions Engineering, July 23–26, Orono, ME: Reston, VA, American Society of Civil Engineers, 11 p.
- Linell, K.A., 1973, Long-term effects of vegetative cover on permafrost stability in an area of discontinuous permafrost, in Proceedings of Permafrost—North American contribution, Second International Conference; Principles of construction in permafrost: Washington, DC, National Academy of Sciences, National Research Council, p. 688–693.
- Lobacz, E.F. and Quinn, W.F., 1966, Thermal regime beneath buildings constructed on permafrost, in Proceedings, International Conference on Permafrost, Purdue University, Indiana: Washington, DC, National Academy of Sciences, National Research Council, Publication 1287, p. 247–252.
- U.S. Army Corps of Engineers, Permafrost Division, 1950, Investigation of military construction in arctic and subarctic regions, comprehensive report 1945-48; Main Report and Appendix III—Design and construction studies at Fairbanks research area: Arctic Construction and Frost Effects Laboratory Technical Report 28, 68 p.

This page was intentionally left blank.



## Site 3: Trans Alaska Pipeline and Permafrost

Elden Johnson<sup>1</sup>

### TRANS-ALASKA PIPELINE SYSTEM

The 800-mile Trans-Alaska Pipeline System (TAPS) is operated by Alyeska Pipeline Service Co. (Alyeska) on behalf of the pipeline owners. The pipeline originates at the Prudhoe Bay oil fields on the North Slope of Alaska and ends at the ice-free port of Valdez. The pipeline route is underlain with continuous permafrost in the north, where the climate is the coldest. South of the Brooks Range, across interior Alaska, the permafrost is discontinuous, transitioning to sporadic permafrost along the southern portion of the Copper River basin. Climate records indicate a gradual warming trend along the entire pipeline route. Permafrost temperature monitoring shows similar trends but with slower warming. Alyeska has focused much of its attention on discontinuous and sporadic permafrost, which are close to the melting temperature of ice. Climate and ground-temperature monitoring is ongoing to track and appropriately respond to temperature changes.

### MONITORING THE EFFECTS OF CLIMATE CHANGE

Alyeska monitors climate change in several ways. Alyeska constructed and operates 43 instrumented thermal-monitoring sites along the pipeline corridor from the Brooks Range to Thompson Pass. At these sites, air, surface, subsurface ground, and permafrost temperatures are recorded three or four times a day, 365 days a year. Alyeska also analyzes local weather station data available from the Western Regional Climate Center (<http://www.wrcc.dri.edu/>) along the pipeline corridor. In addition, there are over 80 thermistor strings installed in the ground along the pipeline route that measure soil temperatures. These strings are monitored every year or two with the temperature data available through Alyeska's Engineering Data Management system for trend monitoring. Alyeska records subsurface ground temperatures at the base of select vertical support members (VSMs) following heat pipe maintenance as part of its trend-monitoring program.

### TAPS PIPELINE SUPPORT SYSTEM

Vertical support members (VSMs) are pipe pilings embedded in the ground to support the above-ground pipe in areas of thaw-unstable permafrost. Most VSMs south of the Brooks Range have heat pipes installed to keep the ground frozen around the embedded portion of the VSMs. These heat pipes are sealed thermosiphons that begin to remove heat from the ground when air temperatures fall below ground temperatures. Over the length of the pipeline, 78,000 VSMs are embedded 15 to 70 feet in the ground. In total, 61,000 thermal VSMs are configured with 122,000 individual heat pipes, two per VSM.

Alyeska heat-pipe monitoring and other thermal studies indicate that the ground around the VSM piling is being maintained in a frozen state. The vast majority of VSMs are not moving, which means climate changes are not presently affecting VSM stability. VSM settling or movement can be caused by a variety of reasons. When settling or movement is discovered, engineering studies determine the appropriate action necessary to re-establish stability.

### CLIMATE MONITORING

Recorded climate data are used in computer models by Alyeska to determine the amount of thermal energy that must be removed from the ground to maintain frozen conditions of the permafrost surrounding the VSMs.

### HEAT-PIPE INFRARED EVALUATIONS

Infrared surveys of all the heat pipes on the Trans-Alaska Pipeline occur on a three-year cycle. These data are used to predict the performance of the heat pipes installed at every thermal VSM. Heat pipes not meeting the required performance criteria are then listed for repair. The repair procedure requires recharging the listed heat

<sup>1</sup>Alyeska Pipeline Service Company, Fairbanks, Alaska

pipe with refrigerant and designating subsequent infrared surveys to ensure the heat pipes are working properly after maintenance.

After the heat pipe has been recharged, the temperature of permafrost at the base of the VSM is determined through pressure measurements that are converted to temperatures. If the permafrost temperature is approaching 32°F, additional temperature monitoring is conducted. Other spot checks measure permafrost temperatures where heat pipes have been recharged and where heat pipe recharging is not required to verify that methods used to maintain frozen conditions are working.

## **HEAT PIPE AND VSM SETTLEMENT MONITORING**

The segment of the pipeline corridor where the majority of the heat-pipe recharging has occurred is at the southern fringe of permafrost in the Copper River Basin. This area of discontinuous permafrost is transitional to sporadic permafrost. The temperature of the permafrost is relatively warm, often approaching the freezing point. At this southern boundary north of Thompson Pass, some permafrost has thermally degraded.

Alyeska has replaced or modified a few thermal VSMS with standard non-thermal friction VSMS at several locations. However, permafrost in most of this region remains stable. Heat-pipe recharge monitoring and other thermal studies, in addition to settlement surveys, indicate that the ground around thermal VSM pilings is effectively being maintained in a frozen state where needed and that the VSMS are stable.

## Site 4: Studying the Effectiveness of an Underground, Adjustable Foundation for Alleviating the Problems Associated with Building on Permafrost

Danielle L. Ayers<sup>1</sup> and Michael R. Lilly<sup>2</sup>

The Cold Climate Housing Research Center (CCHRC) is a non-profit corporation that researches and provides education on energy-efficient, affordable, and sustainable building techniques, designs, and materials. A business and education approach helps turn ideas into solutions. CCHRC conducts investigations in its research and testing facility (RTF) (fig. 1). The entire RTF building is an ongoing experiment in cold climate building technology. More than 1,000 on-site sensors monitor moisture and temperature throughout the building and the surrounding environment. The monitoring systems collect data on foundation and background soil and geotechnical conditions. One of the major research projects at CCHRC is to observe and record data on the permafrost below the building to determine how the permafrost is affected by the building and how the uniquely designed, underground adjustable foundation performs if permafrost does degrade.

The research and testing facility is constructed on Eolian silt that has been cleared of trees for 40–50 years, and is adjacent to wetlands that are covered by a black spruce forest. After the trees were cleared from the RTF

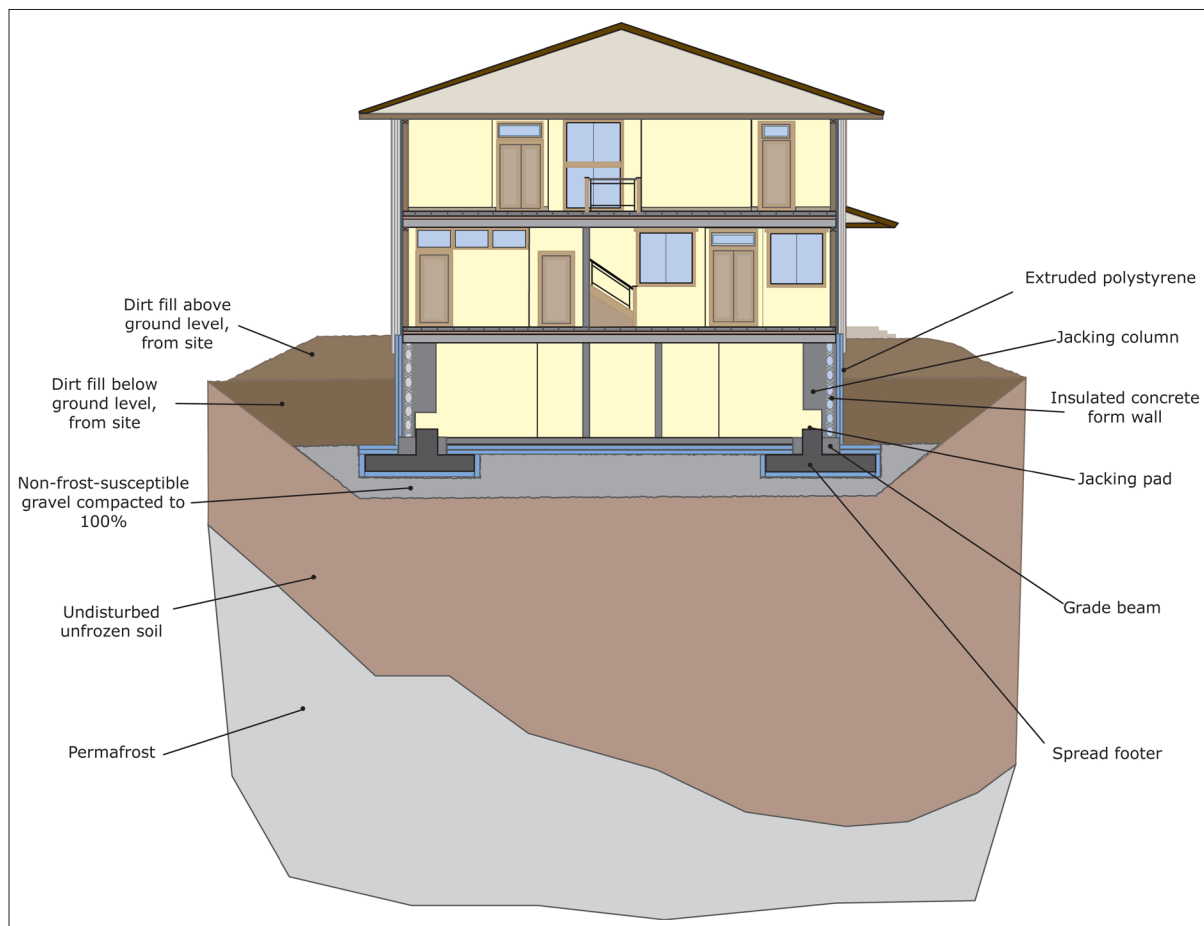


Figure 1. Cold Climate Housing Research Center (CCHRC) Research and Testing Facility cross section illustrating adjustable foundation components.

<sup>1</sup>Cold Climate Housing Research Center, P.O. Box 82489, Fairbanks, Alaska 99708-2489

<sup>2</sup>Geo-Watersheds Scientific, 650 Eaton Blvd., Fairbanks, Alaska 99709-6771

site, the underlying permafrost receded to depths between 12 and 30 feet. Thermistor strings were installed to track changes in the permafrost over time by reporting the direct effects of the building on permafrost degradation. Thermistor strings monitor soil temperature profiles and temperature changes in the foundation systems and the underlying soils, and in background sites from ground surface to the top of permafrost (fig. 2). Data are recorded by Campbell Scientific data loggers. Additionally, ground-water wells were drilled so manual measurements could be made of the water table.

Ground-water observation wells were positioned at the four corners of the property and range between 18 and 25 feet deep. The underlying permafrost in each corner ranges between 15 and 25 feet deep. A solid-stem auger was used to drill boring holes in which a galvanized pipe was driven to a set depth below the water table. The wells were screened to account for vertical seasonal variation in the water table. Initial drilling provided information on preliminary ground-water levels and direction of flow, which is generally from west to east. Wells placed in shallow permafrost areas were driven into the permafrost to track changes in the elevation of the permafrost table.

Temperature profiles are reported by thermistor strings buried in two sites adjacent to the building. The first profile, near the southwestern corner of the facility, provides data that can indicate minor disturbance near the building. The second profile section, on the east side of the facility, monitors changes closer to the building. Thermistor strings were installed into boring holes using a custom driving rod. The boreholes were refilled with the soil removed during the drilling process. The soil was compacted with a tamping rod as it was replaced to minimize the air spaces left in the drilled area. Each data-gathering string has 12 thermistors spaced to gather relevant data at different depths; each hole may have multiple thermistor profile strings installed. Hourly readings are made by each thermistor set and recorded by an attached Campbell Scientific data acquisition system. Sensor spacing was designed to provide information on the active soil layer, ground water, and permafrost. This information will help with understanding standard changes in permafrost over time as well as the effects the building has on permafrost degradation.

The building's foundation was engineered to facilitate adjustments to changes in the underlying permafrost (figs. 1–3). It was constructed using individually adjustable spread footers placed under a continuous, reinforced grade beam. These two support systems are designed to work together and can move independently of each other; they can be adjusted to accommodate movement of the underlying permafrost.

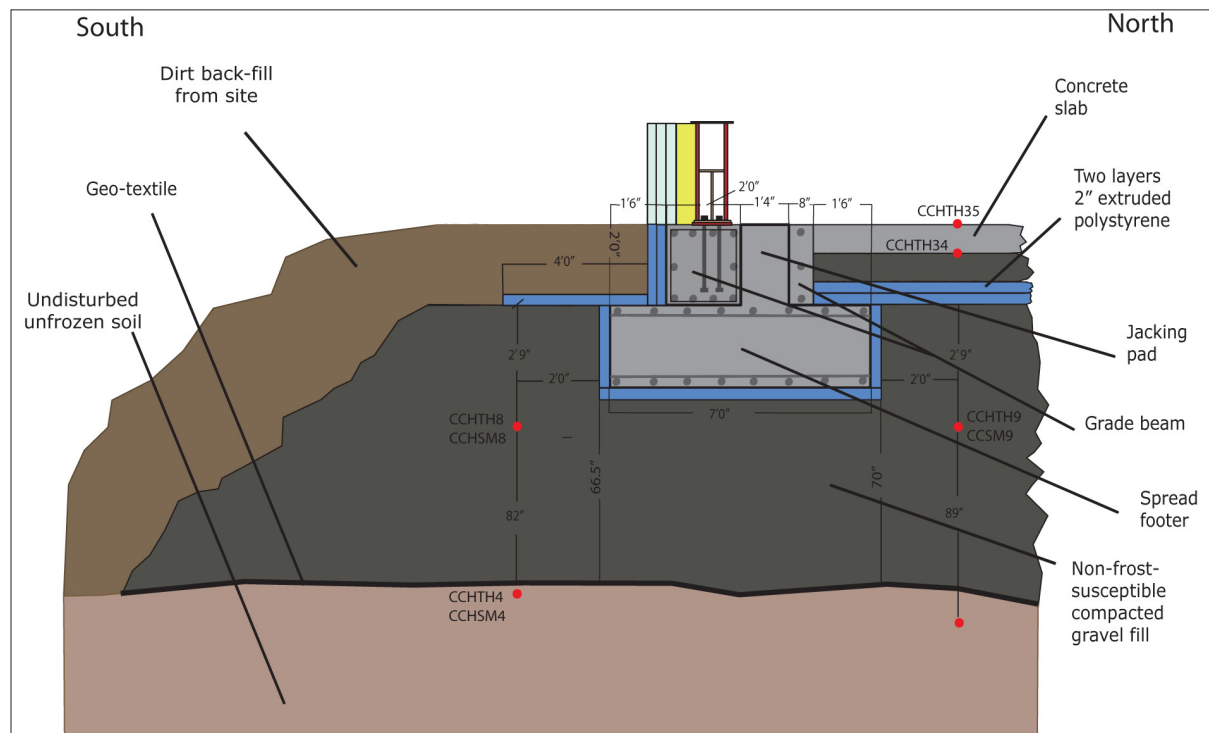


Figure 2. Selected test area of the Research and Testing Facility Foundation showing detailed foundation specifications.

To install the foundation, native soils were removed and replaced with gravel back-fill that was compacted to form the base of the spread footers. Spread footers of reinforced concrete with integrated jacking pads were poured on the compacted fill, and non-frost-susceptible gravel back-fill was compacted around each footer up to the bottom of the jacking pad. Next, the frame for the reinforced grade beam was constructed on top of the spread footers so that the grade beam surrounded each jacking pad. The reinforced grade beam was poured as a separate unit on top of the spread footers and around each jacking pad. Attached to and resting on the grade beam is an insulated concrete-form wall with built-in jacking columns that protrude inside the basement. The jacking columns align with each jacking pad. Insulation was added to the exterior of all basement surfaces that contact the ground. Following the construction of the foundation and basement walls, non-frost-susceptible gravel fill was compacted around the exterior of the basement.

If changes occur in the underlying permafrost, the building can be leveled from the interior of the basement. If the frozen ground starts to recede, hydraulic jacks can be placed on the jacking pads below the jacking columns in the basement. The jacks push individual spread footers down until the soils reach a stable compaction state, while the reinforced grade beam supports the weight of the building. Structural foam can be injected through pre-installed tubes to fill the space between the grade beam and the spread footers. The building can be adjusted at 52 interior access points around the basement of the building, allowing the structure to be leveled.

Data are collected continuously regarding the soil surrounding the building, and control points are checked every 6 months to monitor relative changes in the height of those points around the basement and first floor levels of the building. This monitoring of the building foundation enables researchers to assess changes in the building's level over time and to adjust the foundation accordingly.

Research on adjustable underground foundations is important because if this technique proves to be effective, it will offer another long-term option for building on permafrost. This flexibility is especially important in areas of discontinuous permafrost where melting and subsidence are more likely to occur.

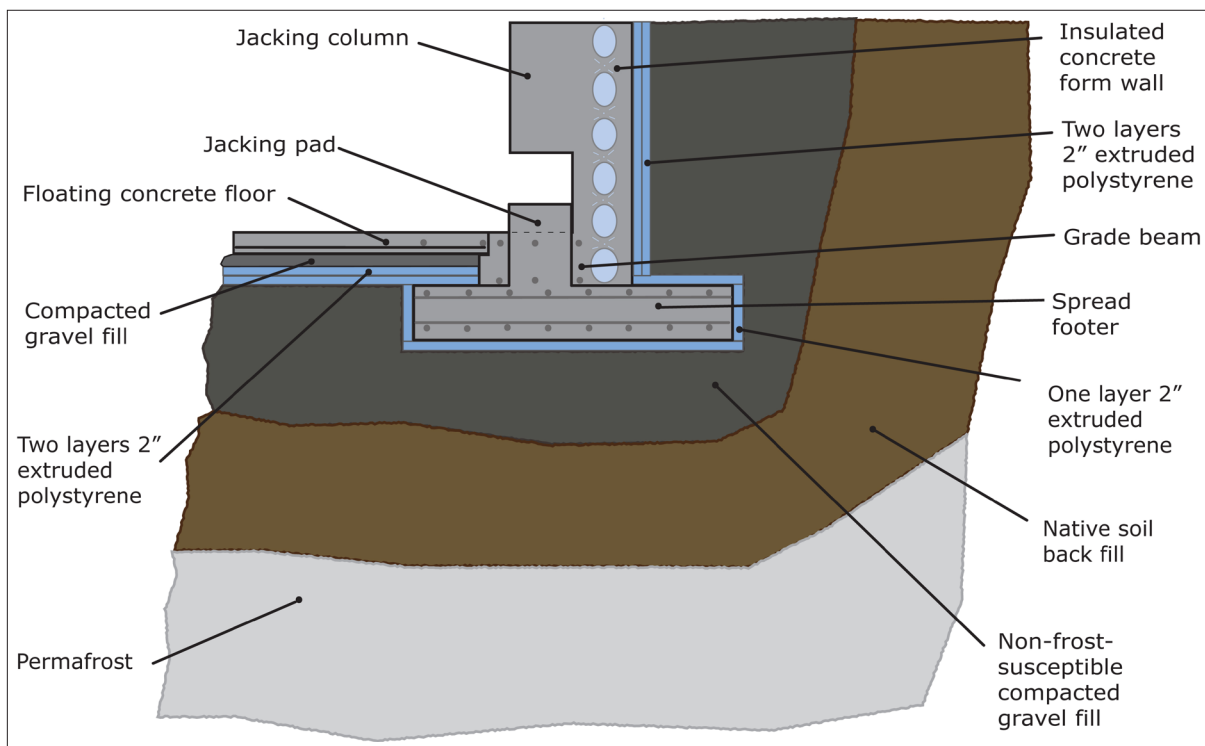


Figure 3. Adjustable foundation detail.

This page was intentionally left blank.

## Site 5: Sunnyside House Building on Permafrost: Failures and Solutions

Michael Lilly<sup>1</sup> and Dennis Filler<sup>2</sup>

This stop helps illustrate some common problems and solutions for building on permafrost and problems associated with water-supply wells in permafrost. Please do not walk to either house, as one house is currently occupied and the vacant house has some hazard conditions. The abandoned house on the west was built in several stages. The well is located in the garage and was drilled before the garage was built. The well went through permafrost, primarily in colluvial deposits from the adjacent hillside. Massive ice lenses are probably present in the local permafrost. Water-supply wells tend to be drilled down to underlying weathered bedrock, where adequate flow rates can be obtained from the fracture and foliation planes. The permafrost acts as a local confining zone for the regional ground-water system. In this area, ground-water generally flows from the bedrock aquifer in the hills directly to the north and enters the alluvial aquifer south of the property. The transition between the hills and alluvial floodplain typically has colluvial silt, which is rich in permafrost. In areas that have not been cleared in the past, the top of permafrost is relatively shallow. In areas cleared for farming, roads, and residential development, permafrost typically is significantly thawed. The ground-water system below permafrost occupies a subpermafrost aquifer, and ground-water on top of permafrost occupies a suprapermafrost aquifer. In this area, the silts provide relatively poor aquifers and are not frequently used for water supply.

So, you have a well through permafrost. How do you keep it from freezing? If the well is artesian (flowing), you may let it run continuously so that it does not freeze up. This practice wastes a lot of water and can create problems with excess water on the land surface in summer and ice in winter. Flowing artesian wells also cause thawing of soils outside of the well, enabling water to flow up outside of the well casing, where it is difficult to control. Another method to prevent freezing of wells in permafrost is to use heat tape, which is installed down the well. Heat tape use needs to be carefully managed so the heat is turned on only enough to keep the inside of the well casing from freezing and not enough to cause excessive thawing on the outside of the well. When heat tape is left on, it can melt the permafrost on the outside of the well, which can lead to well failure. Where massive ice or ice-rich permafrost exists, thawing can produce large subsurface voids, which can cause settlement around the well casing. These types of problems can be very costly to fix and can pose a problem in areas of warming permafrost.

The house at this site had a well drilled through permafrost and housed in a heated garage, so that conditions around the well could not easily be seen. This area was developed as a potato farm many years ago; the associated land clearing likely resulted in melting of the top of the permafrost. The well had heat tape installed, which was reported to be left on for an extended period of time, causing melting of permafrost, so that water flowed up and into the house during periods when it was vacant, causing serious structural and environmental problems in the house. The increased settlement around the well and under the house is creating an escalating series of structural failures.

In comparison, the house built to the east was designed to accommodate permafrost conditions. Before the house was built, there was a homestead log cabin with adjacent artesian well that was allowed to freely flow year-round. During periodic freeze-ups, an installed electric heat tape was used to thaw the well until it flowed again. The house was built on pilings into permafrost to help keep the permafrost stable. The house is typical of structures found on the North Slope. The area under the house remains relatively snow free, which helps cool permafrost during the winter months. The artesian well pressure originally supplied the first floor of the house with water until problems caused the well and foundation to fail at the house to the east. The free-flowing well likely dropped the artesian pressure enough that the water flow to this properly built house will need to be augmented with an electric pump.

These two properties help illustrate one of the common methods to build on permafrost, and one approach that frequently leads to problems. These examples show the results of not properly maintaining an adequate ground-water well through permafrost.

<sup>1</sup>Geo-Watersheds Scientific, 650 Eaton Blvd., Fairbanks, Alaska 99709

<sup>2</sup>College of Engineering and Mines, Civil and Environmental Engineering, PO Box 755900, Fairbanks, Alaska 99775-5900





## Site 6: O'Connor Creek Pingos

Kenji Yoshikawa<sup>1</sup>

Five small open-system pingos near O'Connor Creek, at the toe of an alluvial fan, are among the oldest research pingos in Alaska. In the 1950s, Troy Péwé named these pingos, from largest to smallest, as alpha, beta, and gamma (Péwé, 1982). Alpha pingo is an elliptical mound about 100 m long, 60 m wide, and 10.4 m high, with a breached crater ~6 m deep in the center. Most of the pingo's overburden is composed of dry silt; active layer thickness is 1–3 m. Pingo ice was present from 6 m to 10 m below the ground surface, including organic layers (fig. 1). The area surrounding the pingos was originally black spruce, muskeg, and bog that were cleared for farming. Ground temperature at this pingo is close to thawing point (fig. 2).

Beta pingo is about 120 m to the northeast of Alpha pingo and is about half the size. There is no depression in the center. On the south side, which is steep and slumping, growing trees are deformed and several have split trunks. However, the mounds have been relatively stable for more than 40 years (fig. 3). Some of the old benchmarks installed in September 1964 by Péwé and his student still exist without deformation.

In a nearby drill hole, the silt is 27 m thick and overlies 15 m of creek gravel. The permafrost is 43 m thick. The hydraulic potential of the pingos and the nearby alluvium deposits is high (>68kPa), creating artesian conditions. Most of the homeowners in this area have installed groundwater wells for domestic use. Heating the well to prevent freezing by the permafrost is critically important and tricky work. Permafrost is very warm (>-1°C) and subpermafrost groundwater is close to the freezing point. Groundwater leaking around the outside of the well casing is a typical problem in artesian wells. In some cases the resulting discharge from the wells continued to flow through the winter, creating large masses of aufeis (icings), some of which destroyed houses and covered roads. In November 2005 serious well leakage occurred near the pingo site. On February 24, 2006, liquid nitrogen was injected to freeze the seepage around the well; the well was completely frozen, stopping the groundwater discharge. We monitored subpermafrost groundwater potentials during and after this event. After the well leakage was stopped, the groundwater hydraulic potential immediately began rising and in a few weeks, returned to the original pressure (fig. 4).

## REFERENCE

Péwé, T.L., 1982, Geologic hazards of the Fairbanks area: Alaska Division of Geological & Geophysical Surveys Special Report 15, 119 p.

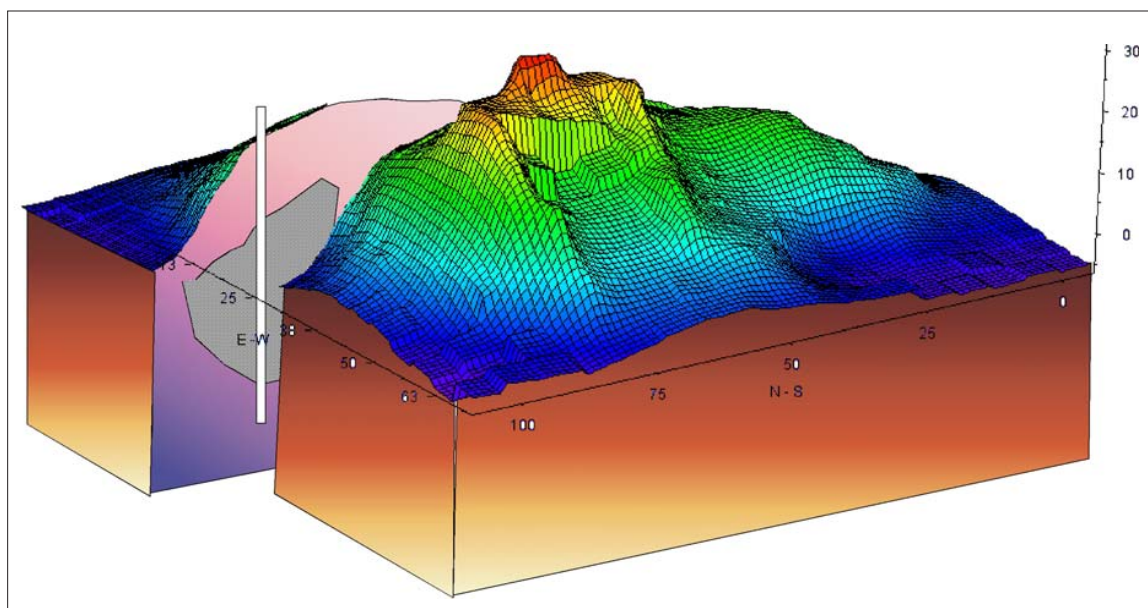


Figure 1. Sketch of Alpha pingo viewed from the northwest side. A massive ice core is present 6–10 m deep on the north side of the pingo (drilled by Yoshikawa in 2005).

<sup>1</sup>Water and Environmental Research Center, Institute of Northern Engineering, University of Alaska, PO Box 755860, Fairbanks, Alaska 99775-5860; email: [kyoshikawa@alaska.edu](mailto:kyoshikawa@alaska.edu)

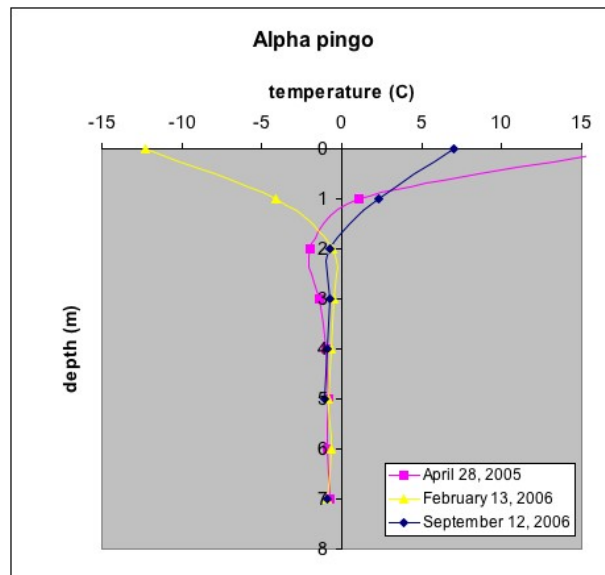


Figure 2. The temperature profile at Alpha Pingo displays stable cold temperatures below 2 m. A massive ice core is present between 6 and 10 m depth.



Figure 3. South-facing slope of Beta pingo (but may be palsa, judging from the ice structure drilled by Yoshikawa). Top photo taken in 1965 by D. Hopkins; bottom photo taken in 1998 by K. Yoshikawa.

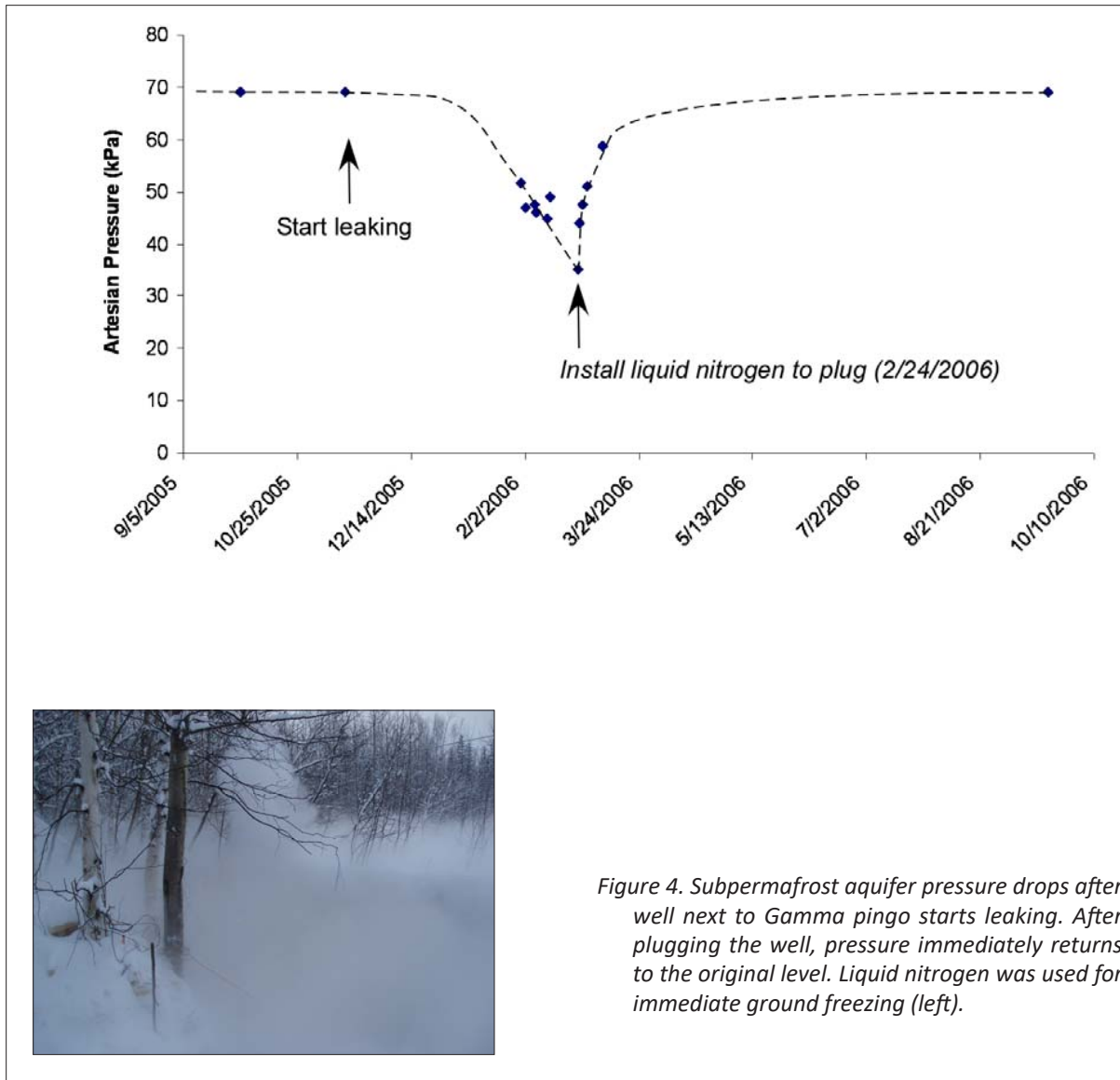


Figure 4. Subpermafrost aquifer pressure drops after well next to Gamma pingo starts leaking. After plugging the well, pressure immediately returns to the original level. Liquid nitrogen was used for immediate ground freezing (left).

This page was intentionally left blank.

## Site 7: Murphy Dome

De Anne S.P. Stevens<sup>1</sup>

Murphy Dome is a scenic upland approximately 30 km northwest of Fairbanks (fig. 1). The Dome is accessible via Murphy Dome Road, which starts at Goldstream Road and follows the Alaska Railroad along Goldstream Creek valley for 12 km before heading north onto higher ground after crossing Spinach Creek. The road is unpaved after the Spinach Creek bridge. A very large parking area is located at the end of the road on top of Murphy Dome, with expansive views of the Alaska Range, Mount McKinley, Minto Flats, and the Steese–White Mountains. Numerous trails lead from the parking area and offer visitors abundant opportunities to explore alpine tundra and periglacial features.

Murphy Dome is a popular recreation area for Fairbanks residents, who use it for hiking, hunting, biking, camping, berry picking, snowshoeing, snowmobiling, and all-terrain vehicle (ATV) riding. It is also a key access point for overland travel to the lower Chatanika River and to Minto Flats and beyond, via ATV in summer and snowmobile in winter.

The accordant rounded ridges north of Fairbanks, including Murphy Dome, have never been glaciated (Péwé, 1953, 1975; Péwé and Rivard, 1961). During past glaciations eolian loess derived from braidplains originating in the Alaska Range to the south and sediment sources along the Yukon River to the north was transported by winds and blanketed the area. This loess was reworked into thick slopewash and alluvial aprons that are visible in road cuts along Murphy Dome Road. Gullying is prevalent on the lower slopes of these reworked silt deposits. The broad valleys surrounding Murphy Dome are filled with thick alluvial deposits and overlying silt and peat. These valley deposits grade smoothly into the slopewash and alluvial aprons of the slopes.

Fairbanks is in the zone of discontinuous permafrost (Péwé, 1975), leading to many problems during road, railroad, and building construction projects. Frost heave and thermokarst settling continue to be serious problems for roads and improperly built structures. Murphy Dome Road is in a constant state of disrepair due to these processes, as are most paved roads in interior Alaska.

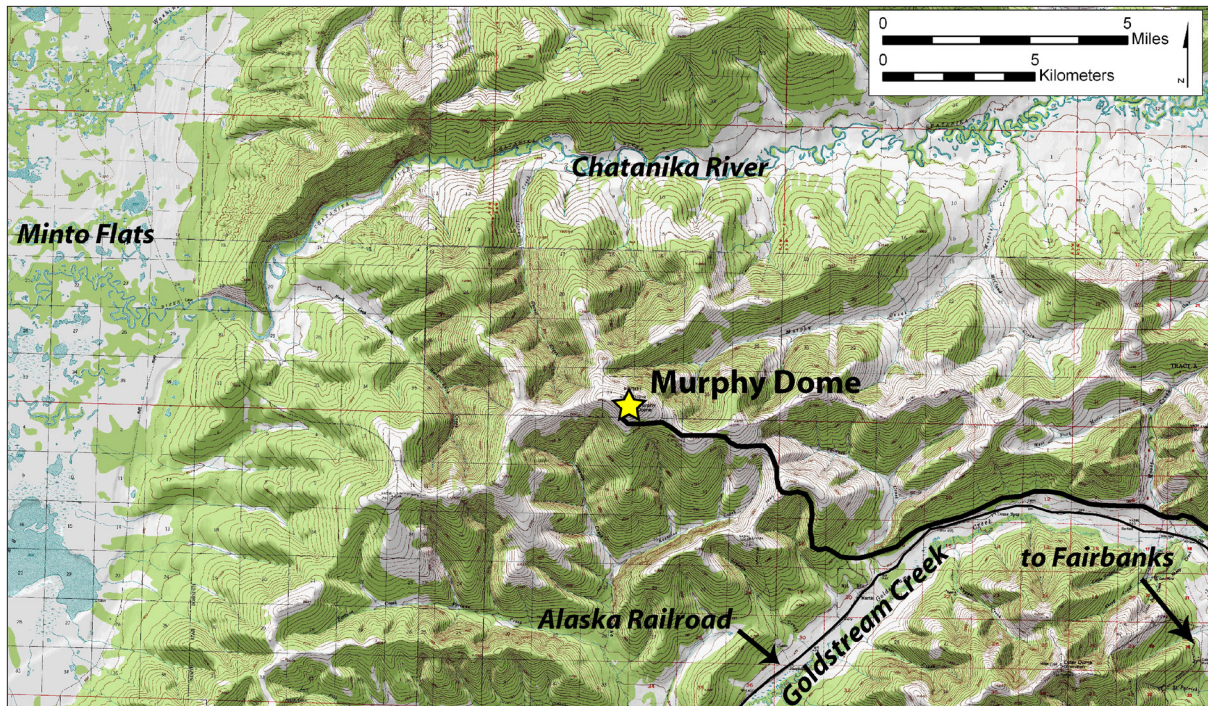


Figure 1. Murphy Dome, a scenic upland approximately 30 km northwest of Fairbanks, is a popular recreation area for local residents.

<sup>1</sup>Alaska Division of Geological & Geophysical Surveys, 3354 College Rd., Fairbanks, Alaska 99709-3707, [deanne.stevens@alaska.gov](mailto:deanne.stevens@alaska.gov)

The greater Fairbanks area, including Murphy Dome, is part of the Fairbanks mining district in the western portion of the Yukon–Tanana Terrane, a displaced portion of the North American continental margin. The Yukon–Tanana Terrane consists of upper Paleozoic and older metasedimentary, metavolcanic, and metaplutonic rocks that crop out for more than 2,000 km, reaching from western Canada and southeastern Alaska to western Alaska (Newberry and others, 1996). The bedrock of Murphy Dome is a very resistant, tor-forming metasandstone (fig. 2). This light to medium gray, quartz-rich, muscovite–biotite grit was probably originally a quartz-rich sedimentary rock that was deposited in a continental margin environment (Newberry and others, 1996).

Vegetation in this area is predominantly taiga, although the top of Murphy Dome is above treeline and is characterized by tundra vegetation (fig. 3). The taiga forest of interior Alaska is part of the circumpolar boreal forest and consists of a mosaic of forest, grassland, shrublands, bogs, and alpine tundra that has formed primarily as a result of differences in slope, aspect, elevation, parent material, and succession following disturbance. On Murphy Dome, the transition from taiga on the lower slopes to tundra at the top is primarily a function of elevation, and the effects of wind above treeline.

Environmental conditions at the top of Murphy Dome have resulted in a variety of phenomena typical of alpine–periglacial settings in interior Alaska. Characteristic landforms include tors, felsenmeers, stone stripes and polygons, nivation hollows, frost-jacked stones, and gelifluction lobes (fig. 4). Tors are pinnacles of bedrock resulting from subsurface physical and chemical weathering along joint surfaces followed by exhumation and stripping of the weathered material from around the residual rock masses (fig. 4a). Felsenmeers, or block fields, are accumulations of frost-rived angular blocks with little or no fine matrix material (fig. 4b). Stone stripes and polygons are linear and polygonal accumulations of coarse blocks that form primarily by intense freeze–thaw activity in substrates with heterogeneous grain sizes (fig. 4c). Nivation hollows are shallow depressions that develop on hillsides as a result of sheetwash, rivulet flow, and solution under and immediately adjacent to perennial snowbanks, where an abundant supply of moisture is available due to melting snow (fig. 4d). Frost jacking, or frost pull, lifts stones and



*Figure 2. Tors formed of the resistant metasandstone bedrock of Murphy Dome.*

other objects out of the ground. Freezing ground adheres to the sides of the object and lifts it as it heaves in response to the expansion of interstitial water upon freezing (fig. 4e). Gelifluction is a form of solifluction involving slow downslope flow of soil due to freeze–thaw processes and the development of excess pore-water pressures in the layer just above a frozen layer (fig. 4f).

Many of the scattered small spruce trees that have managed to take root in the upper slopes of Murphy Dome exhibit flagging due to persistent high winds, especially in winter, or an absence of intermediate branches due to winter wind scour and small animal activity at a level just above typical snow-drift height (fig. 5). Disruption of the surface and subsequent modification of the local hydrology by the major ATV trail leading northwest from the top of Murphy Dome has resulted in thick stands of water-loving alder shrubs growing along the trail margins. Off-road traffic across the fragile tundra to the lower group of tors has led to the development of areas of bog and mud that continue to expand as trail riders seek to circumvent the difficult trail conditions of prior disturbed areas.

The single radar tower and associated generator backup outbuilding at the summit of Murphy Dome are all that remain of a former Air Force NORAD control center (fig. 6). This long-range radar site is currently remotely operated and maintained, with technicians dispatched from Fairbanks as needed. Murphy Dome Air Force Station became operational in 1951 and included extensive facilities, including personnel living quarters and multiple radar towers. Operations were scaled back as remote control and maintenance became possible, and all military personnel were phased out by September 1983. The aircraft control and warning (AC&W) site was redesignated a long-range radar site and a small number of contract civilian personnel remained to provide maintenance. The final phase of radar modernization was completed in the late 1980s with the transition from the older radar to the current AN/FPS-117 minimally attended radar (MAR).



*Figure 3. View northwest from Murphy Dome, with the lower group of tors in the middleground. The upper elevations of Murphy Dome are characterized by tundra vegetation, transitioning into taiga on the lower slopes and surrounding hills. Note frost-jacked stones and stone polygons.*

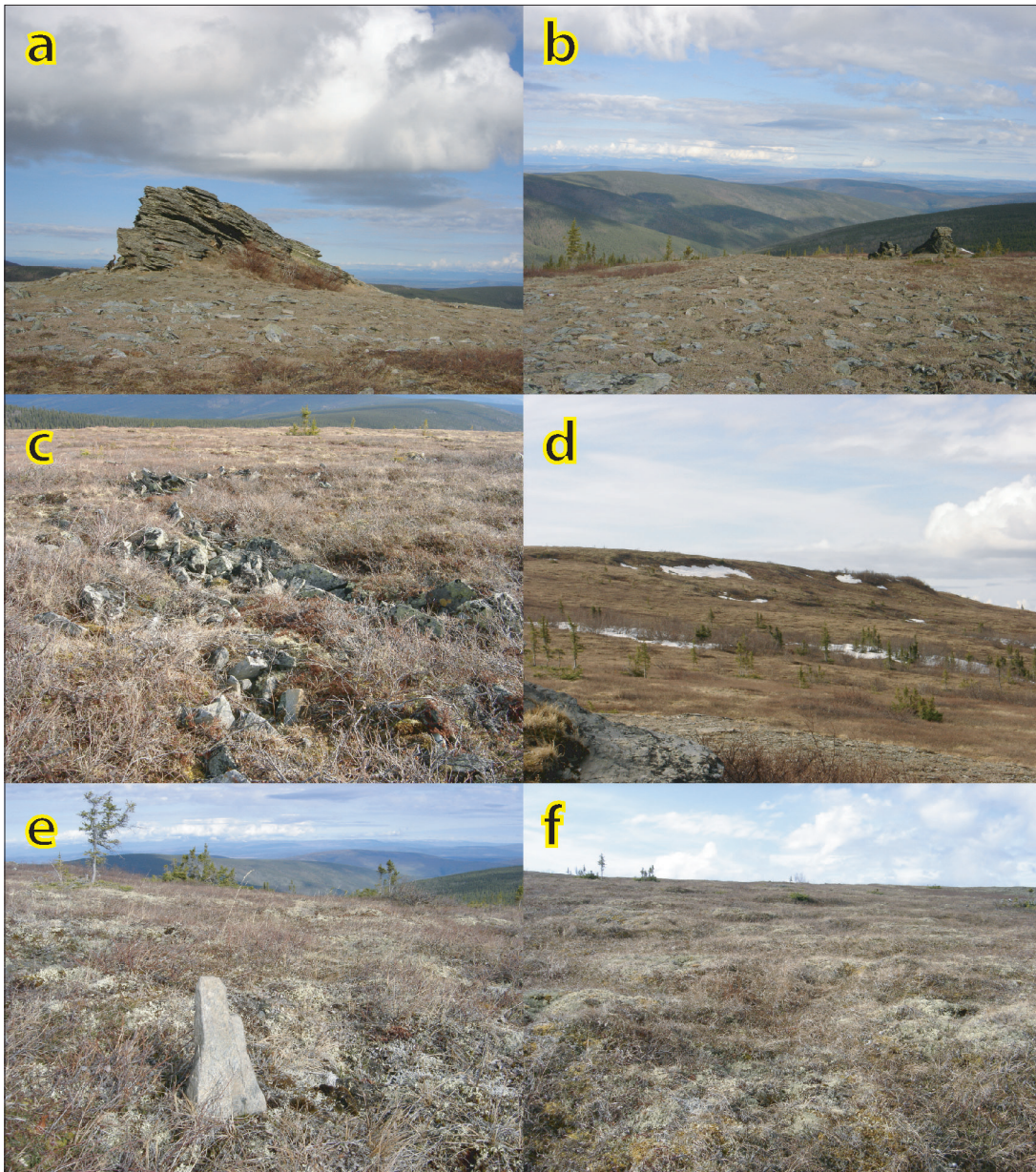


Figure 4. Some characteristic periglacial landforms of Murphy Dome include: (a) tors; (b) felsenmeers (block fields); (c) stone stripes and polygons; (d) nivation hollows; (e) frost-jacked stones; and (f) gelifluction lobes.



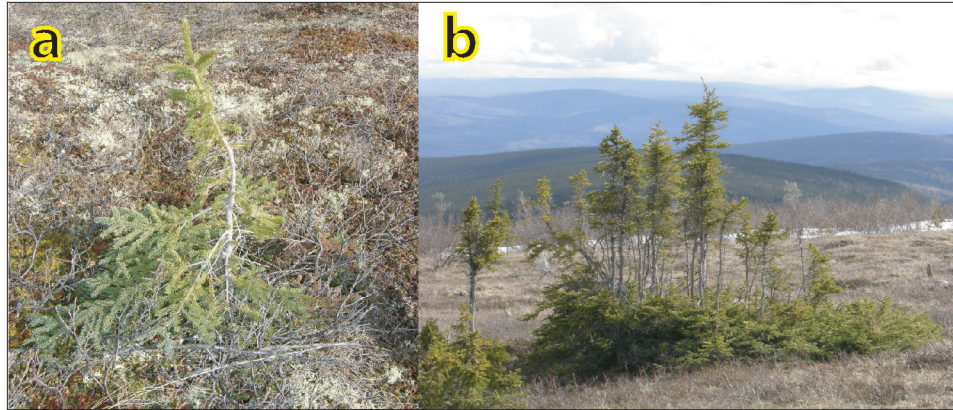


Figure 5. Spruce that have managed to take root in the alpine tundra of Murphy Dome are subjected to high winds and drifting snow. Evidence of the extreme conditions include: a) flagging; and b) absence of intermediate branches.



Figure 6. Radar tower at summit of Murphy Dome.

## REFERENCES CITED

- Newberry, R.J., Bundtzen, T.K., Clautice, K.H., Combellick, R.A., Douglas, Tom, Laird, G.M., Liss, S.A., Pinney, D.S., Reifentuhl, R.R., and Solie, D.N., 1996, Preliminary geologic map of the Fairbanks mining district, Alaska: Alaska Division of Geological & Geophysical Surveys Public Data File 96-16, 17 p., 2 sheets, scale 1:63,360.
- Péwé, T.L., 1953, Multiple glaciation in Alaska; a progress report: U.S. Geological Survey Circular 289, 13 p., 1 sheet, scale 1:3,168,000.
- Péwé, T.L., 1975, Quaternary geology of Alaska: U.S. Geological Survey Professional Paper 835, 145 p., 3 sheets, scale 1:500,000.
- Péwé, T.L., and Rivard, N.R., 1961, Geologic map and section of the Fairbanks D-3 quadrangle, Alaska: U.S. Geological Survey Miscellaneous Investigations Map 340, 1 sheet, scale 1:63,360.

This page was intentionally left blank.

## Site 8: Gold Hill (Péwé Climatic Change Permafrost Reserve)

James E. Begét<sup>1</sup>, David Stone<sup>1</sup>, Paul Layer<sup>1</sup>, Jeffrey Benowitz<sup>1</sup>, and Jason Addison<sup>1</sup>

### TIME NEEDED FOR THIS SITE

Allow anywhere from 5 minutes to 2 hours for this stop. Begin near the Troy Péwé memorial stone. You can see and photograph much of the 35-m-high loess cliffs from that area. Alternatively, if you want to spend more time at this locality, follow the signs and the trail 0.5 km to the east, where exposures of loess, volcanic ash, and ancient ice wedge casts are visible.

### THE TROY L. PÉWÉ CLIMATIC CHANGE PERMAFROST RESERVE

In 1999 the University of Alaska Fairbanks became the owner of 25 acres of Gold Hill; the area before you was set aside as the “Troy L. Péwé Climatic Change Permafrost Reserve.” Troy Péwé first studied the site while working for the U.S. Geological Survey in 1949. During the 1950s and 1960s, Dr. Péwé was a professor at the University of Alaska Fairbanks (UAF) and continued his work on loess. He then moved to Arizona State University, but continued working with new colleagues in Alaska until the end of his career. Péwé received an honorary degree from UAF in 1991 for his contributions to the understanding of Alaska geology and his pioneering permafrost research.

The cliffs of wind-blown silt preserved at Gold Hill in the Péwé Climatic Change Permafrost Reserve contain the oldest loess deposits recognized anywhere in Alaska. The loess here is rich with clues to the last several million years of Alaska’s geological history.

From the area near the stone, a dark layer extends across the loess cliff just below the top; this dark layer is the last interglacial (Marine Isotope Stage 5) paleosol. The loess nearest and just north of the stone is more than a million years old at the base and overlies much older, gold-bearing gravel. The trail to the east leads to the field-trip stop where the loess is thickest and the base of the loess is about 4 million years old. If you want to spend more time at this stop, hike the trail to the exposure.

### GRAVEL DEPOSITS LEFT BY HYDRAULIC GOLD MINING

As you walk along the trail, notice the coarse gravel around you; these are mine tailings. Gold was discovered in creeks around Fairbanks in 1902, causing a gold rush the next spring that left many piles of such tailings throughout the area.

By November 1903, Fairbanks had a population of several thousand and was an incorporated city. Two years later, annual gold production had risen to six million dollars (\$205,800,000 in 2023 dollars), and gold was already being produced from underground tunnels dug to the gravels under the loess deposits. By 1908 there were 18,500 people in the Fairbanks mining district; however, by 1920 the town’s population had shrunk to 1,100 as the miners had mined most of the easily accessible surface gold and were unable to dig through thick loess like that exposed here at Gold Hill.

*Figure 1. Location of the field trip stop at Gold Hill.*

*You can see the 35-m-high loess cliffs from the bus stop at the Péwé Memorial Stone, or you can walk the trail to the exposure.*



<sup>1</sup>Department of Geology & Geophysics, University of Alaska, P.O. Box 755780, Fairbanks, Alaska 99775-5780

Figure 2. Example of gold-mining dredges used at Gold Hill. The gravel was taken into the dredge using the excavator buckets on the right. The gold was separated from the gravel in the dredge using mechanical and chemical processes, and the processed gravel was dumped behind the dredge by the large boom on the left.



Mining revived in the 1920s when a large corporation bought up the claims of individual miners and began industrial-scale dredge mining. The Gold Hill loess cliffs were excavated during this period. Miners used hydraulic giants (giant hoses) to direct streams of water at the loess cliffs to thaw and remove the frozen silt. They injected steam into the frozen gravel beneath the loess and used dredges to mine the gold. The gold dredges were floating factories that slowly chewed their way through the gravel beds, excavating the gravel with huge buckets and creating a small pond in which the dredge floated. The waste gravel was left behind and refilled the pond. Dredges operated in several of the valleys around Fairbanks until 1959.

## LOESS DEPOSITS AT GOLD HILL

Loess deposits are common across central Alaska and the northwestern Yukon Territory, especially on river terraces and low areas near the Tanana and Yukon and other glacier-fed rivers. Large areas of frozen ground are hosted in loess and reworked eolian silts in valley bottoms in central Alaska. River erosion or human disturbance of loess caused by building or highway construction can provide spectacular views of ice wedges, ice lenses, and other varieties of permafrost.

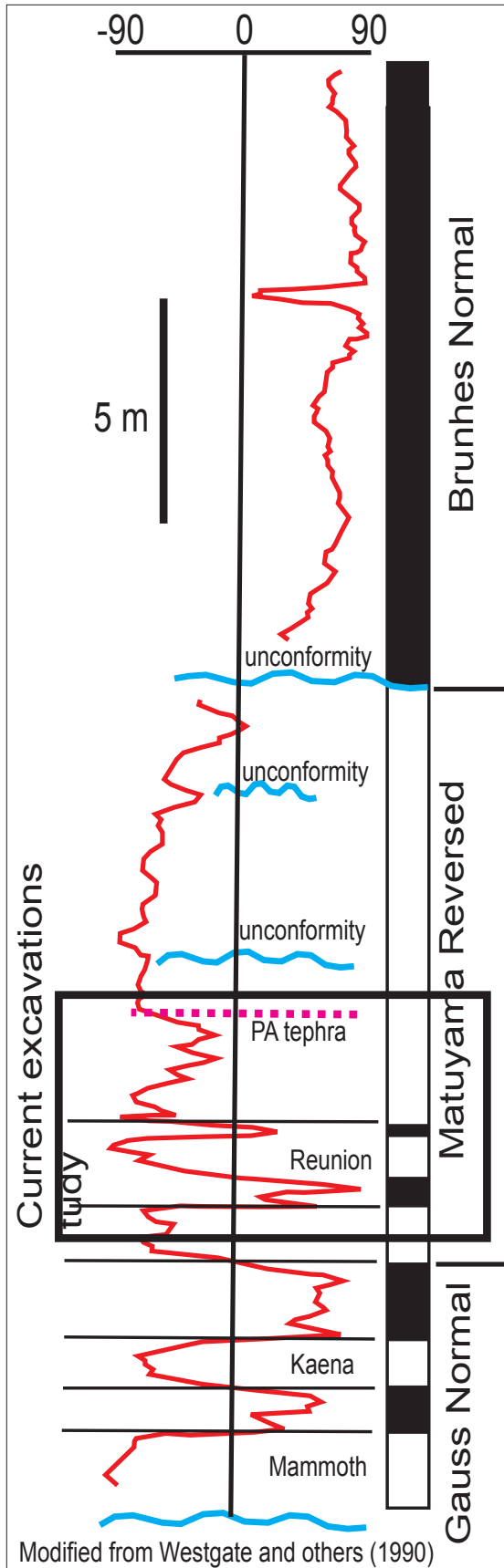
Péwé (1951) first recognized that the silts that blanket hillslopes and form thick deposits in valley bottoms near Fairbanks and other areas were eolian in origin, and suggested that the ice wedges and other periglacial features found in the loess were produced during the last ice age.

Huge volumes of valley-filling loess deposits were washed away and destroyed by hydraulic excavation and dredging during 20th century industrial-scale gold-mining operations near Fairbanks, Ester, Chicken, and other mining areas in central Alaska. When the mining operations stopped, cliffs of loess and other sediments 10–40 m thick were left in some areas. As a result of the gold mining, numerous bones and rare frozen carcasses of bison, mammoths, and other extinct Pleistocene megafauna were collected from the loess and the alluvial gravels beneath the loess (Guthrie, 1990).

The Gold Hill site, along the north side of the Parks Highway beginning about 3 km southwest of the University of Alaska Fairbanks campus, preserves an almost 5-km-long vertical bluff of loess produced by hydraulic mining in the Fairbanks area. The highest loess cliffs are at the eastern end of the exposure and are as high as 35 m. The surface of the loess originally sloped gently downwards to the south, and small “islands” of the original loess valley fill left by the mining operations are preserved on the south of the Parks Highway.

Péwé (1975a, b) divided the loess at Gold Hill into four main stratigraphic units. An upper loess section locally overlies a zone of buried logs and is named the Eva Creek Forest Bed; it was formed during the last interglaciation (Péwé and others, 1997). This section overlies thick deposits of loess termed the Gold Hill silt. A basal forest bed present in a few sites was named the Bonanza Creek Forest Bed (Péwé, 1975b). The base of the Gold Hill loess section was assumed to be “Illinoian” in age, or less than 200,000 years old (Péwé, 1975a; Péwé and Reger, 1983).

The first indication that Alaska loess deposits were much older came from the discovery that the loess contained numerous paleosols recording many more warm periods than those recorded by the Eva Creek and Bonanza Creek forest beds (Begét, 1988; 1991). The sequences of multiple paleosols and interstratified loess deposits found at Gold Hill and other sites were interpreted as glacial–interglacial cycles, requiring an age for the loess much older than originally inferred by Péwé. Subsequently, Begét and Hawkins (1989) showed that the loess deposited in glacial and interglacial periods had different geophysical properties, and that changes in environmental magnetic signals recorded in the loess could be used to produce proxy climate records through loess sections in Alaska that correlated with Milankovitch models of insolation changes and marine isotope records (Begét and others, 1990). The environmental magnetic properties of loess and interglacial soils were reversed from those found in loess–paleosol



sequences in China because of local differences in source material and high-latitude pedogenic processes, including gleying associated with permafrost (Begét, 1996; 2001).

Westgate and others (1990; 2003) used tephrochronology and paleomagnetic stratigraphy to determine that the PA tephra, found at about 21 m depth at Gold Hill, was deposited  $2.02 \pm 0.14$  million years ago, and loess at the base of the Gold Hill section was as much as 3.1 million years old (fig. 3). Westgate and his co-workers took samples at 10 cm intervals and found the upper loess is normally magnetized and correlates with the Brunhes paleomagnetic epoch. The lower part of the loess records mainly reversed magnetic fields, but contains intervals of loess recording normal polarity at about 2.5, 3.5, 5.5, and 8.2 m below the PA tephra layer. The initial transition from normal to the reversely magnetized loess was correlated with the Brunhes–Matuyama boundary, and the two normal epochs below the PA tephra were assigned to the Huckleberry Ridge and Reunion subchrons.

Recent work at Gold Hill has resulted in the discovery of ice-wedge casts, thermokarst features, and interstratified loess and paleosol sequences below the PA tephra at the base of the Gold Hill section. The paleosols and ice-wedge casts were dated using a new paleomagnetic reversal stratigraphy developed for the Gold Hill loess (Begét and others, 2008). The new data show that Alaska loess deposits are surprisingly good recorders of short-lived geologic events, including transient shifts in climate and fluctuations in the earth's magnetic field. Loess can provide long paleoclimatic records of events in terrestrial areas during the last several million years.

## FIELD STRATIGRAPHY AT GOLD HILL

The PA tephra layer is 11 m from the bottom of the loess section and forms a distinctive marker bed that can be traced for more than 30 m across the lower part of the Gold Hill loess. In places the tephra is as thick as 5 cm, although in most places it is broken into pods or several thinner layers. The PA tephra records the position of the ground surface about 2 million years ago. Because the PA tephra can be traced across the exposure, the tephra was used as the datum from which local stratigraphic measure-

Figure 3. Preliminary chronostratigraphy for the Gold Hill loess. Black vertical bars indicate zones of normal magnetization; white bars are reversed zones. The red line shows changes in paleomagnetic declination. Current excavations expose ice-wedge casts and thermokarst collapse features formed during glacial to interglacial climate cycles after the Reunion subchron (2.2 million years ago) but before the PA tephra was deposited 2.0 million years ago.

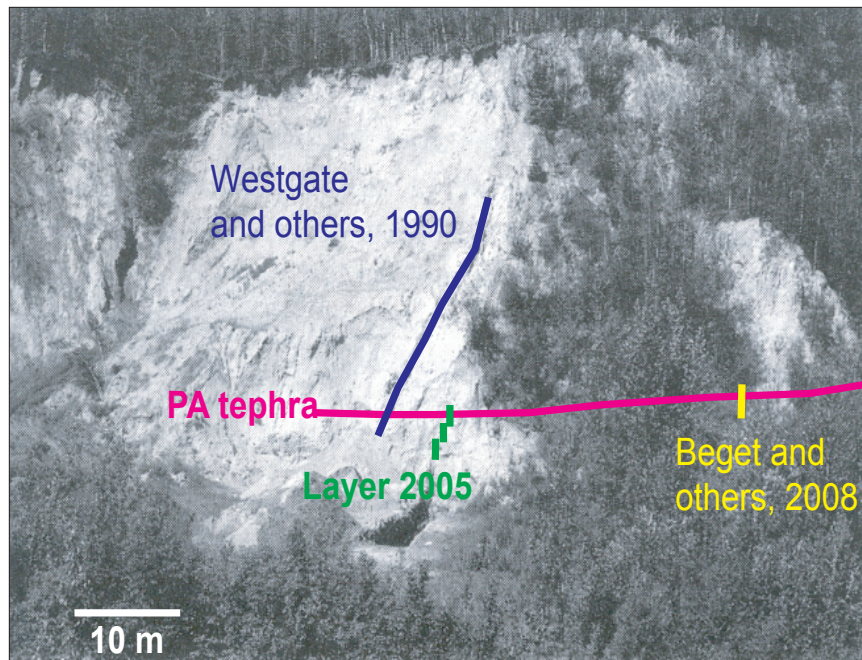


Figure 4. Location of the PA tephra and trenches exposing ancient periglacial features at Gold Hill, Alaska.

ments were taken. The PA tephra is also used as the tie point to correlate the magnetic work of Westgate and others (1990) with our current work.

Trenching and sampling were done at two new sites, one about 5 m east of the long section studied by Westgate and others (1990) and a second site about 20 m farther east (fig. 4). The three trenches expose features we have interpreted as evidence of ice-wedge casts and thermokarst collapse pits extending as much as several meters below the PA tephra. Thermokarst collapse features of similar size are forming today in Fairbanks where permafrost is thawing.

## FEATURES AT THE FIELD SITE

During our trenching and logging it became apparent that loess just below the PA tephra had been involved locally in a series of post-depositional collapses. The PA tephra was deposited on the ground surface about 2 million years ago, and thus sediments at Gold Hill that are overlain by the tephra can be precisely dated. Our trenching locations were chosen specifically at sites where we can demonstrate the trench sediments are overlain by the PA tephra (Naibert and others, 2005).

Our excavations reveal the PA tephra was incorporated in local depressions in four separate areas along the 30-m-long exposure. At the eastern pit, the tephra and the intercalated loess, which elsewhere are preserved in sub-horizontal beds, abruptly drop in elevation on each side of a 2-m-wide V-shaped depression. Further excavations found pellets of the tephra and blocks of loess in a compact silt matrix within the depression. The V-shaped depression was excavated to a depth of 2 m, where it became narrower and then terminated. This feature is interpreted as an ice-wedge cast (Beget and others, 2008).

At the western pit, a well developed, organic-rich paleosol about 20–60 cm thick above the PA tephra was involved with the tephra in a high-angle slump. This paleosol can be traced along much of the exposure above the PA tephra. Excavations in the western trench exposed crudely bedded organic sediment and loess and pods of PA tephra that had apparently accumulated in a broad depression. This feature is interpreted as a thermokarst collapse pit.

At the far eastern end of the PA exposure, a loess cliff exposed a 3-m-thick diamicton that can be traced 5 m across the section. The diamicton contains rounded to elongate silt and multicolored paleosol clasts ranging from 0.5 to 10 cm in diameter disseminated within a dense, fine-grained matrix. The eastern margin of this deposit cuts across undisturbed loess below the PA tephra, locally underlies the PA tephra, and incorporates pods of the tephra. We interpret that the diamicton was formed by progressive collapse of wet, thawed pellets and blocks of sediment into a large thermokarst pit. Similar large pits can be seen today at several sites around Fairbanks where frozen loess is thawing, and bits of the thawed ground can frequently be heard falling into the pit. We believe this large thermokarst collapse feature formed in a similar fashion 2 million years ago.

The presence of ice-wedge casts and thermokarst features below the PA tephra indicates climate in the Fairbanks area had cooled sufficiently by 2 million years ago to allow the formation of permafrost. The climate subsequently warmed and caused the permafrost to degrade. The well-developed paleosol found above the PA tephra records an interglaciation that occurred soon after the PA tephra fall. These features record a glacial-to-interglacial climate cycle similar in duration and intensity to those that occurred during late Pleistocene time.

## REFERENCES

- Begét, J.E., 2001, Continuous late Quaternary proxy climate records from loess in Beringia: *Quaternary Science Reviews*, v. 20, p. 499–507.
- Begét, J.E., 1996, Tephrochronology and paleoclimatology of the last interglacial–glacial cycle recorded in Alaskan loess deposits: *Quaternary International*, v. 34–36, p. 121–126.
- Begét, J.E., 1991, Paleoclimatic significance of high latitude loess deposit, *in* Weller, G., Wilson, C.L., and Severin, B.A.B., eds., *Proceedings of the International Conference of the Role of the Polar Regions in Global Change: Fairbanks, Alaska*, Geophysical Institute, p. 594–598.
- Begét, J.E., 1988, Tephros and sedimentology of frozen Alaskan loess, *in* Senneset, I.K., ed., *Fifth International Conference on Permafrost, Trondheim, Norway, 1988: International Conference on Permafrost [Proceedings]*, v. 5, p. 672–677.
- Begét, J.E., and Hawkins, D.B., 1989, Influence of orbital parameters on Pleistocene loess deposition in central Alaska: *Nature*, v. 337, p. 151–153.
- Begét, J.E., Layer, P.W., Stone, D.B., Benowitz, J.A., and Addison, J., 2008, Evidence of permafrost formation two million years ago in central Alaska: *Proceedings of the Ninth International Permafrost Conference, Fairbanks, Alaska*, p. 95–100.
- Begét, J.E., Stone, D.B., and Hawkins, D.B., 1990, Paleoclimatic forcing of magnetic susceptibility variations in Alaskan loess: *Geology*, v. 18, p. 40–43.
- Guthrie, D.R., 1990, *Frozen fauna of the Mammoth Steppe—The story of Blue Babe*: Chicago, University of Chicago Press, 338 p.
- Naibert, T.J., Domeier, M.M., Robertson, K.L., Fallon, J.F., Stone, D.B., Begét, J.E., and Layer, P.W., 2005, Re-evaluation of the magnetostratigraphy of the Gold Hill loess, Interior Alaska: *American Geophysical Union, AGU Fall Meeting Abstracts*, p. A96.
- Péwé, T.L., 1951, An observation on wind-blown silt: *Journal of Geology*, v. 59, p. 399–401.
- Péwé, T.L., 1975a, *Quaternary Geology of Alaska*: U.S. Geological Survey Professional Paper 835, 145 p.
- Péwé, T. L., 1975b, *Quaternary stratigraphic nomenclature in central Alaska*: U.S. Geological Survey Professional Paper 862, 32 p.
- Péwé, T.L., and Reger, R.D., 1983, *Guidebook to permafrost and quaternary geology along the Richardson and Glenn Highways between Fairbanks and Anchorage, Alaska*: Alaska Division of Geological & Geophysical Surveys Guidebook 1, 263 p., 1 sheet, scale 1:250,000.
- Péwé, T.L., Berger, G.W., Westgate, J.A., Brown, P.M., and Leavitt, S.W., 1997, *Eva interglaciation forest bed, unglaciated east-central Alaska—Global warming 125,000 years ago*: *The Geological Society of America Special Paper* 319, 54 p.
- Westgate, J.A., Stemper, B.A., and Péwé, T.L., 1990, A 3 m.y. record of Pliocene–Pleistocene loess in interior Alaska: *Geology*, v. 18, p. 858–861.
- Westgate, J.A., Preece, S.J., Péwé, T.L., 2003, The Dawson cut forest bed in the Fairbanks area, Alaska, is about two million years old: *Quaternary Research*, v. 60, p. 2–8.

This page was intentionally left blank.



## Site 9: Thermokarst Pits and Fens in Goldstream Valley Torre Jorgenson<sup>1</sup>

Thermokarst pits and fens surrounded by collapsing forests can be found just south of the peat mine near the intersection of Murphy Dome and Goldstream Road (fig. 1). Parking is available at the peat mine, which is filling with water and recovering naturally with abundant wetland vegetation. A 300-m-long trail leads around the east side of the mine to a deep thermokarst pit, a thermokarst fen, and a site with actively collapsing trees. The peat mine, which provided organic matter for landscaping for several years during the early 2000s, took advantage of thick peat deposits that long had been locked in permafrost.

Thermokarst is abundant in ice-rich lowland areas around Fairbanks on fine-grained soils associated with lowland loess, retransported deposits, and abandoned floodplains. Typical thermokarst landforms include shallow thermokarst lakes, bogs (isolated water bodies fed by precipitation and dominated by *Sphagnum* mosses), fens (connected waterbodies fed by groundwater and dominated by sedges, grasses, and forbs), and pits (isolated open waterbodies dominated by submergent or floating aquatic forbs). Recent analysis indicates that permafrost covers ~62 percent of the discontinuous permafrost zone in central Alaska; thermokarst covers 5 percent of the landscape; 21 percent is unfrozen; and on 12 percent, permafrost status remains undetermined. Thermokarst landforms are



Figure 1. Southeast of the peat mine are thermokarst pits, fens, and actively collapsing forests. A “moat” surrounds the margins of areas with rapidly collapsing permafrost. After collapse, the groundwater-fed water body quickly becomes colonized by sedges and cattails to become a fen.

<sup>1</sup>ABR—Environmental Research and Services, Inc. P.O. Box 80410, Fairbanks, Alaska 99708-0410; [tjorgenson@abrinc.com](mailto:tjorgenson@abrinc.com)

dominated by thermokarst fens (1.8 percent of area), bogs (1.0 percent), lakes (1.0 percent), and pits (0.3 percent). Fens and bogs predominate because the shallow water formed after collapse quickly fills in with either herbaceous fen- or Sphagnum bog-dominated vegetation.

At this site, both thermokarst pits and fens are evident. The pit in figure 2 has collapsed 2.5 m, causing the trees to lean inward and fall into the water. The pit remains isolated from groundwater movement. Due to nutrients released from the previously frozen peat and silt, the water is quickly colonized by duckweed and algae. Stirring the bottom sediments with a stick can cause vigorous bubbling of methane gas. Adjacent to the pit is a thermokarst fen that has become connected to groundwater moving downslope from the nearby hillside. In this minerotrophic environment, the collapsed area quickly becomes colonized by aquatic sedges and cattails. Immediately next to the steep collapsing bank, an open-water “moat” forms, where vegetation has not yet colonized. The soil next to the fens has become well drained and vegetation has converted from black spruce to birch trees. Beavers and waterbirds have colonized the open water in the fen and the beavers have felled many of the birch trees along the margins. Thus, the thermokarst has created a radical conversion in habitat and wildlife use.

Thawing of ice-rich soil also severely damages roads and creates costly maintenance problems. Nearby Goldstream Road develops long, shallow longitudinal cracks (0.5 m wide by 0.1-0.2 m deep) in the roadbed every year from thawing and slumping of permafrost at the margins of the roadbed. Thawing along the margins is accelerated by insulating snow that is plowed off the road during winter and shallow ponds are developing in the ditches. Nearly every year, road-maintenance crews fill in the long cracks with additional asphalt and add substantial amounts of gravel to the slumping shoulders of the road.



*Figure 2. The ice-rich lowlands in Goldstream Valley are susceptible to permafrost degradation that takes the form of thermokarst lakes, pits, bogs, and fens. The deep thermokarst pit (left) has relatively warm, nutrient-rich water, and abundant methane emissions. At an area of rapid collapse (right), the trees fall into the pit so quickly over a summer that they don't have a chance to adjust their growth, as evident by the curving trees along the edge of the pit.*

## Site 10: College Peat Ice Wedges

Kenji Yoshikawa<sup>1</sup> and Vladimir Romonovsky<sup>2</sup>

A landscaping company that sells organic topsoil from a pit on the north side of Fairbanks (fig. 1) excavated into the muskeg layer and exposed a polygonal network of ice wedges that are possibly still active. The ice wedges are present in peat that has accumulated since about 3,500 yr BP and has grown episodically as the permafrost table fluctuated in response to fires, other local site conditions, and perhaps regional climatic changes (Hamilton and others, 1983). Radiocarbon dates indicate one or two episodes of ice-wedge growth between about 3,500 and 2,000 yr BP as woody peat accumulated at the site (Hamilton and others, 1983). At one of the Water and Environmental Research Center's sites near the College Peat pit, with similar landscape characteristics and in current climatic conditions, we observed a low ( $< -4^{\circ}\text{C}$ ) annual mean permafrost-surface temperature event every 5–10 years, usually in concert with low snow years. The College Peat site is one of the coldest temperature permafrost locations in Fairbanks ( $-3.1^{\circ}\text{C}$  at 10 m) (fig. 2); convective heat transfer is a major ground-cooling process at

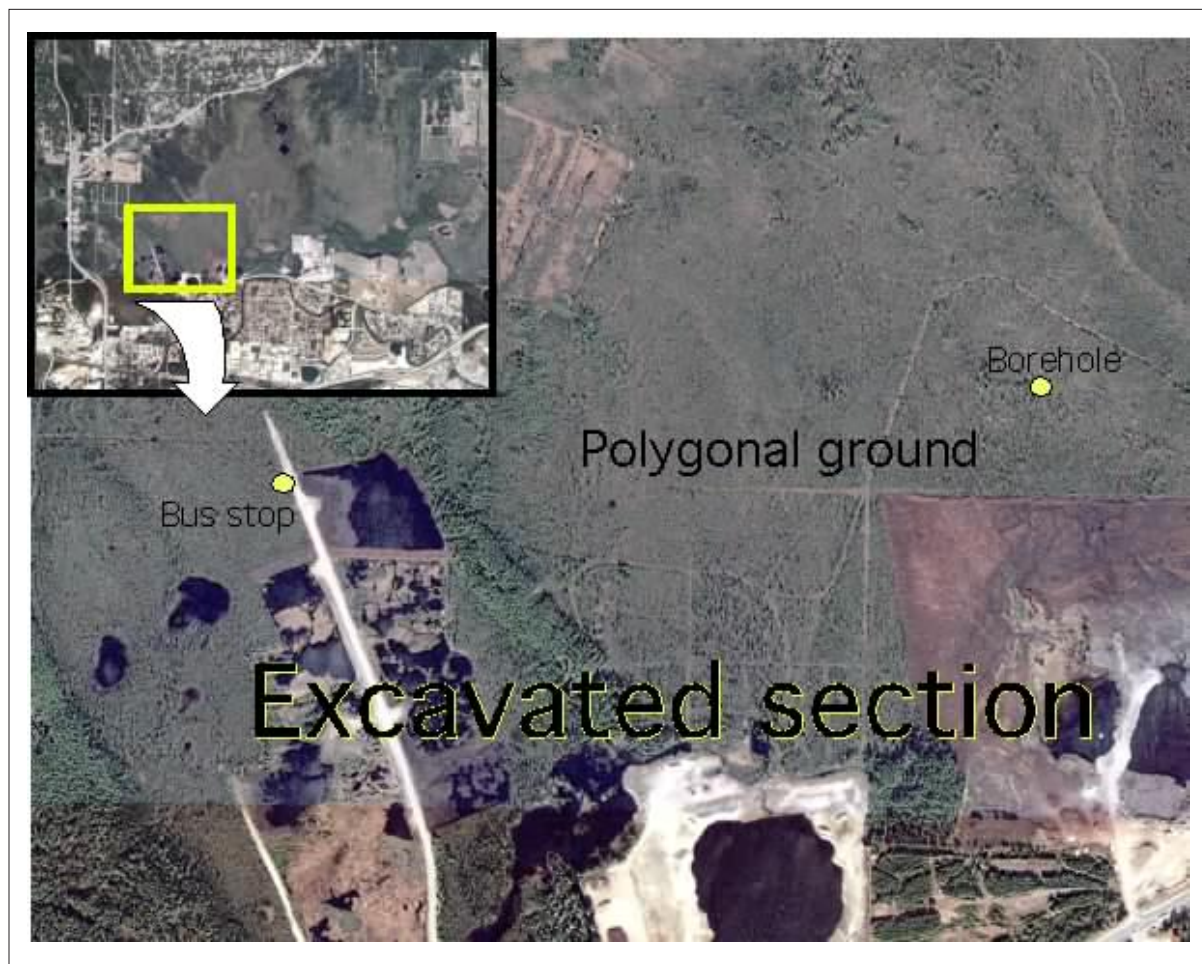


Figure 1. Great Northwest peat site on College Road. White northwest–southeast road marked with bus stop is a private road on the west border of the peat site, just north of College Road. This peat site is operated by Great Northwest, Inc. The polygonal network of ice wedges that are possibly still active were exposed when the operators excavated into the muskeg layer. Peat has accumulated in this location since about 3,500 yr BP and grows episodically with fluctuations in the permafrost table. Aerial photography from GoogleEarth.

<sup>1</sup>Water and Environmental Research Center, Institute of Northern Engineering, University of Alaska, PO Box 755860, Fairbanks, Alaska 99775-5860; [kyoshikawa@alaska.edu](mailto:kyoshikawa@alaska.edu)

<sup>2</sup>Geophysical Institute, PO Box 757320, University of Alaska, Fairbanks, Alaska 99775-7320

this site. A thicker organic (moss) layer also developed strong thermal resistance during the summer and much less persistence during the winter, promoting a large thermal offset (up to  $-3.8^{\circ}\text{C}$ ) (Yoshikawa and others, 2004). Thermal conductivity of the organic strata (such as feathermoss, fibric, and humic layers) is strongly affected by moisture content (Yoshikawa and others, 2002). Recent human activities (excavation) lowered the near-surface groundwater level in some areas of these polygonal terrains, which could change thermal offsets in the near future. Frost-contraction cracking can still be observed during winter periods and wedge ice probably continues to form, although not every year. Secondary generation of syngenetic ice wedges occurred in the past few hundred years, most likely during the Little Ice Age.

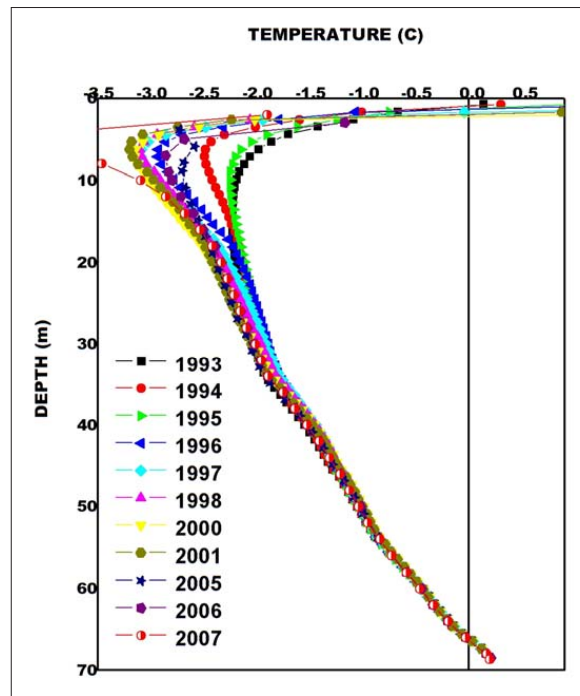


Figure 2. Permafrost temperatures near the Great Northwest peat site since 1993. Permafrost temperature was  $-3.09^{\circ}\text{C}$  at 10 m depth on July 13, 2007.

## REFERENCES

- Hamilton, T.D., Ager, T.A., Robinson, S.W., 1983, Late Holocene ice wedges near Fairbanks, Alaska, U.S.A.; environmental setting and history of growth: *Arctic and Alpine Research*, v. 15, no. 2, p. 157–168.
- Yoshikawa, K., Bolton, W.R., Romanovsky, V.E., Fukuda, M., and Hinzman, L.D., 2002 Impacts of wildfire on the permafrost in the boreal forests of Interior Alaska: *Journal of Geophysical Research*, v. 107, p. 8148, doi:[10.1029/2001JD000438](https://doi.org/10.1029/2001JD000438), 2002 [printed 108(D1), 2003].
- Yoshikawa, K., Overduin, P.P., and Harden J.W., 2004, Moisture content measurements of Moss (*Sphagnum* spp.) using recently developed commercial sensors: *Permafrost and Periglacial Process*, v. 15, no. 4, p. 309–318.

## Site 11: GeoData Center – Map Office – Alaska Satellite Facility User Services Office

Patricia Burns<sup>1,2</sup>

Many products and services relevant to permafrost researchers are currently available in Room 204 of the Syun-Ichi Akasofu Building.

The GeoData Center (GDC) provides data management and archive services for the Geophysical Institute and maintains a variety of geophysical data collections in support of scientific research. GDC collections include, but are not limited to, historic aerial photography and early satellite image acquisitions valuable for landscape change studies.

The Map Office sells statewide USGS topographic of Alaska in 1:250,000, 1:63,360, and 1:25,000 scales (limited to certain areas). In addition, thematic maps are available that describe permafrost, ecology, and geology. Various trail maps and selected maps of Yukon Territory and British Columbia are also available for purchase. Selected nautical charts published by the National Oceanic and Atmospheric Administration (NOAA) are available, including charts for Prince William Sound, Resurrection Bay, and Kachemak Bay.

The Alaska Satellite Facility (ASF) is involved in a wide range of activities—from downlinking satellite data to developing data-analysis tools, value-added products, and training for Synthetic Aperture Radar (SAR) users. SAR is the only satellite imagery that can be acquired at any time of the day or night and during adverse weather conditions. ASF's User Services Office provides a wide range of products, services and information to ASF data users.



*Examples of maps and imagery available at the joint offices of the GeoData Center, Map Office, and Alaska Satellite Facility User Services Office include: BAR aerial photography, Barrow, Alaska, 1945 (GDC); National Oceanic and Atmospheric Administration (NOAA) aerial photography, Barrow, Alaska, 1977 (GDC); Circum-Arctic Map of Permafrost and Ground-Ice Conditions (Map Office); Circumpolar Arctic Vegetation Map (Map Office); AVNIR-2 satellite image of Barrow, Alaska, 2007 (ASF); and PRISM satellite image of Barrow, Alaska, 2007 (ASF).*

<sup>1</sup>Geophysical Institute GeoData Center, P.O. Box 757320, University of Alaska, Fairbanks, Alaska 997756-7320

<sup>2</sup>Current: Alaska Division of Mining, Land, and Water, 3700 Airport Way, Fairbanks, Alaska 99709; [patricia.burns@alaska.gov](mailto:patricia.burns@alaska.gov)



## Site 12: Thermokarst and Drunken Forest <sup>1</sup>Katey Walter Anthony<sup>1</sup> and Dragos Vas<sup>1</sup>

### SITE DIRECTIONS

Parking is available at Creamer's Field, College Road access. Follow the trails and boardwalk through the drunken forest to observe ice wedge polygon terrain, thermokarst mounds, and thermokarst lakes.

This area is perennially frozen with well developed thermokarst terrain. The broad lowland valley in which Creamer's Field sits is underlain by retransported silt of late Quaternary origin. The silt is relatively organic, typically dated to 20,000–40,000 yr BP, and forms the valley-bottom facies of Péwé's Goldstream formation (Péwé, 1975). Permafrost is prevalent except under the talik of creeks and rivers; shallow ice wedges and large masses of ground ice are relatively common; and sites where groundwater flow emerges at the surface are associated with pingos.

In the severe cold of winter, permafrost soils contract, crack, and split into polygonal shapes. In spring, meltwater seeps into the cracks and refreezes. Over many years, these events create a pattern of troughs and raised mounds, which create polygons. In many places, degradation of permafrost leads to deep troughs where surrounding trees slump into the growing trenches. These tilted trees are often referred to as 'drunken forest.' Thawing ground ice also results in formation of thermokarst pits, mounds, and lakes. Lakes enlarge as permafrost along margins thaws and banks retreat.

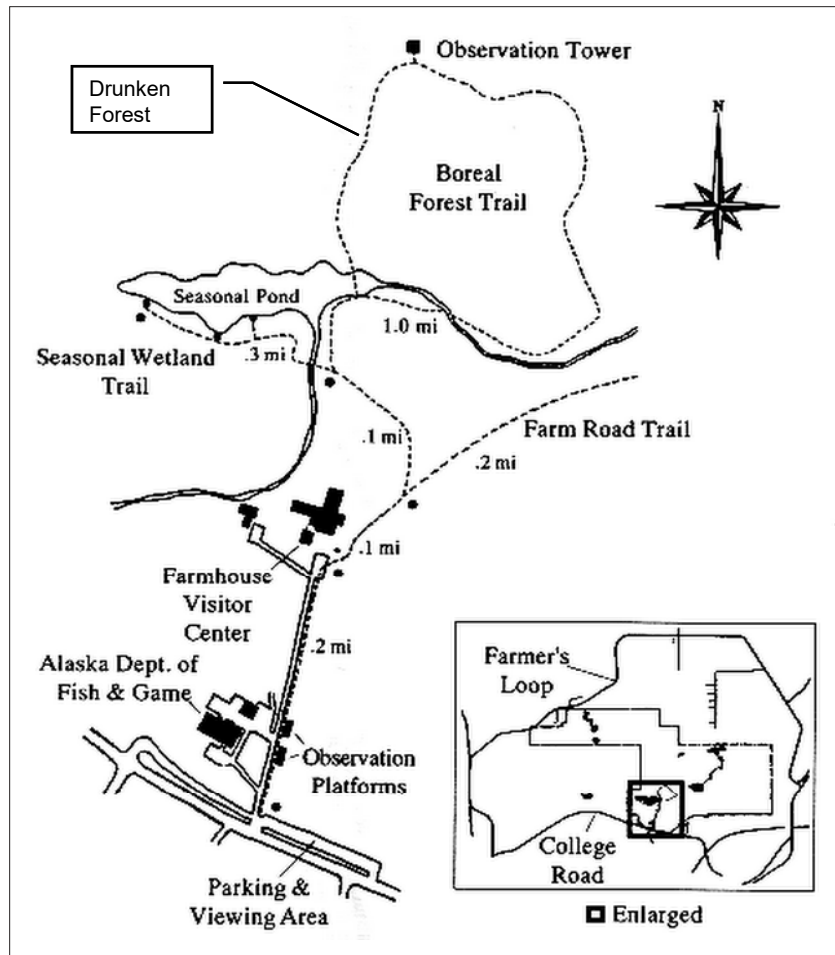


Figure. 1 Map of Creamer's Field site. Follow the dotted trail marks to the "Drunken Forest" site marked on the map. [http://wildlife.alaska.gov/index.cfm?adfg=refuge.creamers\\_trails](http://wildlife.alaska.gov/index.cfm?adfg=refuge.creamers_trails).

<sup>1</sup>Assistant Professor, Water & Environmental Research Center, P.O. Box 755960, University of Alaska, Fairbanks, Alaska 99775-5960



Figure 2. Boardwalk at Creamer's Field. This photo shows flooding of the forest floor as a result of ground surface subsidence associated with thermokarst. Photo by: <http://static.panoramio.com/photos/original/9986023.jpg>.



Figure 3. "Drunken forest" results when ground ice melts and surface subsidence alters the rooting foundation of trees, causing them to tilt or fall over. Photo by: <http://www.flickr.com/photos/cysewski/165084192>.





Figure 4. “Drunken forest” along thermokarst margin of Reindeer Lake, north of Creamer’s Field visitor center. Photo by K. Walter Anthony, 2007.

#### Site information from the Creamer’s Field Visitor’s Guide, 2008

- Winter:** Air temperature for Creamer’s Field: Varies from an average of 27°F (-3°C) in October to -11°F (-24°C) in January. Extremes of -61°F to +38°F (-52°C to 3°C) have been recorded in January. Extreme temperature fluctuations over short time periods (as much as 50°F [28°C] in 24 hours) can occur in any month.
- Vegetation:** Black spruce, white spruce, aspen, balsam poplar. Forest cover is less than 50 years old in this area.
- Wildlife:** More than 20 species of mammals, 30 species of birds, and hundreds of plants, fungi, insects, and smaller organisms remain in the boreal forest through winter. Many organisms endure the winter in a state of dormancy, a state where life is temporarily suspended. Other animals produce antifreezes, special chemicals that lower the temperature at which their cells and body fluids will freeze, allowing the animals to survive severe cold. Yet other animals remain active throughout winter, including voles, red squirrels, snowshoe hares, porcupines, martens, red fox, moose, and weasels.

## REFERENCES CITED

- Creamer’s Field Visitor’s Guide, 2008 (<http://wildlife.alaska.gov/index.cfm?adfg=refuge.creamers>).
- Péwé, T.L., 1975, The Quaternary Geology of Alaska: U.S. Geological Survey Professional Paper 385, 145 p.

This page was intentionally left blank.

## Site 13: Late-Pleistocene Syngenetic Permafrost in the CRREL Permafrost Tunnel, Fox Alaska

M.Z. Kanevskiy<sup>1</sup>, H.M. French<sup>2</sup>,  
Y.L. Shur<sup>1</sup>, K.L. Bjella<sup>3</sup>, M.T. Bray<sup>1</sup>, C.M. Collins<sup>3</sup>, T.A. Douglas<sup>3</sup>, and D. Fortier<sup>1</sup>  
(M.Z. Kanevskiy, H.M. French, and Y.L. Shur, eds.)

### ABSTRACT

Late-Pleistocene syngenetic permafrost exposed in the walls and ceiling of the CRREL permafrost tunnel consists of ice- and organic-rich silty sediments penetrated by ice wedges. Evidence of long-continued syngenetic freezing under cold-climate conditions includes the dominance of lenticular and micro-lenticular cryostructures throughout the walls, ice veins, and wedges at many levels, the presence of undecomposed rootlets, and organic-rich layers that reflect the former positions of the ground surface. Fluvio-thermal modifications are indicated by bodies of thermokarst-cave ('pool') ice, by soil and ice pseudomorphs, and by reticulate-chaotic cryostructures associated with freezing of saturated sediments trapped in underground channels.

### INTRODUCTION

The CRREL permafrost tunnel is located at Fox, approximately 16 km north of Fairbanks, Alaska. Constructed 40 years ago, this facility is one of the few underground exposures of syngenetic Pleistocene-age permafrost. Natural exposures of ice-rich permafrost quickly degrade and provide only opportunistic study. The permafrost tunnel allows hundreds of visitors the unhurried opportunity to become acquainted with ice-rich permafrost and for professionals to study the peculiarities of syngenetic permafrost and its history.

This guide summarizes recent cryostratigraphic observations made in the tunnel and re-evaluates earlier interpretations. Some observations have been described in previous publications (Shur and others, 2004; Bray and others, 2006) while others are presented in the NICOP proceedings volume (Bray, 2008; Fortier and others, 2008; Kanevskiy and others, 2008).

### THE CRREL TUNNEL

The CRREL permafrost tunnel was constructed in the early 1960s by the U.S. Army Cold Regions Research and Engineering Laboratory (CRREL) to test mining, tunneling, and construction techniques in permafrost. It continues to be maintained by CRREL for research. An isometric view of the floor plan of the tunnel is shown in figure 1. The tunnel entrance is on the eastern margin of Goldstream Creek valley, where a steep 10-m-high escarpment was created by placer-gold mining activities in the first part of the previous century. The surface of the valley that lies immediately above the long axis of the tunnel rises gently from the top of the escarpment in which the entrance is located toward the east side of Goldstream Creek valley. The active layer of the terrain that overlies the tunnel is between 0.7 and 1 m thick, which is typical of the Fairbanks area.

The tunnel is composed of two portions (fig. 1). The adit (a nearly horizontal passage from the surface into the hillside) was driven by the U.S. Army Corps of Engineers using continuous mining methods in the winters of 1963–64, 1964–65, and 1965–66 (Sellmann, 1967). The winze (an inclined adit) was driven by the U.S. Bureau of Mines (USBM) from 1968 to 1969 using drill and blast, thermal relaxation, and hydraulic relaxation methods (Chester and Frank, 1969). The adit extends approximately 110 m in length and is located predominantly in the frozen silt unit. The winze begins approximately 30 m into the adit and drops obliquely at an incline of 14 percent for 45 m, passing into the frozen gravel unit and ultimately into the weathered bedrock, where the Gravel Room was excavated (Pettibone and Waddell, 1973). At the time of excavation, portions of the Gravel Room roof consisted of 2 m of frozen gravel lying below the silt unit. After the winze levels out adjacent to the Gravel Room, it continues for another 10 m into what is known as the CRREL Room. The tunnel is chilled by natural ventilation

<sup>1</sup>Institute of Northern Engineering, College of Engineering & Mines, University of Alaska Fairbanks, P.O. Box 755910, Fairbanks, Alaska 99775-5910

<sup>2</sup>Departments of Geography and Earth Sciences, University of Ottawa, ON, K1N 6N5, Canada

<sup>3</sup>Cold Regions Research and Engineering Laboratory (CRREL), P.O. Box 35170, Fort Wainwright, Alaska 99703-0170

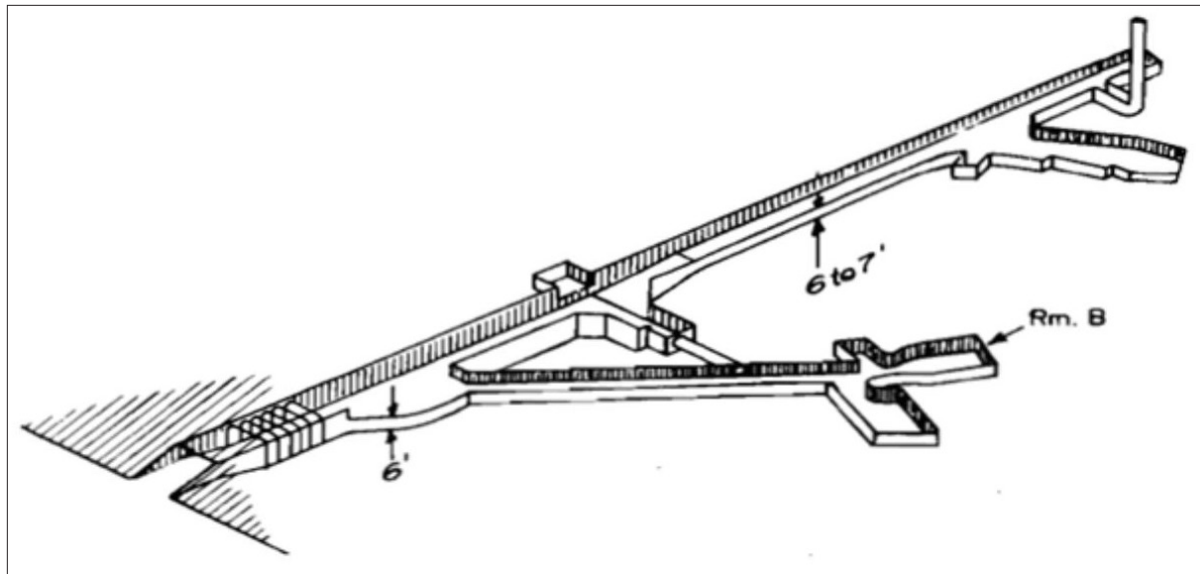


Figure 1. Isometric view of the CRREL permafrost tunnel.

in winter and by artificial refrigeration in summer, supporting permafrost stability.

Many papers have been published on the geology, paleoecology, and cryostratigraphy of the sediments exposed in the tunnel (Sellmann, 1967, 1972; Watanabe, 1969; Hamilton and others, 1988; Long and Péwé, 1996; Shur and others, 2004; Pikuta and others, 2005; Bray and others, 2006; Katayama and others, 2007; Wooler and others, 2007; Fortier and others, 2008; Kanevskiy and others, 2008) as well as their engineering properties (Chester and Frank, 1969; Pettibone and Waddell, 1971, 1973; Thompson and Sayles, 1972; Johansen and others, 1981; Johansen and Ryer, 1982; Garbeil, 1983; Weerdenburg and Morgenstern, 1983; Arcone and Delaney, 1984; Delaney and Arcone, 1984; Huang and others, 1986; Delaney, 1987; Bray 2008). The problems of tunnel construction have also been described (Chester and Frank, 1969; Dick, 1970; Swinzow, 1970; Linnell and Lobacz, 1978).

Sediments exposed in the tunnel consist mainly of frozen silts that range in age from Wisconsinan to Holocene (fig. 2) and are derived largely from the outwash gravels and braided stream deposits of the Tanana lowlands and surrounding hills. Ice-rich silts of eolian origin were also partly reworked and retransported by slope and fluvial processes (Péwé, 1975; Hamilton and others, 1988). The silts overlie the Fox Gravel, fluvial gravels of early Pleistocene age, that are derived from the surrounding hills of the Yukon–Tanana Uplands. These gravels overlie Pre-Cambrian schist bedrock.

The silt is as thick as ~14 m over the adit and 18 m over the Gravel Room. Silts formed between 30,000 and 43,000 yr BP (Hamilton and others, 1988). Near the tunnel portal, fanlike deposits of poorly sorted debris uncon-

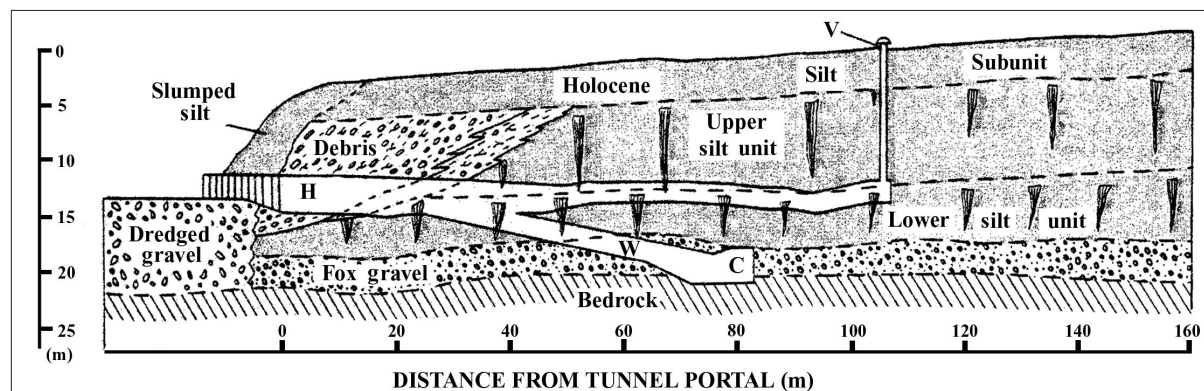


Figure 2. Generalized geologic section of Fox permafrost tunnel showing horizontal tunnel (H), ventilation shaft (V), winze (W), and chamber within Fox Gravel, known as a “Gravel Room” (C). (Hamilton and others, 1988)

formably overlie the silts; the poorly sorted debris formed between 12,500 and 11,000 yr BP during deep erosion of the Goldstream Creek valley slopes (Hamilton and others, 1988).

**PREVIOUS OBSERVATIONS on the tunnel permafrost**

Sellmann (1967, 1972) was the first to provide information on the tunnel geology and permafrost. He described segregation ice, foliated wedge ice, and large clear masses of ice (buried ‘aufeis’) and identified two ‘unconformities.’ The upper unconformity was marked by the tops of small wedges and a change in soil color. The lower unconformity was identified by (i) a change in size and shape of wedges, (ii) a gap in radiocarbon ages obtained from organic material contained in the silty sediments in the tunnel walls of between 14,000 and 30,000 years BP, and (iii) a 20-fold increase in chemical concentration with depth. Sellmann (1967) suggested “...this unconformity was probably caused by some regional warming or local depositional or erosional event.”

Hamilton and others (1988) reported a diverse assemblage of animals’ bones (bison, horse, mammoth[?], caribou[?], and arctic ground squirrel) and plant macrofossils (grasses and sedges) indicated a tundra or shrub-tundra environment. Hamilton and others (1988) concluded that the tunnel “...provides continuous and undisturbed exposures of ice-rich silt that overlies gravel and bedrock” and that “...most of the pore and segregated ice formed during freezing of silt.” The authors identified four major types of ground ice previously described by Péwé (1975): pore ice, segregated ice, foliated wedge ice, and buried surface ice; they concluded that “most of the pore ice and segregated ice formed during freezing of silt and has been preserved since that time.” They also identified two independent systems of ice wedges (fig. 2) and inferred a thaw unconformity between them. Other bodies of ice, described as “...horizontal, saucer-shaped bodies, 2–6 m wide and 0.5–2 m deep” (Hamilton and others, 1988) were interpreted as buried frozen thaw ponds formed in ice-wedge troughs. According to these authors, these ice bodies “...generally consist of three successive depth zones: (1) clear ice with vertical bubble trains, transitional downward into (2) ice containing reddish brown, suspended organic matter that overlies (3) a lenticular body of unusually ice-rich silt.”

**CRYOSTRATIGRAPHY AND CRYOLITHOLOGY**

Cryostratigraphy refers to the study of frozen layers in the Earth’s crust and is a branch of geocryology. The science was developed first in Russia, where the study of ground ice gained early attention (Shumskii, 1959; Katanonov, 1962, 1969) and subsequently led to highly detailed studies (Vtyurin, 1964; Popov, 1967, 1973; Gasanov, 1969; Gravis, 1969; Zhestkova, 1982; Shur, 1988; Romanovskii, 1993; Dubikov, 2002) that are unparalleled in North America. A summary of cryostratigraphic principles can be found in French (2007, p. 153–185).

Cryostratigraphy differs from traditional stratigraphy by specifically recognizing that perennially frozen sediment and rock contain structures that are different from structures in unfrozen sediment and rock. Cryolithology

is a related branch of geocryology and refers to the relation between the lithologic characteristics of rocks and their ground ice amounts and distribution. The structures, largely determined by the amount and distribution of ice in sediments are termed ‘cryostructures.’ Cryostructures are useful in determining the nature of the freezing process and the conditions under which frozen sediment accumulates.

A distinction must be made between epigenetic and syngenetic permafrost (fig. 3). Epigenetic permafrost refers to permafrost that forms subsequent to deposition of the host sediment and rock. By contrast, syngenetic permafrost refers to permafrost that forms at the same time

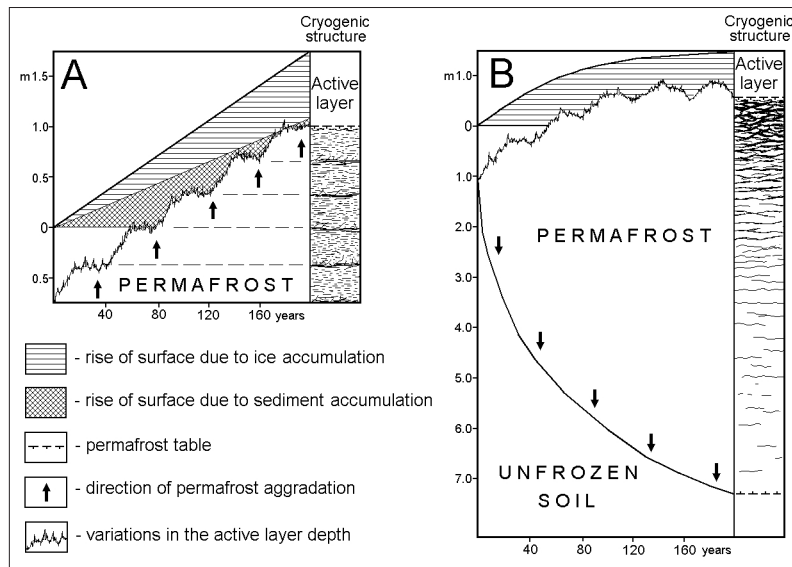









Figure 3. Mechanisms of (A) syngenetic (based on Popov, 1967) and (B) epigenetic permafrost formation.

as the host sediment is being deposited. These types of permafrost can be distinguished by analysis of cryostructures. The epigenetic–syngenetic distinction is extremely useful in the context of Quaternary paleoenvironmental reconstruction.

Cryostratigraphy adopts many of the principles of modern sedimentology. For example, cryofacies are defined according to volumetric ice content and ice-crystal size, and then subdivided according to cryostructure. Finally, where a number of cryofacies form a distinctive cryostratigraphic unit, these are termed a ‘cryofacies assemblage’ (French, 2007).

### (I) CRYOSTRUCTURES

Russian permafrost scientists were the first to systematically identify cryotextures and cryostructures (Gasarov, 1963; Katasonov, 1969; Zhestkova, 1982; Popov and others, 1985; Melnikov and Spesivtsev, 2000). Unfortunately, these classifications are complex and unwieldy. For example, Katasonov’s (1969) classification lists 18 different cryostructures and Popov’s classification (Popov and others, 1985) lists 14 categories.

(A)		CRYOSTRUCTURE AND CODE	SEDIMENT	ICE	OCCURRENCE AS OR WITHIN
	structureless (SI)	sand gravel		pore	ice in sand + gravel
	lenticular (Le)	muddy peat mud (fine sand)	sand	segregated crack infill	ice/sediment lenses massive ice icy sediments (ice wedges) (composite sand-ice wedges) (dilation-crack ice)
	layered (La)	muddy peat mud (fine sand)	sand	segregated intrusive crack infill	ice/sediment layers massive ice icy sediments ice wedges composite sand-ice wedges dilation-crack ice
	regular reticulate (Rr)	mud		segregated	ice in mud
	irregular reticulate (Ri)	mud		segregated	ice in mud
	crustal (Cr)	mud frost-susceptible clasts		segregated	
	suspended (Su)	mud sand gravel	mud sand gravel	segregated intrusive	icy layer at top of permafrost ice dikes in mud ice lenses massive ice icy sediments ice dikes


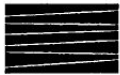

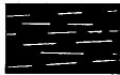
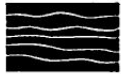
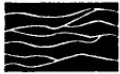
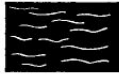
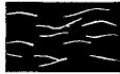
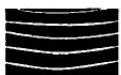



(B)		LAYERED		LENTICULAR	
		parallel	non-parallel	parallel	non-parallel
planar					
wavy					
curved					

Figure 4. A North American classification of cryostructures. (A) Scheme proposed by Murton and French (1994). Ice is shown in white, sediment in black. (B) Terms and illustrations used to describe layered and lenticular cryostructures (Murton and French, 1994).

A simplified North American cryostructural classification by Murton and French (1994) encompasses the range of cryostructures found in permafrost (fig. 4). Several Russian terms are transliterated. All cryostructures can be recognized by the naked eye.

**The common cryostructures are:**

1. ‘structureless’ (Sl) – refers to frozen sediment in which ice is not visible and consequently lacks a cryostructure (this category is termed ‘massive’ in the Russian transliterated literature)
2. ‘lenticular’ (Le) – lens-like ice bodies that are described by inclination, thickness, length, shape, and relation to adjacent cryostructures
3. ‘layered’ (La) – continuous bands of ice, sediment, or a combination of both
4. ‘regular reticulate’ (R) – a regular three-dimensional net-like structure of ice veins surrounding a mud-rich block
5. ‘irregular reticulate’ (Ri) – an irregular three-dimensional net-like structure of ice veins surrounding a mud-rich block
6. ‘crystal’ (Cr) – refers to the ice crust or rim around a rock clast
7. ‘suspended’ (Su) – refers to grains, aggregates, and rock clasts suspended in ice (this category is termed ‘ataxitic’ in the Russian transliterated literature)

Figure 5 shows examples of cryostructures typical for the tunnel.

The micro-morphology of cryostructures can be observed using an environmental scanning electron microscope (ESEM). For example, Bray and others (2006) provide examples of structureless (massive) and lenticular cryostructures viewed conventionally and under ESEM (fig. 6).

## (ii) THAW UNCONFORMITIES

Discontinuities in the nature and distribution of ground-ice bodies related to permafrost thawing are termed ‘thaw unconformities’ (French, 2007). These features are the result of either thawing of frozen materials (primary thaw unconformity) or subsequent refreezing of previously thawed material (secondary thaw unconformity). A primary thaw unconformity forms at depth below a residual thaw layer; for example, it truncates the top of an ice wedge. When permafrost subsequently aggrades, the original thaw unconformity at depth becomes a secondary (paleo-) thaw unconformity and the new active layer–permafrost boundary becomes the primary thaw unconformity. The secondary thaw unconformity can be recognized by both the truncated ice wedge and by different cryostructures in the sediment above and below. Thaw unconformities can be further recognized by differences in stable isotope values, by heavy mineral assemblages above and below the unconformity, and by horizons of enhanced microorganisms.

The manner in which permafrost degrades and subsequently forms again, and the resulting cryostratigraphic evidence are illustrated in figure 7.

## Syngenetic permafrost

The permafrost exposed in the CRREL tunnel is typical of the Pleistocene permafrost referred to in the Russian literature as ‘yedoma’ or ‘ice complex’ (Soloviev, 1959; Katasonov, 1978; Popov and others, 1985; Romanovskii, 1993). Ice-complex sediments have been studied mainly in central and northern Yakutia; similar sediments also were observed in Chukotka, West Siberia, Taimyr, Alaska, and Canada (Vtyurin, 1964; Péwé, 1966, 1975; Popov, 1967; Gasanov, 1969; Katasonov, 1978; Lawson, 1983; Carter, 1988; Hamilton and others, 1988; Shur and others, 2004; French, 2007). This permafrost developed when long periods of uninterrupted cold-climate sedimentation allowed permafrost to form syngenetically.

Syngenetic permafrost forms in response to sedimentation (alluvial, slope, aeolian, and lacustrine) that causes the base of the active layer to aggrade upward. By definition, the permafrost is syngenetic because it is of the same age (approximately) as the host sediment. Thus, transformation of active-layer sediments into a perennially frozen state occurs virtually simultaneously with sedimentation. Typically, syngenetically frozen sediments are silty, or loess-like (up to 70–80 percent silt fraction), and ice rich (the soil gravimetric moisture content may exceed 100–200 percent). They also contain rootlets, buried organic horizons, and exhibit layered cryogenic structures.

The main locations where syngenetic permafrost is forming today are in the alluvial and deltaic environments (Shur and Jorgenson, 1998) of Arctic North America (Colville River, Alaska; Mackenzie River, Canada) and in northern Siberia (Lena, Ob, Yenisey, Yana, Indigirka, and Kolyma River valleys and deltas). Thickness of con-



Figure 5. Photos showing (A) micro-lenticular cryostructure (location marker is 1.25 x 1.25 cm in size) (photo by M. Kanevskiy), and (B) reticulate-chaotic cryostructure (the handle of the knife is about 6 cm long) (Fortier and others, 2008).



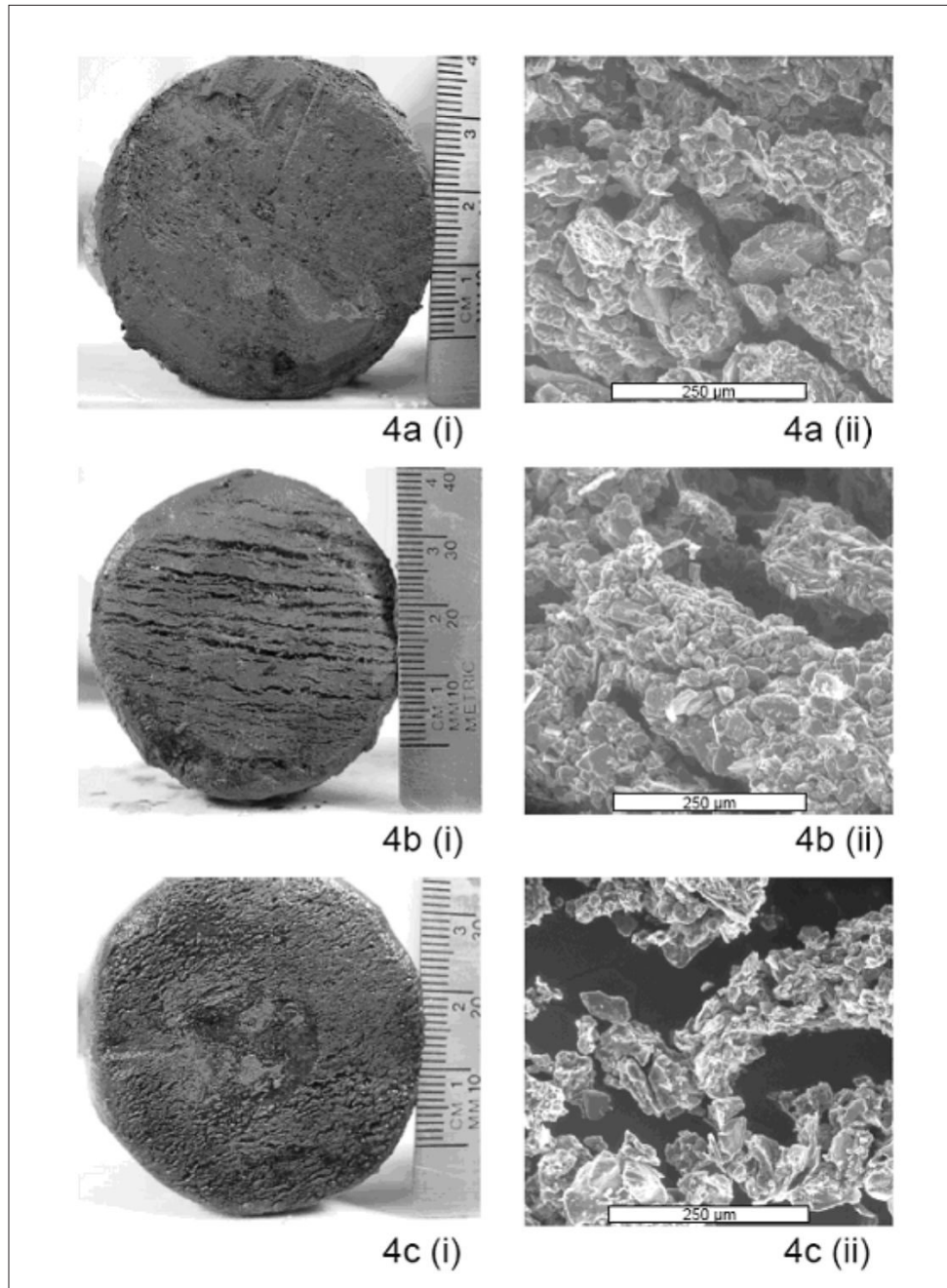


Figure 6. Example of cryostructures from the CRREL tunnel viewed conventionally and under an environmental scanning electron microscope (ESEM). (A) Massive cryostructure. Image (1) is a macro-scale image typical of silt pseudomorphs. Note centimeter scale. Image (2) is a micro-scale image using an ESEM. Bar scale indicates 250  $\mu\text{m}$ . (B) Lenticular-layered cryostructure. Image (1) is a conventional macro-scale image. Note centimeter scale. Image (2) is a micro-scale image using an ESEM that shows the soil and micro ice-lens morphology. Bar scale indicates 250  $\mu\text{m}$ . (C) Micro-lenticular cryostructure. Image (1) is a macro-scale image. Note centimeter scale. Image (2) is a micro-scale image under ESEM in which soil particles are generally suspended in an ice matrix. Bar scale indicates 250  $\mu\text{m}$ . (Bray and others, 2006)

temporary syngenetic permafrost usually does not exceed a few meters.

Pleistocene syngenetic permafrost exists mainly in the continuous permafrost zone of Siberia, and its presence in the discontinuous permafrost zone of Alaska is a rare phenomenon. This type of permafrost is also found in the valleys and lowlands of adjacent unglaciated Yukon Territory, Canada. Under the current climatic conditions of the Fairbanks area, modern ice-wedge formation occurs very rarely and only in peat (Hamilton and others, 1983).

Syngenetic permafrost is often characterized by numerous ice veins and ice wedges. In contrast to epigenetic permafrost, in which ice wedges rarely exceed 4 m in depth, ice wedges in syngenetic permafrost may extend through the entire strata, either as huge wedges reaching 10–40 m in depth and 2–6 m in width or as small ice veins throughout the profile. Their varying width and depth reflect the varying rates of sedimentation and climate conditions. In syngenetic permafrost bodies, wedge ice can occupy 30–50 percent, and even more in some cases, of the total volume. In color, the ice wedges are gray because of the numerous inclusions of fine sediment, and they can easily be distinguished from smaller Holocene and modern ice wedges located in the top part of Yedoma sections, because the latter are usually white and opaque due to fewer soil inclusions and an abundance of air bubbles.

Radiocarbon dating and oxygen-isotope variations indicate that much of the syngenetic Pleistocene permafrost in northern Siberia formed between 40,000 and 12,000 years ago (Vasil'chuk and Vasil'chuk, 1997, 2000). As a

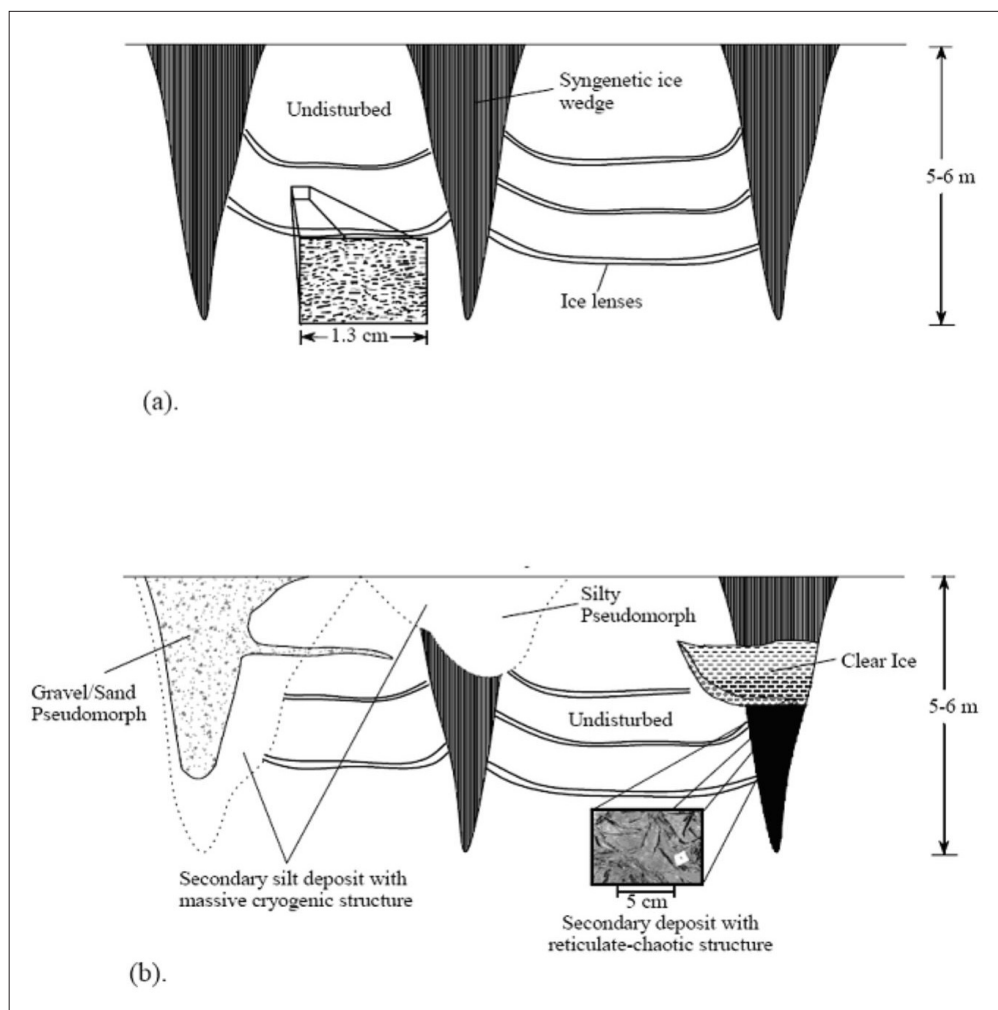


Figure 7. Schematic diagram of (A) undisturbed syngenetic permafrost and (B) typical modified permafrost exposure within the CRREL tunnel. In (A) the expanded image represents a micro-lenticular cryostructure, a reliable indicator of syngenetic permafrost. In (B) an idealized schematic shows typical secondary modification of original syngenetic permafrost. Expanded image represents reticulate-chaotic cryostructures. The reticulate-chaotic cryostructure is associated with 'clear ice,' interpreted as thermokarst-cave ('pool') ice (Bray and others, 2006).

dominant type of permafrost in unglaciated lowlands during the late Pleistocene, this permafrost is the main source of well-preserved late Pleistocene faunal remains (woolly mammoths and other large mammals).

### Cryostratigraphic mapping in the tunnel

Cryostratigraphic mapping uses the cryofacies method (permafrost-facies analysis) first proposed by Katasonov (1962, 1978). This method is based on two concepts, namely, that (1) the shape, size, and spatial pattern of ice inclusions (cryostructures) depend on the conditions under which the sediment was deposited and then frozen, and (2) every cryofacies has its own specific cryostructure.

The results of cryostratigraphic mapping of the main adit of the tunnel (Bray and others, 2006) are shown in figures 8 and 9. Four categories of information are shown:

- a. Mineral sediment is grouped into the general categories of silt, sand, and gravel.
- b. Cryostructures are identified as being either lenticular or micro-lenticular (typical for syngenetic permafrost), massive or reticulate-chaotic (typical for epigenetic permafrost).
- c. Ice bodies are mapped as being either lenses (usually a layered cryogenic structure), wedge ice (formed in thermal-contraction cracks), or clear ice (occurring in association with wedge ice).
- d. Pseudomorphs are mapped where the sediment or ice is interpreted to be the result of ice-wedge modification.

Descriptions of the cryo-lithostratigraphic units, ice bodies, and other features are shown in table 1.

In 2006, the 38-m-long winze section was studied (Kanevskiy and others, 2008). Cryostratigraphic mapping of one wall and the ceiling of the winze was performed in the scale 1:20; several small sections were studied in detail (scale 1:4). Figure 10 shows the general view of the left wall and the ceiling of the winze. More detailed fragments are shown in figures 11 to 13.

*Table 1. Cryo-lithostratigraphic units, ice bodies, and other features that were mapped in the CRREL tunnel (figs. 8 and 9).*

#### 1. CRYO-LITHOSTRATIGRAPHIC UNITS

Sscs:	Fairbanks silt, representative of the original syngenetic permafrost, characterized by micro-lenticular and layered cryostructures. Average gravimetric water content 130%
SnsCs:	Fairbanks silt, characterized by a massive cryostructure that is indicative of secondary modification. It contains no cryostructures typical of syngenetic permafrost. The average gravimetric water content is 69%
Sor:	Fairbanks silt with a massive cryostructure and possessing organics (rootlets, wood, animal bones)
Ssor:	Sandy organic silt with a massive cryostructure and containing rootlets, wood, and animal bones
Gr:	Gravel deposits; sandy, silty, imbricated. Near the tunnel entrance they may represent slope deposits. Deeper in the tunnel, the gravel deposits are directly related to the fluvial erosion and thaw-modification of ice wedges

#### 2. ICE BODIES

Ice lenses:	Lenses of ice that range in length from 10 cm to several meters and thickness between 0.5 and 10 cm. They form part of the micro-lenticular and layered cryostructures
Clear ice:	Lenticular-shaped ice bodies, often with aligned bubbles toward outer edges, and usually associated with reticulate-chaotic cryostructures in adjacent sediments. The ice is interpreted as thermokarst-cave ice
Wedge ice:	Foliated ice with vertical soil laminations, often gray to brownish in color

#### 3. OTHER FEATURES

Pseudomorphs: Bodies of mineral soil ranging in composition from gravel to silt, commonly possessing high organic contents and often possessing reticulate-chaotic cryostructures. Interpreted as replacement deposits in previously thaw-eroded and truncated ice-wedge structures

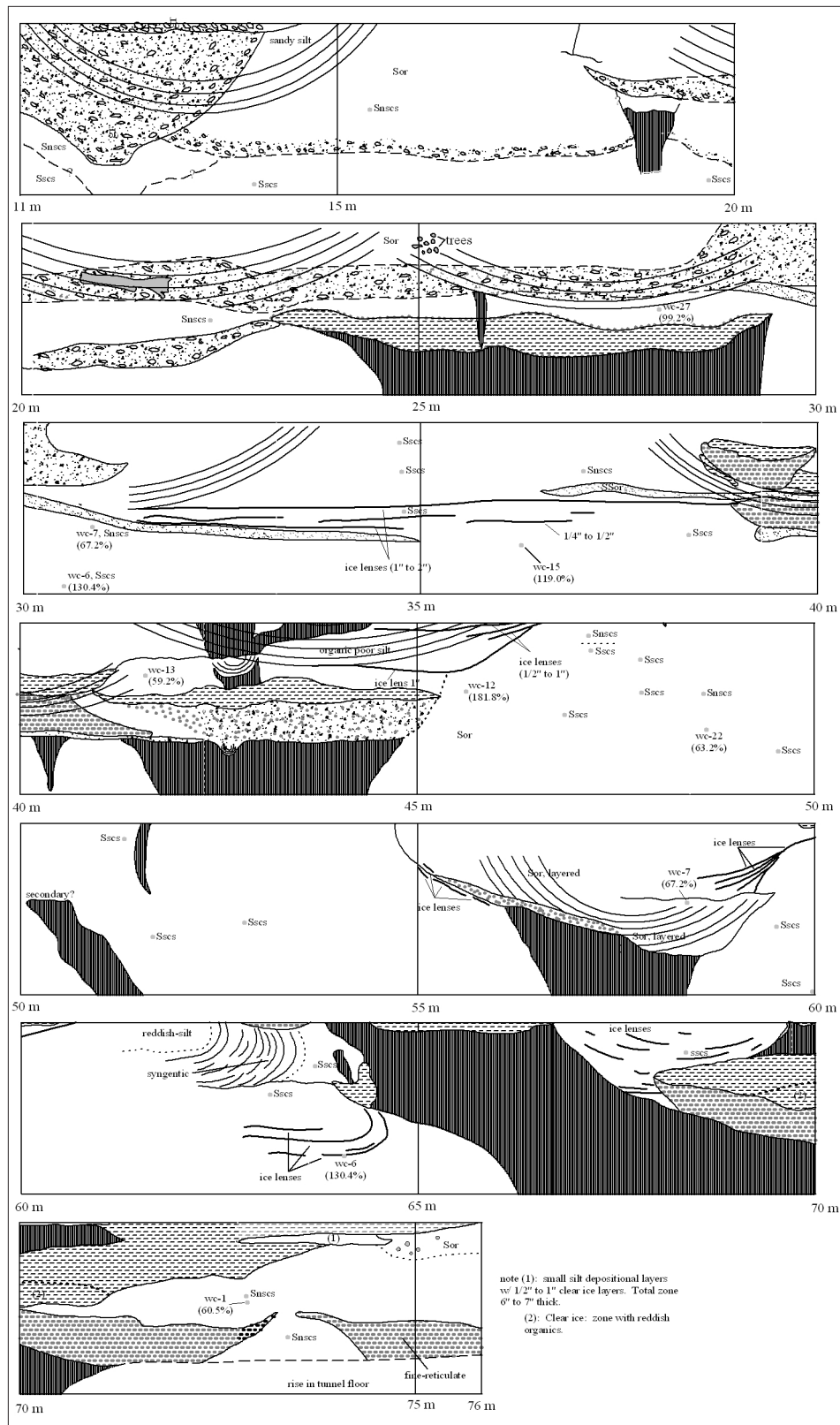


Figure 8. Cryostratigraphic map of part of the main shaft of the CRREL permafrost tunnel, left side (viewed from entrance) of the tunnel. For the legend, see figure 9 and table 1 (Bray and others, 2006).

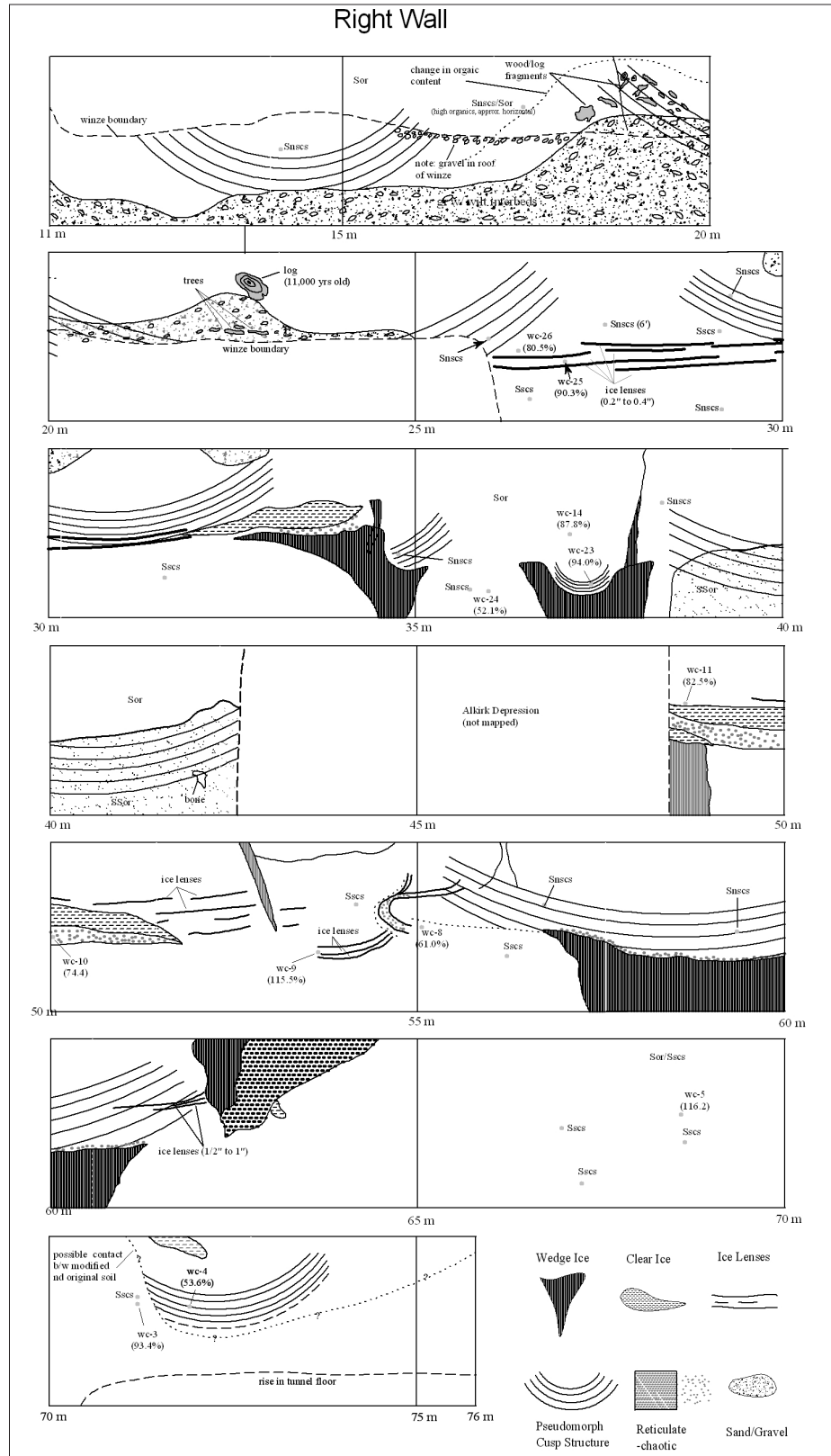


Figure 9. Cryostratigraphic map of part of the main shaft of the CRREL permafrost tunnel, right side (viewed from entrance) of the tunnel. Definitions of symbols are listed in table 1 (Bray and others, 2006).

## CRYOSTRUCTURES

Recent publications (Shur and others, 2004; Bray and others, 2006; Fortier and others, 2008; Kanevskiy and others, 2008) show the variety of cryostructures that are present in the tunnel and describe typical features related to syngenetic permafrost formation.

Four types of cryogenic structure have been identified in the tunnel (Shur and others, 2004):

1. A micro-lenticular cryostructure is the most common structure; it is formed by thin and short lenses of ice practically saturating the soil (fig. 5A). The thickness of straight and wavy ice inclusions is generally less than 0.5 mm.

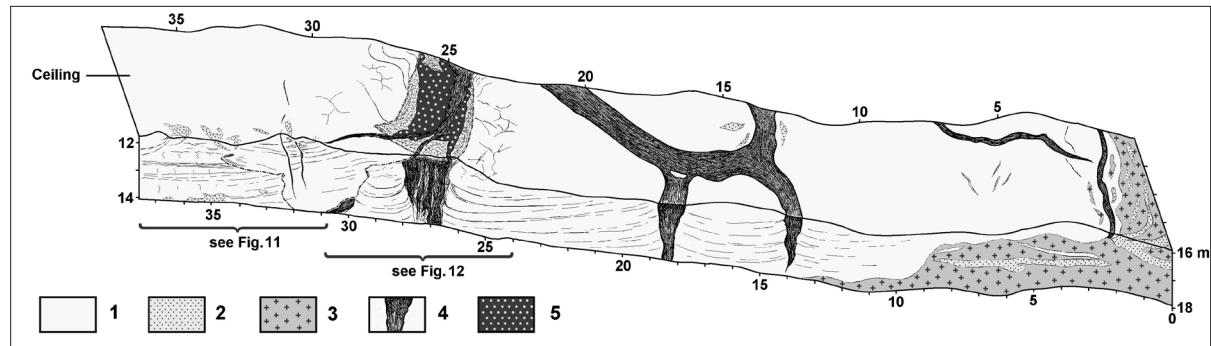


Figure 10. General view of the left wall and the ceiling of the winze. 1—silt; 2—sand; 3—Fox Gravel; 4—ice wedge; 5—thermokarst-cave ice. See figures 11 to 13 for details (Kanevskiy and others, 2008).

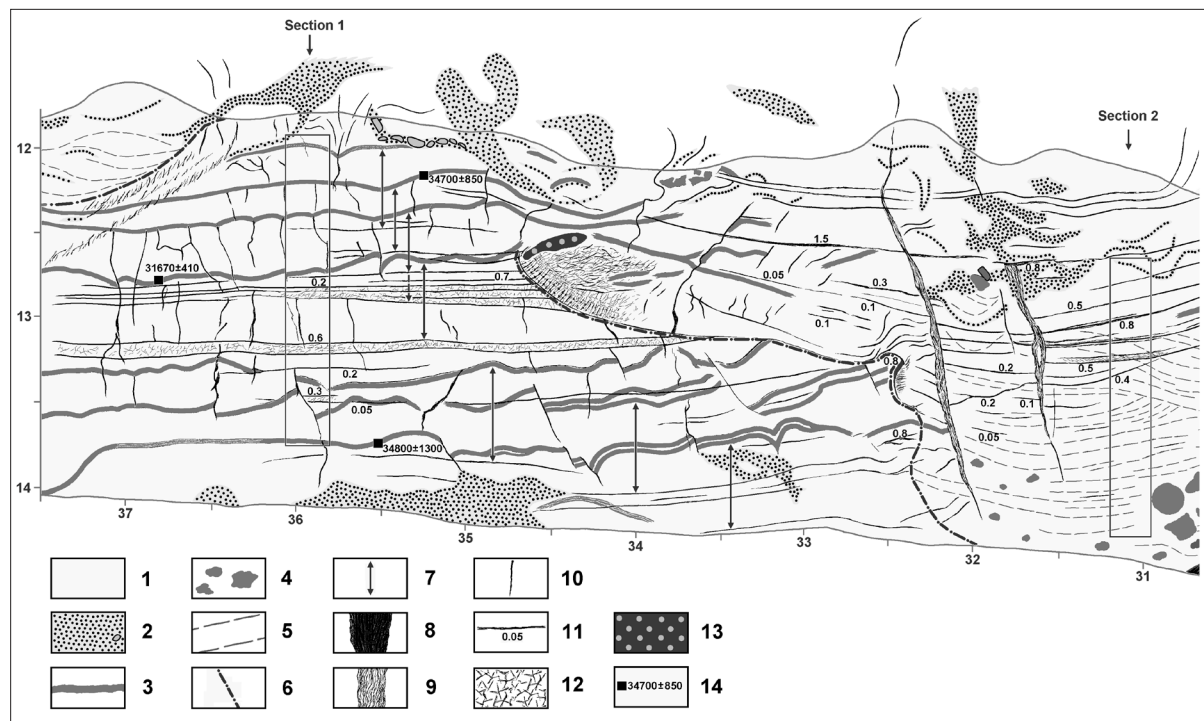


Figure 11. Cryostratigraphic map of the left wall of the winze, interval 31–37 m. 1—silt; 2—sand, gravel inclusion; 3—in situ peat layers; 4—inclusions of retransported organic matter; 5—lamination in silt; 6—erosion boundary; 7—approximate position of active layer at the periods of slower sedimentation; 8—ice wedge; 9—composite wedge (ice/silt); 10—isolated ice vein; 11—ice layer ('belt'), thickness in cm; 12—reticulate-chaotic cryostructure; 13—thermokarst-cave ice; 14—radiocarbon date, yr BP (Kanevskiy and others, 2008).

2. A layered cryostructure is represented by repeated layers of ice with thickness of between 0.2 and 1 cm. The layers form series with the spacing between layers of between 2 and 5 cm.
3. A lenticular-layered cryostructure is formed by ice lenses with a thickness from 0.5 to 1.5 mm and a length from a few millimeters to 1 cm. These lenses form continuous ice layers with soil inclusions.
4. A reticulate-chaotic cryostructure is recognized by relatively thick multi-directional ice lenses (veins), often randomly oriented (fig. 5B). This structure is interpreted as having formed following the closed-system freezing of a tálík or thaw layer.

The dominant cryostructure that can be observed in the CRREL tunnel is micro-lenticular (Shur and others, 2004), which is typical of syngenetic permafrost formation. The micro-lenticular term refers to the presence of very small, sub-horizontal (sometimes wavy), relatively short ice lenses. Usually, the thickness of uniformly distributed ice lenses (and the spacing between them) does not exceed 0.5 mm (fig. 5A). In the winze (section 1, fig. 13A), several varieties of micro-lenticular cryostructure can be distinguished (for example, latent micro-lenticular, micro-braided). Micro-lenticular cryostructures typically form more than 50–60 percent of the entire thickness of the syngenetic permafrost (Kanevskiy, 2003). Usually the micro-lenticular cryostructure is combined with a layered cryostructure. In the tunnel, gravimetric moisture content of the sediments with micro-lenticular cryostructure varies from 80 percent to 240 percent. The great variability of gravimetric moisture content of silts can be associated with existence of the several varieties of micro-lenticular cryostructure mentioned above (fig. 13A), which is typical for syngenetic permafrost, and mostly linked to different rates of sedimentation.

Certain sections of the tunnel expose bodies of clear ice, which are usually underlain by silt that exhibits a reticulate-chaotic cryostructure. This cryostructure is the most obvious type that is visible in the tunnel (Shur and others, 2004), but is not the most common cryostructure and is restricted to a few localities where it can be easily recognized by relatively thick, randomly oriented ice veins (fig. 5B). These multi-directional reticulate ice veins are thought to have formed by inward freezing of saturated sediments trapped in underground channels incised in

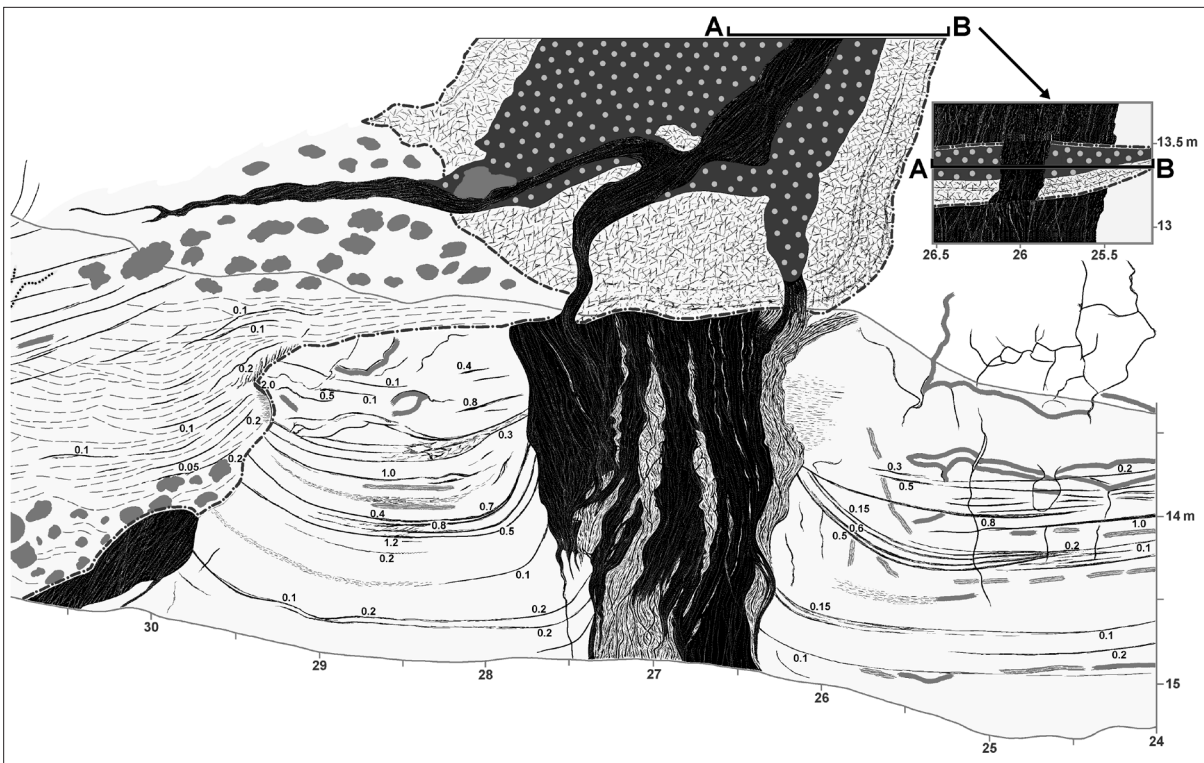


Figure 12. Cryostratigraphic map of the left wall of the winze, interval 24–31 m. For the legend, see figure 11. Segment A–B is a schematic reconstruction of vertical section through the ice pseudomorph, located at the ceiling of the winze (Kanevskiy and others, 2008).

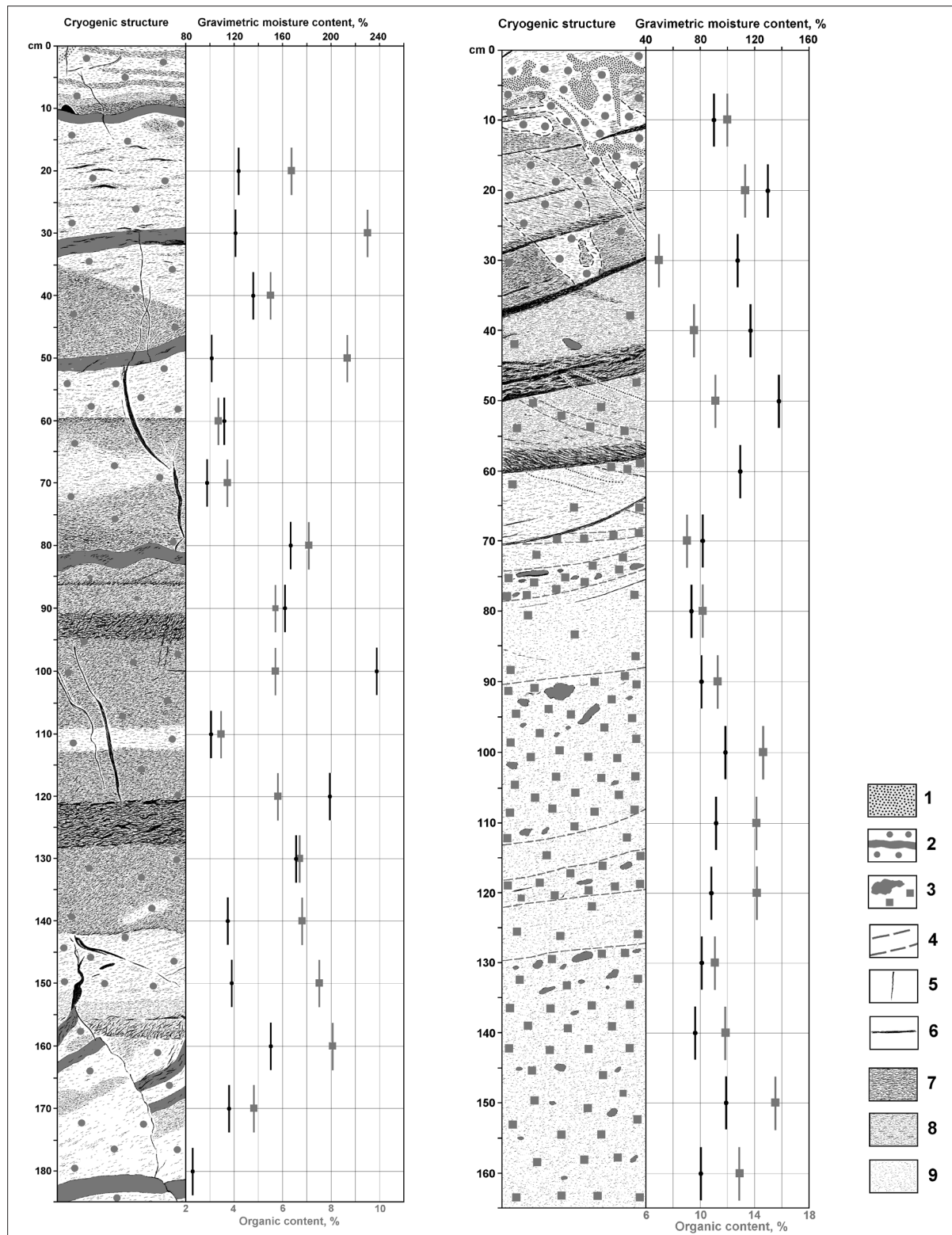


Figure 13. Details of cryogenic structure and properties of sections 1 (A) and 2 (B); location of sections is shown in figure 11. 1—sand; 2—in situ peat layer and inclusions of organic matter; 3—inclusions of retransported organic matter; 4—lamination in silt; 5—isolated ice vein; 6—distinct ice layer ('belt'); 7—micro-braided cryostructure; 8—micro-lenticular cryostructure; 9—latent micro-lenticular/porous cryostructure (Kanevskiy and others, 2008).



the permafrost by thermal erosion. They form following cessation of flow as freezing occurs in sediments either laid down in the channel floor or slumped into the channel from the sides of the gully. Formation of the reticulate-chaotic cryostructure has been reproduced in laboratory experiments (Fortier and others, 2008).

## AGGRADATION OF THE PERMAFROST TABLE

Seven thin organic horizons can be observed in the upper part of the winze at a depth of approximately 12–14 m below the ground surface (fig. 11). The AMS radiocarbon dates for organic layers vary from 31,000 to 35,000 yr BP (fig. 11). Below each peat horizon, at a depth of approximately 0.4 to 0.6 m, are distinct icy layers (so-called ‘belts’ in the Russian literature). These layers are interpreted to be the temporary positions of the former permafrost table (base of the active layer) during the time of peat accumulation. In all probability, the peat reflects an environment of slower sedimentation. The approximate positions of the active layer during these periods are indicated by arrows in figure 11.

Numerous small cracks partially filled with ice (ice veins) extend downward from the peat horizons to depths of up to 0.5 m. These cracks form polygons up to 0.5 m across. Perhaps these cracks were seasonal-frost cracks and the seasonal-ice veins were subsequently incorporated into the syngenetic permafrost.

## MASSIVE ICE BODIES

Bodies of massive ice are exposed in the walls and ceiling of the CRREL tunnel and impress the first-time visitor. These bodies are the most visible expression of the ice-rich nature of Pleistocene syngenetic permafrost. Three types of massive ice can be identified: wedge ice, clear ice, and clear ice with wedge-ice inclusions.

Many of the ice wedges in the CRREL tunnel have been thaw-modified by fluvio-thermal erosion, which promotes the formation of soil and ice pseudomorphs (see below). Figure 6 is a schematic diagram showing how thermal erosional processes may modify syngenetic permafrost.

### (a) Wedge ice

Wedge ice is the main type of massive ice in the CRREL tunnel (fig. 14), and is easy to recognize by its wedge or vertical shape and by its foliated structure. Wedge ice is grey to dark brown in color, reflecting the presence of silt particles and organic staining in the ice. The size of the wedges is difficult to quantify. Although the wedges appear to range in width from 1 to 7 m, their true width probably varies between 0.5 and 3.0 m. We stress that only the middle and lower portions of the wedges are seen in the tunnel. Wedge ice is also present in the winze section, where the wedges have an apparent width of up to 1.8 m. The apexes of wedges terminate at the stratigraphic contact between the overlying silts and the underlying alluvial gravels (fig. 10). The tunnel presents a great opportunity to see crossings of several ice wedges from inside: exposures of the wedge ice in the ceiling of the winze allow one to estimate the dimension of the ice-wedge polygons as 8–12 m across (fig. 10).

Compared to the epigenetic ice wedges commonly described from northern and central Alaska (Leffingwell, 1919; Péwé, 1966), wedges in the CRREL tunnel are average to large in size. However, compared to some of the late Pleistocene syngenetic ice wedges described from Siberia along the Yana or Kolyma rivers in northern Siberia (Dostovalov and Popov, 1966; Popov, 1973; Vasil’chuk and Vasil’chuk, 1997), or the anti-syngenetic wedges inferred from the Pleistocene Mackenzie River Delta, Canada (Mackay, 1995; French, 2007, p. 181), they appear to be average to small in size.

### (b) Clear ice

We interpret the clear ice bodies in the CRREL tunnel to be thermokarst-cave ice (Shur and others, 2004; Bray and others, 2006). In North America, this type of ice is known colloquially as ‘pool’ ice (Mackay, 1997). Ice-rich syngenetic permafrost is highly susceptible to thermal erosion that promotes the formation of subterranean channels. When these channels are finally closed by sediment, water that is ponded behind the blockage begins to freeze. This process results in formation of thermokarst-cave (‘pool’) ice. The clear ice bodies are lenticular shaped. Their visible thickness in the tunnel ranges from a few centimeters to about 2 m and their extent beyond the ceiling is not known. The largest apparent horizontal extent of this type of ice that can be viewed in the tunnel is approximately 7 m. The alternative interpretation that these clear ice bodies are buried surface, or pond, ice (Sellmann, 1967; Hamilton and others, 1988) is not supported by the cryostructures present in the tunnel.

In the winze, a horizontal body of thermokarst-cave ice crosscutting the ice wedge is exposed on the ceiling (figs. 12, 14). Ice thickness varies from 0.2 to 0.35 m; the ice body is underlain by a silt layer (0.1–0.4 m thick)



Figure 14. Photo showing ice wedge dissecting a horizontal lens of white thermokarst-cave ice (ice pseudomorph), right wall of the winze. The width of the wedge is 1 m. The thermokarst-cave ice body is underlain by several silt layers with reticulate-chaotic cryostructure. The same wedge exposed on the opposite wall of the winze is shown in figure 12. (Photo by M. Kanevskiy.)

having a reticulate-chaotic cryostructure (Shur and others, 2004; Fortier and others, 2008). This massive ice body is aligned with the width of the ice wedge, but is wider than the wedge, indicating that the initial subterranean channel eroded laterally across the ice wedge into the enclosing sediments (fig. 11, section A–B).

### **(c) Clear ice crossed by ice veins**

There are many places in the tunnel where veins of wedge ice penetrate horizontal bodies of clear thermokarst-cave ice (fig. 15). This relation demonstrates that the formation of wedge ice did not terminate when the cavity was filled with water and the water subsequently froze. Instead, it indicates that thermal-contraction cracking, ice-wedge formation, and permafrost growth continued after emplacement of the thermokarst-cave ice. The other example of where a horizontal body of thermokarst-cave ice is penetrated (crossed) by an ice wedge can be seen in the ceiling of the winze (fig. 12, section A–B).

## **THERMAL EROSION, SOIL, AND ICE PSEUDOMORPHS**

Numerous sites of former gullies and underground channels can be observed in the silty sediments at various depths. They appear to have been cut by running water and later filled with thermokarst-cave ice and soil whose structure and properties differ from the original syngenetic permafrost (Shur and others, 2004; Bray and others, 2006; Fortier and others, 2008).

The formation of thermokarst-cave ice is related to the gully erosion that must have occurred, especially during the spring snowmelt, during growth of the syngenetic permafrost on the relatively gently sloping terrain of Gold-



Figure 15. Photo showing veins of wedge ice penetrating a near-horizontal layer of thermokarst-cave ice. The location marker is 2.5 x 2.5 cm in size (Shur and others, 2004).

stream valley where the CRREL tunnel is located (Shur and others, 2004). We stress that syngenetic permafrost, composed predominantly of ice-rich silty sediments, is especially susceptible to fluvio-thermal erosion (Shur and others, 2004; Bray and others, 2006; Fortier and others, 2007). Fluvio-thermal erosion occurs when surface runoff from snowmelt, summer precipitation, or thawing permafrost becomes concentrated mainly along ice wedges, causing preferential thaw. The gullies that result typically assume an inverted ‘T’ cross-profile because water first erodes vertically and then laterally as the bed becomes armored with transported sediment. This process often leaves an organic-mat overhang. Slumping, piping and the creation of small tunnels above and adjacent to the partially eroded ice wedge are also common. Fluvio-thermal erosion, which causes thaw-modification of ice wedges, is a well known process in Arctic regions today (French, 2007, p. 191–192; Fortier and others, 2007). What is less well known is that standing water bodies sometimes accumulate in the channel floor behind slumped masses to form the ice bodies that Shumskii (1959) termed ‘thermokarst-cave ice.’

The formation of pseudomorphs is related to the thaw modification of ice wedges that also would have occurred during fluvio-thermal or underground-erosion episodes. Soil pseudomorphs are formed by silt or gravel filling the void left by the eroded ice wedge; ice pseudomorphs are formed by thermokarst-cave ice filling the void (fig. 6). These structures represent secondary infilling. Ice, sediment, or an ice-sediment mix constitute the infill. It is not surprising that the cryogenic properties of this infill material differ from the enclosing syngenetic permafrost. Formation of these structures is regarded as typical of syngenetic permafrost growth.

Both types of pseudomorphs (soil and ice) exist in the CRREL tunnel. However, they are difficult to recognize, especially ice pseudomorphs, because some have been subsequently modified by the penetration of ice veins. The incorporation of ice veins into ice pseudomorphs demonstrates that the formation of wedge ice is not terminated by the formation of thermokarst-cave ice (Shur and others, 2004). An ice pseudomorph modified by the penetration of ice veins is shown in figure 15.

Recent examination of the main adit revealed that, of 20 ice wedges identified, 19 had been subject to thermal erosion. Approximately 60 percent of the channels cutting through the ice wedges and the enclosing syngenetic permafrost were partially or entirely filled by thermokarst-cave ice (Fortier and others, 2008).

In the winze, a gully filled with sediments can be observed at interval 29–35 m (figs. 10–13). Beneath the gully is a truncated ice wedge affected by thermal erosion. The sediments filling the gully are mostly ice-poor stratified silts with lenses of sands. Soils contain numerous inclusions of organic material that are interpreted as having been reworked by water. The organic content of the sediments in the gully varies from 7 to 22.8 percent by weight and is much higher in comparison with the original permafrost (section 2, fig. 13B).

Cryostructures in the lower part of section 2 (fig. 13B, 60–165 cm) vary from latent micro-lenticular to porous (structureless). The gravimetric moisture content of this part of section 2 varies from 70 to 100 percent, which is smaller than the water content of the original syngenetic permafrost. Such water content is unusual for sediments with a very small amount of visible ice and can be attributed to the higher organic content (fig. 13B). Sediments with an organic content of 9–12 percent have a gravimetric moisture content of 70–80 percent, whereas sediments with organic content of 14–16 percent have a moisture content of 90–100 percent. The cryostructures and ice contents of the upper part of section 2 (fig. 13B, 0–60 cm) are similar to those of the original permafrost; the gravimetric moisture contents vary from 110 to 140 percent, indicating change of sedimentation mode and decrease of sedimentation rate at the last stages of gully infilling.

## ICE CONTENT

The ice content of sediments exposed in the tunnel varies widely. Although the weathered schist exposed in the lowest part of the Gravel Room contains a very small amount of visible ice, its gravimetric moisture content varies from 6.5 to 19.9 percent, averaging 11.7 percent (Hamilton and others, 1988). Gravimetric moisture content of alluvial gravel exposed in the lowest part of the winze generally is 8.9 to 10.3 percent (Hamilton and others, 1988). Typically, the gravel contains crustal cryostructures with thin ice crusts enclosing gravel clasts. Close to the contact with overlying silt the thickness of ice crusts increases, sometimes reaching 0.5–2 cm. Silt is generally ice-rich; its gravimetric moisture content varies from 39 to 139 percent (Hamilton and others, 1988).

Recent studies show that the ice content of silt strongly depends on its cryostructure. For sediments with micro-lenticular cryostructure, gravimetric moisture content in the main adit varies from 80 to 180 percent, averaging 130 percent (Bray and others, 2006). A similar range (100–240 percent) is found in the winze (section 1, fig. 13A). For modified sediments with structureless (or massive) cryostructure, which fill gullies and soil pseudomorphs, gravimetric moisture content in the main adit varies from 50 to 95 percent, averaging 69 percent (Bray and others, 2006). For similar sediments in the winze, gravimetric moisture content is 70 to 100 percent (section 2, fig. 13B, 60–165 cm). We associate the unusually high moisture content of ice-poor silt with the high content of reworked organic material in these sediments. The average gravimetric moisture content of the cross-stratified sands with structureless (or massive) cryostructure, filling underground channels, is 44.6 percent, whereas it is 107.7 percent in the surrounding permafrost with micro-lenticular cryostructure (Fortier and others, 2008). For sediments with reticulate-chaotic cryostructure, gravimetric moisture content in the main adit varies from 60 to 115 percent, averaging 85 percent (Bray and others, 2006).

## TWO SILT UNITS?

The early studies in the tunnel (Sellmann 1967, 1972; Hamilton and others, 1988) did not adequately recognize the syngenetic nature of the permafrost. Two independent systems of ice wedges and an inferred thaw unconformity that separated the silts into an upper and a lower unit were recognized (fig. 2). Some ice bodies, described as “... horizontal, saucer-shaped bodies,” and interpreted as buried frozen thaw ponds formed in ice-wedge troughs, are better explained as bodies of thermokarst-cave (“pool”) ice formed in underground channels.

There is now evidence that thermal-erosion processes were simultaneous with permafrost formation. First, the clear ice bodies are best explained as thermokarst-cave ice. Second, the ice veins that penetrate thermokarst-cave ice mean that ice wedges continued to grow after their partial thaw-modification and destruction by fluvio-thermal erosion and the subsequent pooling of water in the erosional void. Third, the dominant cryogenic structure is similar throughout the silt section. Fourth, the radiocarbon ages obtained from sediments in the tunnel do not reveal any sufficient break in sedimentation. In fact, no clear evidence of regional or widespread thermokarst can be found in the tunnel; instead, the thaw unconformities appear localized and connected with previous gullies and underground channels.

In summary, the cryostratigraphic data do not confirm the existence of two silt units divided by a continuous thaw unconformity, as described previously. Cryostructures, truncated ice bodies, and soil and ice pseudomorphs indicate a single sequence of continuous sedimentation and syngenetic permafrost aggradation in late Pleistocene time. This permafrost has been reworked by local thermal-erosional events.

## REFERENCES CITED

- Arcone, S.A., and Delaney, A.J., 1984, Field dielectric measurements of frozen silt using VHF pulses: *Cold Regions Science and Technology*, v. 9, p. 29–37.
- Bray, M.T., 2008, Effects of soils cryostructure on the long term strength of ice-rich permafrost near melting temperatures, *in* Kane, D.L., and Hinkel, K.M., eds., *Proceedings of the Ninth International Conference on Permafrost*, June 29–July 3, 2008, Fairbanks, Alaska: Institute of Northern Engineering, University of Alaska Fairbanks, v. 1, p. 183–188.
- Bray, M.T., French, H.M., and Shur, Y., 2006, Further cryostratigraphic observations in the CRREL permafrost tunnel, Fox, Alaska: *Permafrost and Periglacial Processes*, v. 17, no. 3, p. 233–243.
- Carter, L.D., 1988, Loess and deep thermokarst basins in Arctic Alaska, *in* *Proceedings of the Fifth International Conference on Permafrost: Trondheim, Norway*, Tapir publishers, p. 706–711.
- Chester, J.W., and Frank, J.N., 1969, Fairbanks placers fragmentation research, final report: U.S. Department of Interior, Bureau of Mines, Metals Program, Auth. no. L1115-33, 52 p.
- Delaney, A.J., 1987, Preparation and description of a research geophysical borehole site containing massive ground ice near Fairbanks, Alaska: Hanover, New Hampshire, U.S. Army CRREL Special Report 87-7, 22 p.
- Delaney, A.J., and Arcone, S.A., 1984, Dielectric measurements of frozen silt using time domain reflectometry: *Cold Regions Science and Technology*, v. 9, p. 37–49.
- Dick, R.A., 1970, Effects of type of cut, delay and explosive on underground blasting in frozen gravel: U.S. Bureau of Mines, Report of Investigations 7356, 17 p.
- Dostovalov, B.N., and Popov, A.I., 1966, Polygon systems of ice wedges and conditions of their development, *in* *Permafrost: International Conference Proceedings: Washington, DC*, National Academy of Sciences – National Research Council, Publication 1287, p. 102–105.
- Dubikov, G.I., 2002, Composition and cryogenic structure of permafrost in West Siberia: Moscow, Russian Federation, GEOS, 246 p. (in Russian).
- Fortier, D., Allard, M., and Shur, Y., 2007, Observation of rapid drainage system development by thermal erosion of ice wedges on Bylot Island, Canadian Arctic Archipelago: *Permafrost and Periglacial Processes* v. 18, no. 3, p. 229–243.
- Fortier, D., Kanevskiy, M., and Shur, Y., 2008, Genesis of reticulate-chaotic cryostructure in permafrost, *in* Kane, D.L., and Hinkel, K.M., eds., *Proceedings of the Ninth International Conference on Permafrost*, June 29–July 3, 2008, Fairbanks, Alaska: Institute of Northern Engineering, University of Alaska Fairbanks, v. 1, p. 451–456.
- French, H.M., 2007, *The periglacial environment*, third edition: Chichester, U.K., John Wiley and Sons Ltd, 458 p.
- Garbeil, H.M., 1983, Temperature effects upon the closure of a gravel room in permafrost: Fairbanks, Alaska, M.S. thesis, University of Alaska Fairbanks.
- Gasarov, S.S., 1963, Morphogenetic classification of cryostructures of frozen sediments: Magadan, Russia, *Trudy SVKNII*, v. 3 (in Russian).
- 1969, Structure and history of formation of permafrost in Eastern Chukotka: Moscow, Nauka, 168 p. (in Russian).
- Gravis, G.F., 1969, Slope sediments of Yakutia: Moscow, Nauka, 128 p. (in Russian).
- Hamilton, T.D., Ager, T.A., and Robinson, S.W., 1983, Late Holocene ice wedges near Fairbanks, Alaska, USA; Environmental setting and history of growth: *Arctic and Alpine Research*, v. 15, no. 2, p. 157–168.
- Hamilton, T.D., Craig, J.L., and Sellmann, P.V., 1988, The Fox permafrost tunnel; A late Quaternary geologic record in central Alaska: *Geological Society of America Bulletin*, v. 100, p. 948–969.
- Huang, S.L., Aughenbaugh, N.B., and Wu, M.C., 1986, Stability study of CRREL permafrost tunnel: *Journal of Geotechnical Engineering*, v. 112, p. 777–790.
- Johansen, N.I., and Ryer, J.W., 1982, Permafrost creep measurements in the CRREL tunnel, *in* *Proceedings of the Third International Symposium on Ground Freezing*, Hanover, New Hampshire: Hanover, New Hampshire, U.S. Army CRREL, p. 61–63.
- Johansen, N.I., Chalich, P.C., and Wellen, E.W., 1981, Sublimation and its control in the CRREL permafrost tunnel: Hanover, New Hampshire, U.S. Army CRREL Special Report 81-8, 12 p.
- Kanevskiy, M., 2003, Cryogenic structure of mountain slope deposits, northeast Russia, *in* *Proceedings of the Eighth International Conference on Permafrost*, Zurich, Switzerland, July 21–25, 2003: International, various publishers, v. 1, p. 513–518.

- Kanevskiy, M., Fortier, D., Shur, Y., Bray, M., and Jorgenson, T., 2008, Detailed cryostratigraphic studies of syngenetic permafrost in the winze of the CRREL permafrost tunnel, Fox, Alaska, *in* Kane, D.L., and Hinkel, K.M., eds., Proceedings of the Ninth International Conference on Permafrost, June 29–July 3, 2008, Fairbanks, Alaska: Institute of Northern Engineering, University of Alaska Fairbanks, v. 1, p. 889–894.
- Katasonov, E.M., 1962, Cryogenic textures, ice and earth wedges as genetic indicators of perennially frozen Quaternary deposits; *Issues of Cryology in Studies of Quaternary Deposits*: Moscow, Izd-vo AN SSSR, p. 86–98 (in Russian).
- 1969, Composition and cryogenic structure of permafrost: Ottawa, Ontario, National Research Council of Canada, Technical Translation 1358, p. 25–36.
- 1978, Permafrost-facies analysis as the main method of cryolithology, *in* Proceedings of the Second International Conference on Permafrost, July 13–28, 1973, USSR Contribution: Washington, DC, National Academy of Sciences, p. 171–176.
- Katayama, T., Tanaka, M., Moriizumi, J., Nakamura, T., Brouchkov, A., Douglas, T.A., Fukuda, M., Tomita, F., and Asano, K., 2007, Phylogenetic analysis of bacteria preserved in a permafrost ice wedge for 25,000 years: *Applied Environmental Microbiology*, v. 73, no. 7, p. 2,360–2,363.
- Lawson, D.E., 1983, Ground ice in perennially frozen sediments, northern Alaska, *in* Proceedings of the Fourth International Conference on Permafrost: Washington, DC, National Academy Press, p. 695–700.
- Leffingwell, E. de K., 1919, The Canning River region, northern Alaska: U.S. Geological Survey Professional Paper 109, 251 p.
- Linell, K.A., and Lobacz, E.F., 1978, Some experiences with tunnel entrances in permafrost, *in* Proceedings of the Third International Conference on Permafrost, Edmonton, July 10–13, 1978: Ottawa, Ontario, National Research Council of Canada, p. 814–819.
- Long, A., and Péwé, T.L., 1996, Radiocarbon dating by high-sensitivity liquid scintillation counting of wood from the Fox permafrost tunnel near Fairbanks, Alaska: *Permafrost and Periglacial Processes*, v. 7, p. 281–285.
- Mackay, J.R., 1995, Ice wedges on hillslopes and landscape evolution in the late Quaternary, western Arctic coast: *Canadian Journal of Earth Sciences*, v. 32, p. 1,093–1,105.
- 1997, A full-scale experiment (1978–1995) on the growth of permafrost by means of lake drainage, western Arctic coast; A discussion of the method and some results: *Canadian Journal of Earth Sciences*, v. 34, p. 17–33.
- Melnikov, V.P., and Spesivtsev, V.I., 2000, Cryogenic formations in the earth's lithosphere: Novosibirsk, Siberian Publishing Center UIGGM, Siberian Branch, Russian Academy of Sciences, 343 p.
- Murton, J.B., and French, H.M., 1994, Cryostructures in permafrost, Tuktoyaktuk coastlands, western arctic Canada: *Canadian Journal of Earth Sciences*, v. 31, p. 737–747.
- Pettibone, H.C., and Waddell, G.G., 1971, Stability of an underground room in frozen gravel, *in* Proceedings of the 9th Annual Engineering Geology and Soils Engineering Symposium, Boise, Idaho: Boise, Idaho, Department of Highways, p. 3–30.
- 1973, Stability of an underground room in frozen gravel, *in* Proceedings, American contribution, Second International Conference on Permafrost, Yakutsk, U.S.S.R.: Washington, DC, National Academy of Science, Publication 2115, p. 699–706.
- Péwé, T.L., 1966, Ice wedges in Alaska; Classification, distribution and climatic significance, *in* Permafrost: International Conference Proceedings: Washington, DC, National Academy of Sciences – National Research Council, Publication 1287, p. 76–81.
- 1975, Quaternary geology of Alaska: United States Geological Survey, Professional Paper 835, 145 p.
- Pikuta, E.V., Marsik, D., Dej, A., Tang, J., Krader, P., and Hoover, R.B., 2005, *Carnobacterium pleistocenium* sp. nov., a novel psychrotolerant, facultative anaerobe isolated from permafrost of the Fox Tunnel in Alaska: *International Journal of Systematic and Evolutionary Microbiology*, v. 55, p. 473–478.
- Popov, A.I., 1967, Cryogenic phenomena in the Earth crust (Cryolithology): Moscow, Moscow University Press, 304 p. (in Russian).
- 1973, Album of cryogenic formations in the Earth's crust and relief: Moscow, Moscow State University, 56 p. (in Russian).
- Popov, A.I., Rozenbaum, G.E., and Tumel, N.V., 1985, Cryolithology: Moscow, Moscow University Press, 239 p. (in Russian).
- Romanovskii, N.N., 1993, Fundamentals of cryogenesis of lithosphere: Moscow, Moscow University Press, 336 p. (in Russian).

- Sellmann, P.V., 1967, Geology of the USA CRREL permafrost tunnel, Fairbanks, Alaska: Hanover, New Hampshire, U.S. Army Cold Regions Research & Engineering Laboratory, Technical Report 199, 22 p.
- Sellmann, P.V., 1972, Geology and properties of materials exposed in the USA CRREL permafrost tunnel: Hanover, New Hampshire, U.S. Army Cold Regions Research & Engineering Laboratory, Special Report 177, 16 p.
- Shumskii, P.A., 1959, Ground (subsurface) ice, *in* Principles of geocryology, Part I, General geocryology: Academy of Sciences of the USSR, Moscow, Chapter IX, 274–327 (in Russian) (English translation: C. de Leuchtenberg, 1964, National Research Council of Canada, Ottawa, Technical Translation 1130, 118 p).
- Shur Y.L., 1988, Upper horizon of the permafrost soils and thermokarst: Novosibirsk, Nauka, Siberian Branch, 210 p. (in Russian).
- Shur, Y.L., and Jorgenson, M.T., 1998, Cryostructure development on the floodplain of the Colville River Delta, northern Alaska, *in* Proceedings of the Seventh International Conference on Permafrost, June 23–27, 1998, Yellowknife, Canada: Québec, Université Laval, p. 993–999.
- Shur, Y.L., French, H.M., Bray, M.T., and Anderson, D.A., 2004, Syngenetic permafrost growth: Cryostratigraphic observations from the CRREL tunnel near Fairbanks, Alaska: *Permafrost and Periglacial Processes*, v. 15, no. 4, p. 339–347.
- Soloviev, P.A., 1959, Permafrost of northern part of Lena–Amga plain: Moscow, Academy of Sciences of the USSR Publishing House, 144 p. (in Russian).
- Swinzow, G.K., 1970, Permafrost tunneling by a continuous mechanical method: Hanover, New Hampshire, U.S. Army Cold Regions Research & Engineering Laboratory, Technical Report 221, 37 p.
- Thompson, E.G., and Sayles, F.H., 1972, In-situ creep analysis of room in frozen soil: *Journal of Soil Mechanics and Foundation Division, ASCE*, v. 98, p. 899–915.
- Vasil'chuk, Y.K., and Vasil'chuk, A.C., 1997, Radiocarbon dating and oxygen isotope variations in late Pleistocene syngenetic ice wedges, northern Siberia: *Permafrost and Periglacial Processes*, v. 8, p. 335–345.
- Vasil'chuk, Y.K., and Vasil'chuk, A.C., 2000, AMS-dating of late Pleistocene and Holocene syngenetic ice wedges: *Nuclear Instruments and Methods in Physics Research Series B*, v. 172, p. 637–641.
- Vtyurin, B.I., 1964, Cryogenic structure of Quaternary deposits: Moscow, Nauka, 151 p. (in Russian).
- Watanabe, O., 1969, On permafrost ice: *Journal of Japanese Society of Snow and Ice*, v. 31, no. 3, p.53–62 (in Japanese, translated by CRREL).
- Weerdenburg, P.C., and Morgenstern, N.R., 1983, Underground cavities in ice-rich frozen ground, *in* Proceedings of the Fourth International Conference on Permafrost, Fairbanks, Alaska, July 17–22, 1983: Washington, D.C., National Academy Press, p. 1,384–1,389.
- Wooler, M.J., Zazula, G.D., Edwards, M., Froese, D.G., Boone, R.D., Parker, C., and Bennett, B., 2007, Stable carbon isotope compositions of eastern Beringian grasses and sedges; Investigating their potential as paleoenvironmental indicators: *Arctic, Antarctic and Alpine Research*, v. 39, no. 2, p. 318–331.
- Zhestkova T.N., 1982, Formation of the cryogenic structure of ground: Moscow, Nauka, 209 p. (in Russian).

This page was intentionally left blank.



## Site 14: Sheep Creek Thaw Pond: Thermokarst Lakes and Methane Emissions

Katey Walter Anthony<sup>1</sup> and Laura Brosius<sup>1</sup>

### SITE DESCRIPTION

This site provides an example of a thermokarst (thaw) pond. From the edge of the pond on a still summer day, one can see methane bubbling from active seeps and causing ripples in the water surface. Dead standing trees in the pond and along the thermokarst margins of the pond indicate that, in the recent past, degradation of permafrost led to melting of ice wedges and subsidence of the ground surface as the pond expands. This area is perennially frozen. Thermokarst lakes and ponds lie in broad lowland valleys underlain by retransported silt of late Quaternary origin. The silt is relatively organic, typically dated to 20,000–40,000 yr BP, and forms the valley-bottom facies of Péwé's Goldstream formation (Péwé, 1975).

### Parking

Parking is available in the pullout on the western side of Sheep Creek Road, at the intersection with the connector road to the Parks Highway. From the parking area, cross the road, and follow the bike path northward. Look for a large pond on the east side of the bike path.

### ARTICLE

In some permafrost-dominated regions of the North, thermokarst (thaw) lakes occupy as much as 22–48 percent of the land surface and are major sources of methane, a potent greenhouse gas. Thermokarst lakes form when permafrost thaws, ice melts, and the ground surface subsides. Thermokarst ponds can initiate naturally, in response to climate warming and wetting or in response to both natural (for example, wildfire) or human-caused disturbance (such as road construction). Once initiated, small thermokarst ponds can grow rapidly into large lakes, on time scales of decades to centuries, as a result of thermal and mechanical erosion processes. This thermokarst expansion leads to the release of organic matter previously sequestered in permafrost in anaerobic lake bottoms,



Left: Early winter survey for methane bubbles on lake ice near Chena Ridge, Fairbanks, Alaska; photo by K. Walter Anthony, 2007.



Right: Methane bubbling seeps along the margin of a thermokarst lake in Goldstream Valley, Fairbanks, Alaska; photo by K. Walter Anthony, 2007.

<sup>1</sup>Water & Environmental Research Center, P.O. Box 755960, University of Alaska, Fairbanks, Alaska 99775-5960-5960

providing an organic matter substrate for decomposition by microbes and production and emission of methane. Methane is a potent greenhouse gas, 25 times stronger than CO<sub>2</sub> on a per-molecule basis (IPCC, 2007). Radiocarbon ages of methane bubbles released from thermokarst lakes in the retransported loess valleys of the Fairbanks area range from 12,000 to 28,000 yr B.P. (Walter and others, 2008; Brosius, 2010), demonstrating the important contribution of this ancient permafrost-locked source of organic matter. Modern terrestrial and aquatic ecosystems also contribute organic matter to methanogens. The balance of <sup>14</sup>C-depleted permafrost organic matter versus organic contributions from modern ecosystems in fueling methane production from thermokarst lakes is the subject of ongoing research (Brosius, 2010; Walter and others, 2008–2011 research). Methane bubbling rates are measured with bubble traps and gas collected for geochemical and isotopic analyses to help constrain processes controlling methane production and emission from thermokarst lakes. In winter, researchers map methane bubbles trapped in lake ice, to estimate whole-lake emissions and relate emissions to rates of permafrost thaw.

## REFERENCES

- Brosius, L., 2010, Investigating controls over methane (CH<sub>4</sub>) production and bubbling from Alaskan lakes using stable isotopes and radiocarbon ages: Fairbanks, Alaska, M.S. thesis, University of Alaska Fairbanks.
- Intergovernmental Panel on Climate Change (IPCC), 2007, Climate change 2007; The physical science basis, *in* Solomon, Susan, Oin, Dahe, Manning, Martin, Marquis, Melinda, Averyt, Kristen, Tignor, M.M.B., Miller, H.L. Jr., and Zhenlin, Chen, eds., Contribution of Working Group I to the Fourth Assessment Report of the Intergovernmental Panel on Climate Change: United Kingdom, Cambridge University Press, 996 p.
- Péwé, T.L., 1975, The Quaternary geology of Alaska: U.S. Geological Survey Professional Paper 385, 145 p.
- Walter, K.M., Chanton, J.P., Chapin, F.S., III, Schuur, E.A.G., and Zimov, S.A., 2008, Methane production and bubble emissions from arctic lakes—Isotopic implications for source pathways and ages: *Journal of Geophysical Research*, v. 113, G00A08, doi:[10.1029/2007JG000569](https://doi.org/10.1029/2007JG000569).
- Walter, K.M., Principal Investigator, and others, 2008–2011, “Understanding the impacts of permafrost degradation and thermokarst lake dynamics in the Arctic on carbon cycling, CO<sub>2</sub> and CH<sub>4</sub> emissions, and feedbacks to climate change”: Project data collected for National Science Foundation, International Polar Year Project IPY 07-536, Award 0732735, University of Alaska Fairbanks Institute of Arctic Biology.

# **PART II**

---

## **Permafrost Features in Caribou-Poker Creeks Research Watershed (CPCRW) and Environs of Fairbanks Alaska**



# Permafrost Features in Caribou–Poker Creeks Research Watershed (CPCRW) and Environs of Fairbanks, Alaska

Kenji Yoshikawa<sup>1</sup>, Vladimir Romanovsky<sup>2</sup>, Les Viereck<sup>3</sup>, and Larry Hinzman<sup>4</sup>

---

## SUMMARY OF STOPS

- Pearl Creek Elementary School Permafrost/Active Layer Monitoring Site (active layer, permafrost temperature)
- Goldstream Creek tussock tundra (permafrost condition and Holocene ice wedge)
- O'Connor Creek pingo site open system pingo
- Fox gold mining site permafrost outcrop (Pleistocene ice wedge)
- Chatanika (gold mine and convection heat transfer)
- Caribou–Poker Creeks Research Watershed oil spill experiments: Oil Spill and Frost Fire Experiments
- Aufeis (Icing) and permafrost hydrology
- Isabella Creek bog lake

## INTRODUCTION

### Soil and Permafrost

Most of interior Alaska's boreal forest is underlain by discontinuous permafrost; the discontinuous nature of its distribution creates a complex interrelation between permafrost and vegetation in this region (fig. 1). Permafrost thickness varies in this area from 0 to 150–200 m (Brown and others, 1997) with the most typical thickness between 20 and 120 m. Lateral continuity of the perennially frozen layer changes from practically continuous (90–95 percent) in the southern foothills of the Brooks Range to discontinuous (50–90 percent) in interior Alaska and in most of the Alaska Range, to sporadic (10–50 percent) and isolated patches (0–10 percent) south of the Alaska Range, Talkeetna, and Wrangell Mountains (Brown and others, 1997). The temperature of the permafrost is the most important indicator of its stability. The closer the temperature is to 0°C, the more susceptible permafrost is to surface disturbances. In interior Alaska, permafrost temperature varies seasonally in the upper 3–15 m; therefore, the temperature at the depth of zero seasonal amplitude is usually used to describe the thermal state of permafrost. Permafrost temperatures in Alaska's boreal forest are 0° to -4°C and typically warmer than -2°C (Osterkamp and Romanovsky, 1999). Other natural factors that influence permafrost temperature include the thickness, thermal properties, and duration of the snow cover (Romanovsky and Osterkamp, 1995). The mean annual ground-surface temperatures are usually 3–6°C warmer than the mean annual air temperatures. As a result of relatively warm air temperatures and the effect of snow cover in reducing winter heat loss from soil, the mean annual ground-surface temperatures in the Alaska boreal forest often exceed 0°C and can be as high as 4°C.

## STOP 1: PEARL CREEK ELEMENTARY SCHOOL PERMAFROST/ACTIVE-LAYER MONITORING SITE

### Permafrost monitoring K–12 outreach program

The purpose of this project is to establish long-term permafrost monitoring sites adjacent to schools in the circumpolar permafrost region (fig. 2). Permafrost is one of the important indicators used to monitor climate change. Change in permafrost conditions also affects local ecosystems and hydrological regimes, and may trigger certain natural disasters such as landslides. This long-term permafrost observatory is valuable not only for contemporary and future scientific objectives, but it also can benefit students and teachers in urban and remote village schools. Most remote villages depend on a subsistence lifestyle and will be directly affected by changing climate and permafrost degradation. Monitoring the permafrost temperature in the Arctic to develop a better understanding of the spatial distribution and thermal condition of permafrost, and having students participate in collecting the data, is an ideal International Polar Year (IPY) project. The University of Alaska Fairbanks (UAF) outreach project involves drilling

<sup>1</sup>Institute of Northern Engineering, University of Alaska, PO Box 755910, Fairbanks, Alaska 99775-5910; [kyoshikawa@alaska.edu](mailto:kyoshikawa@alaska.edu)

<sup>2</sup>Geophysical Institute, PO Box 757320, University of Alaska, Fairbanks, Alaska 99775-7320

<sup>3</sup>Deceased 08/31/2008

<sup>4</sup>Director, International Arctic Research Center, PO Box 757340 Fairbanks, Alaska 99775-7340

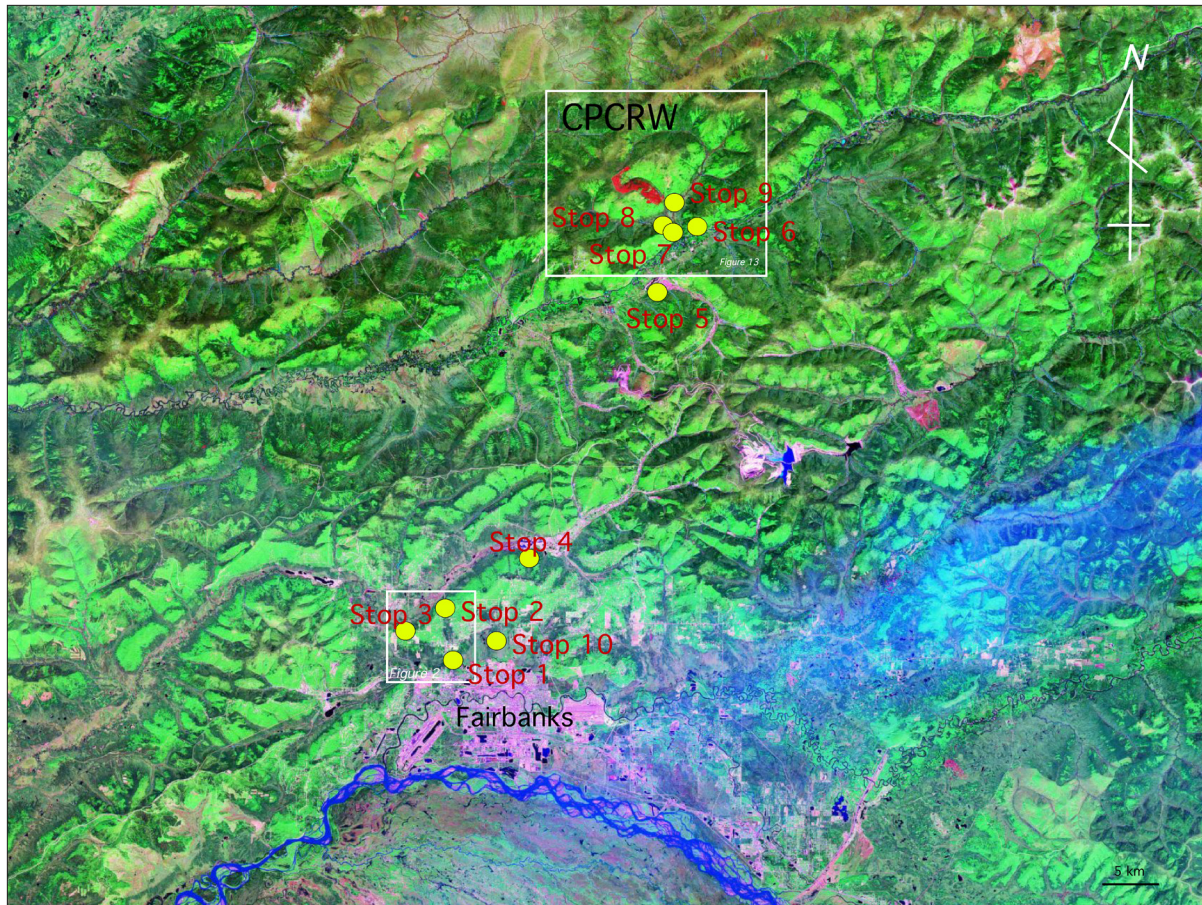


Figure 1. Index map (Landsat image) showing stops during field trip.

boreholes at schools throughout Alaska and western Canada and installing a micro-datalogger with temperature sensors to measure hourly air and permafrost temperatures. Trained teachers help students download data several times a year and discuss the results in class. The data gathered from these stations are shared on the internet ([www.uaf.edu/permafrost](http://www.uaf.edu/permafrost)) and can be viewed by anyone (fig. 3). Using the internet, teachers can also compare their data with data from other monitoring stations.

This project is becoming a useful science project for remote villages, which tend to have limited exposure to science. The National Science Foundation (NSF) funded the preliminary outreach program through UAF. Currently NSF, NASA (National Aeronautics and Space Administration), and the IPY program support this project. The broader impacts of this project are to: (1) provide opportunities for field experience and educational participation at levels ranging from elementary school to high school; (2) provide a high-resolution characterization of the spatial distribution of the thermal state of permafrost, especially in Alaska; and (3) assist in improving the general knowledge of Earth's climatic patterns and provide the opportunity for younger generations to understand the climatic systems. These data and on-line Q&A resources help students improve their understanding of the relation between permafrost conditions and the arctic climate system. In addition to being a strong outreach program to support village science education, the datasets from this project will establish a baseline for future permafrost monitoring investigations.

### Ground-temperature transects

Permafrost temperatures in this region are strongly affected by their slope and aspect. In general, south-facing slopes lack permafrost, and permafrost is usually present on north-facing slopes and in valley bottoms. A series of shallow boreholes were drilled from UAF to Goldstream Creek (figs. 4 and 5). Permafrost temperature in the boreholes varies between  $-1^{\circ}\text{C}$  and  $-0.17^{\circ}\text{C}$ , depending on the site. We estimated the freezing (thawing) point of the local Fairbanks silt to be  $-0.17^{\circ}\text{C}$ . The difference in temperatures of the observed thawing soil (with depressed

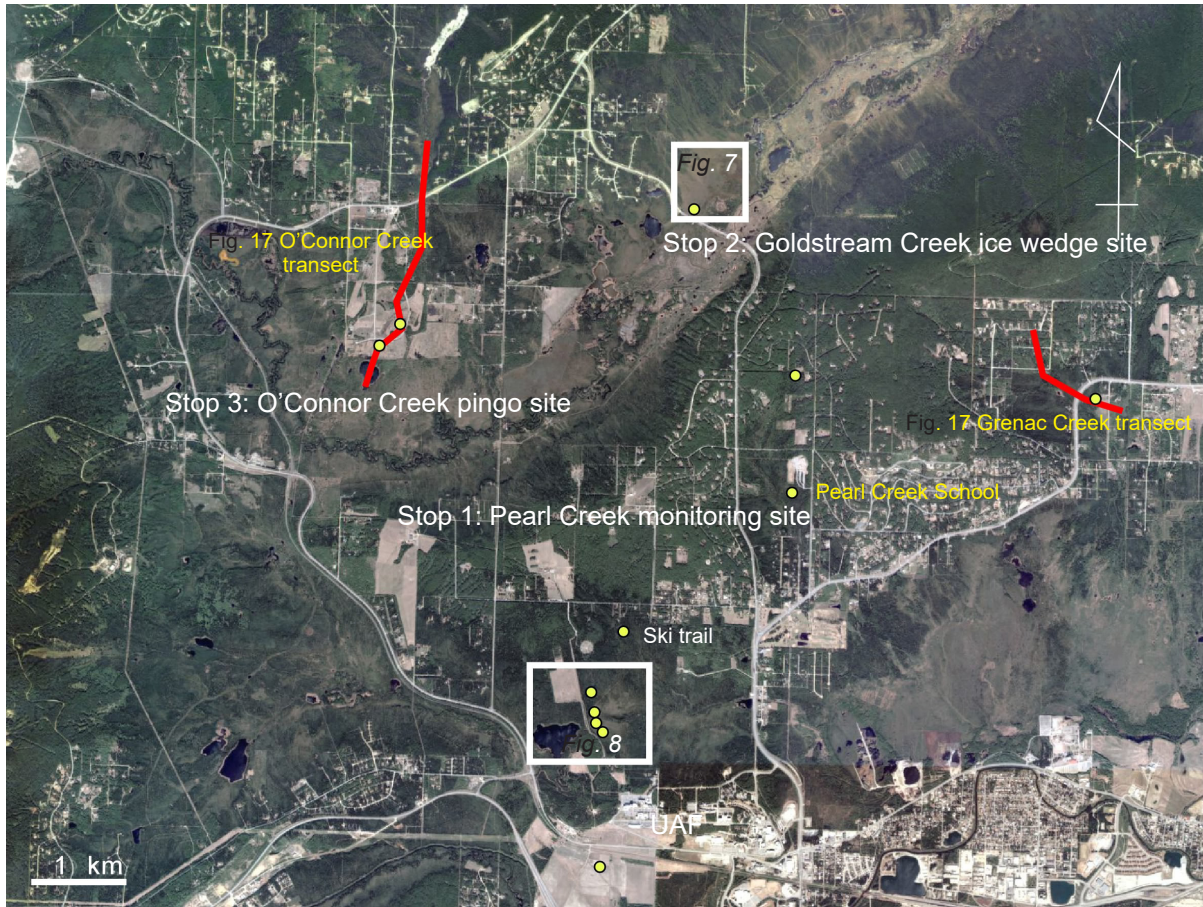


Figure 2. Aerial photograph of first three field stops: Pearl Creek, Goldstream Creek, and O'Connor Creek.

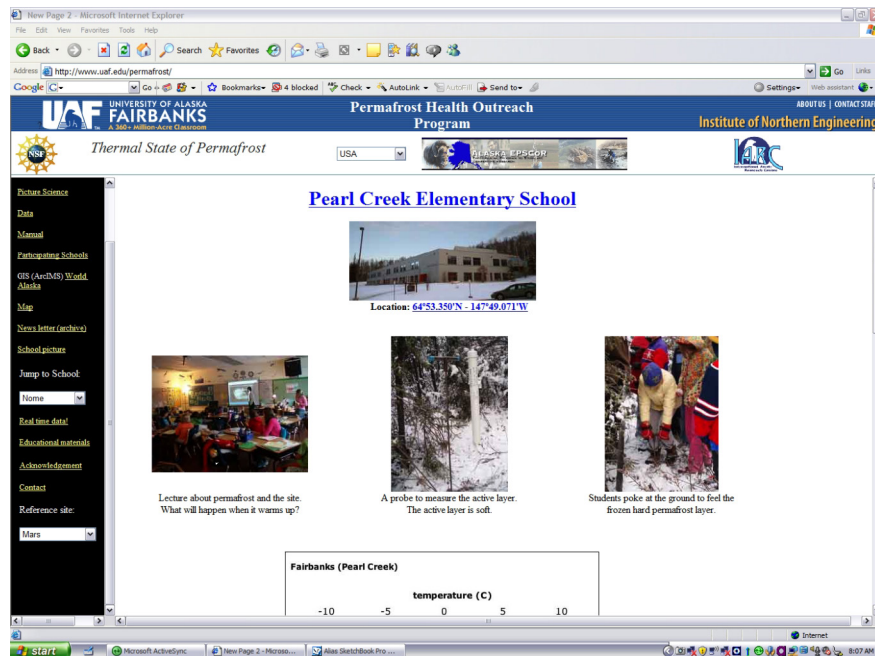


Figure 3. The permafrost data collected at participating schools are available via an internet-based data server. Most of the schools have 5 m boreholes and record temperatures on a 1-hour interval. More than 150 village schools now participate.

thaw point of  $-0.17^{\circ}\text{C}$ ) and thawing free water results from both solutes in the soil water and the matrix potential of the fine-grained soils. The active-layer thickness was measured at UAF and in the Pearl Creek area; thaw depths increased during the last 30 years (fig. 6).

## STOP 2: GOLDSTREAM CREEK

### HOLOCENE ICE WEDGE AND GROUND TEMPERATURE TRANSECTS

Although the frost-contraction process is generally inactive in the Fairbanks area in our current climate, active ice-wedge polygons can be observed in the Goldstream Creek valley (fig. 7). Many of these ice wedges developed 32,000–39,000 yr BP (MIS-3), however, Holocene (current) ice wedges are also present (Boike and Yoshikawa, 2003). Frost-contraction cracking still occurs approximately every 10 or more years, particularly during low-snow winters (figs. 8 and 9) in areas that have substantial microtopography, such as well-developed tussocks.

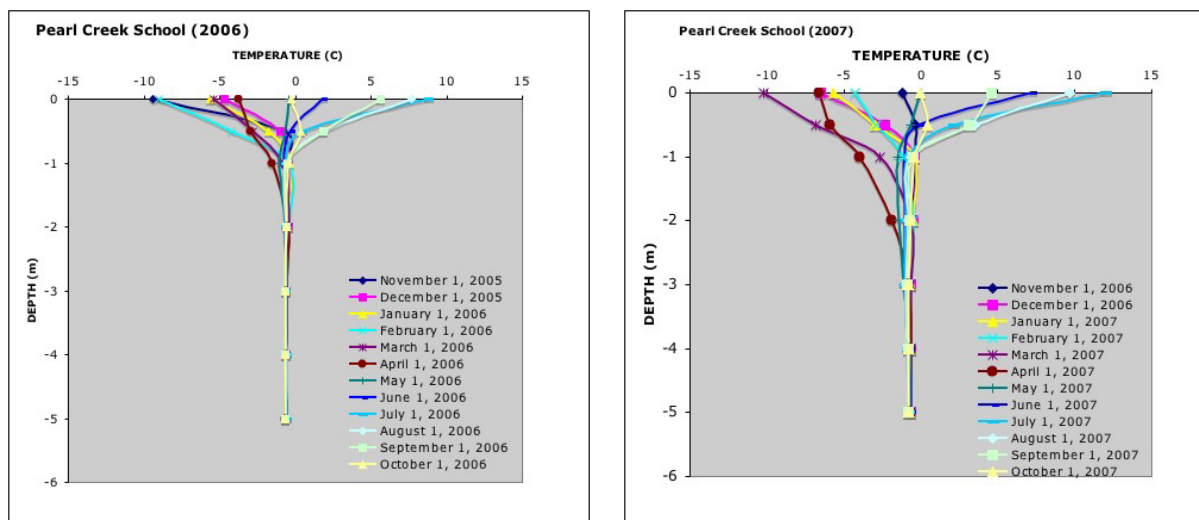


Figure 4. Monthly ground temperatures from the Pearl Creek school site. The spring of 2007 was extremely cold ( $-40^{\circ}\text{C}$ ), affecting April ground temperature.

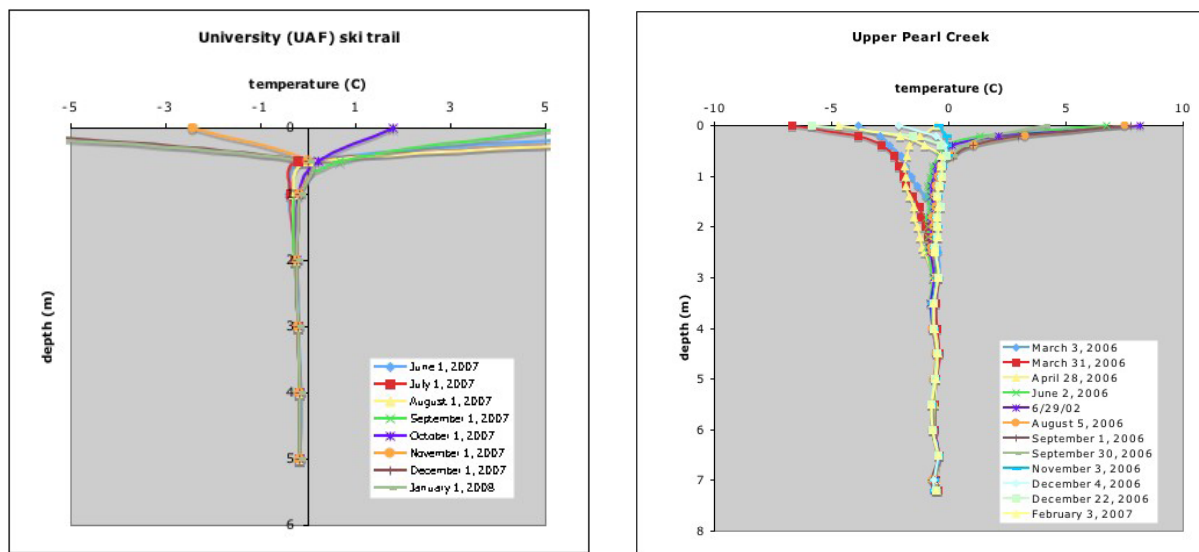


Figure 5. Monthly ground temperatures from University of Alaska Fairbanks (UAF) ski trail and upper Pearl Creek sites. The permafrost temperature at the UAF ski trail site is close to thawing ( $-0.17^{\circ}\text{C}$ ).



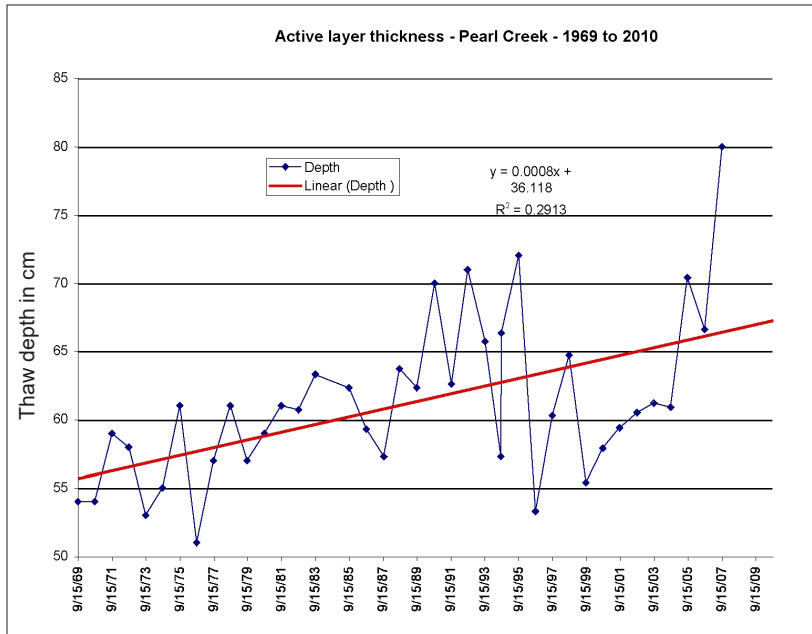


Figure 6. Active-layer thickness during the last 30 years at upper Pearl Creek site. The thaw depths of 1996 and 1999–2002 are similar to the 1970s, otherwise we can see a clear increasing trend. These permafrost temperatures are very close to the thawing point and there is significant unfrozen water in the soil.

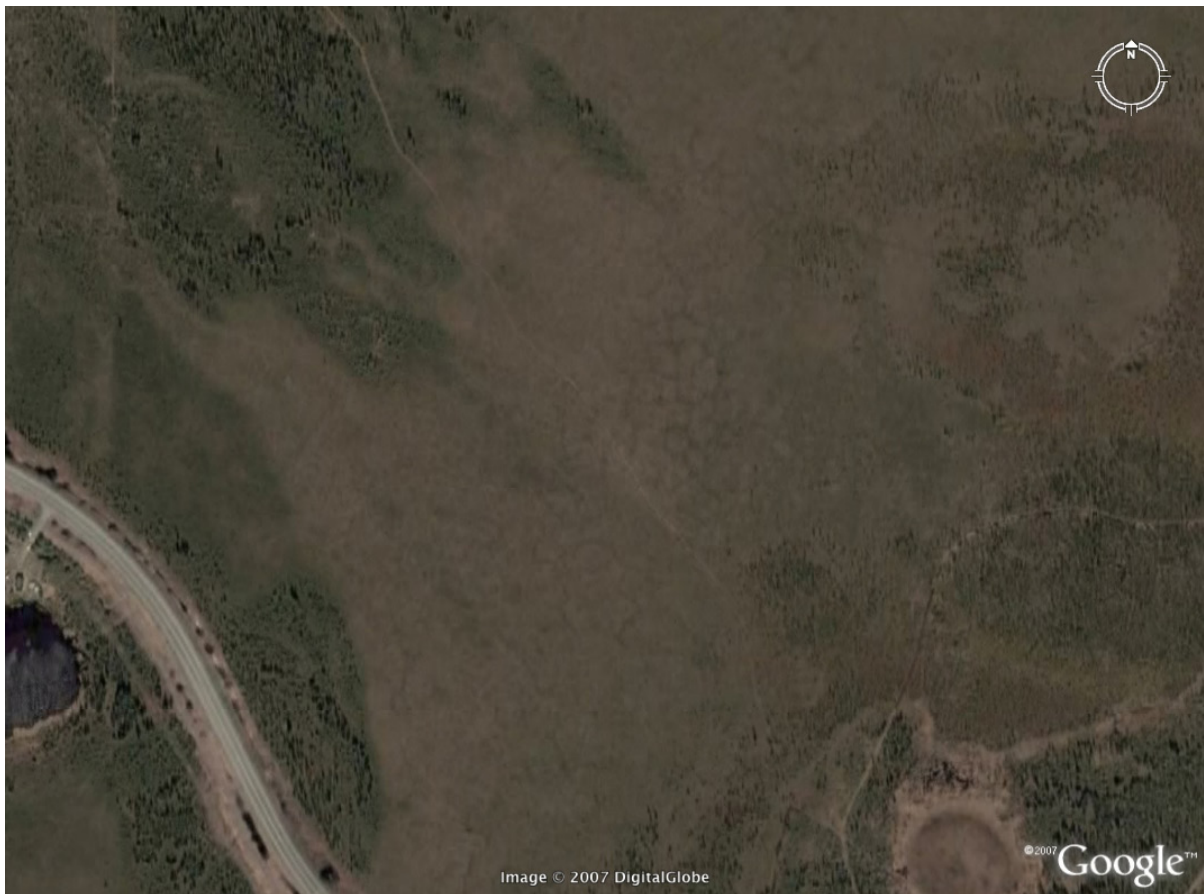


Figure 7. Ice-wedge polygons are present at the bottom of Goldstream Creek valley. These ice wedges crack because of thermal contraction during low-snow winters.

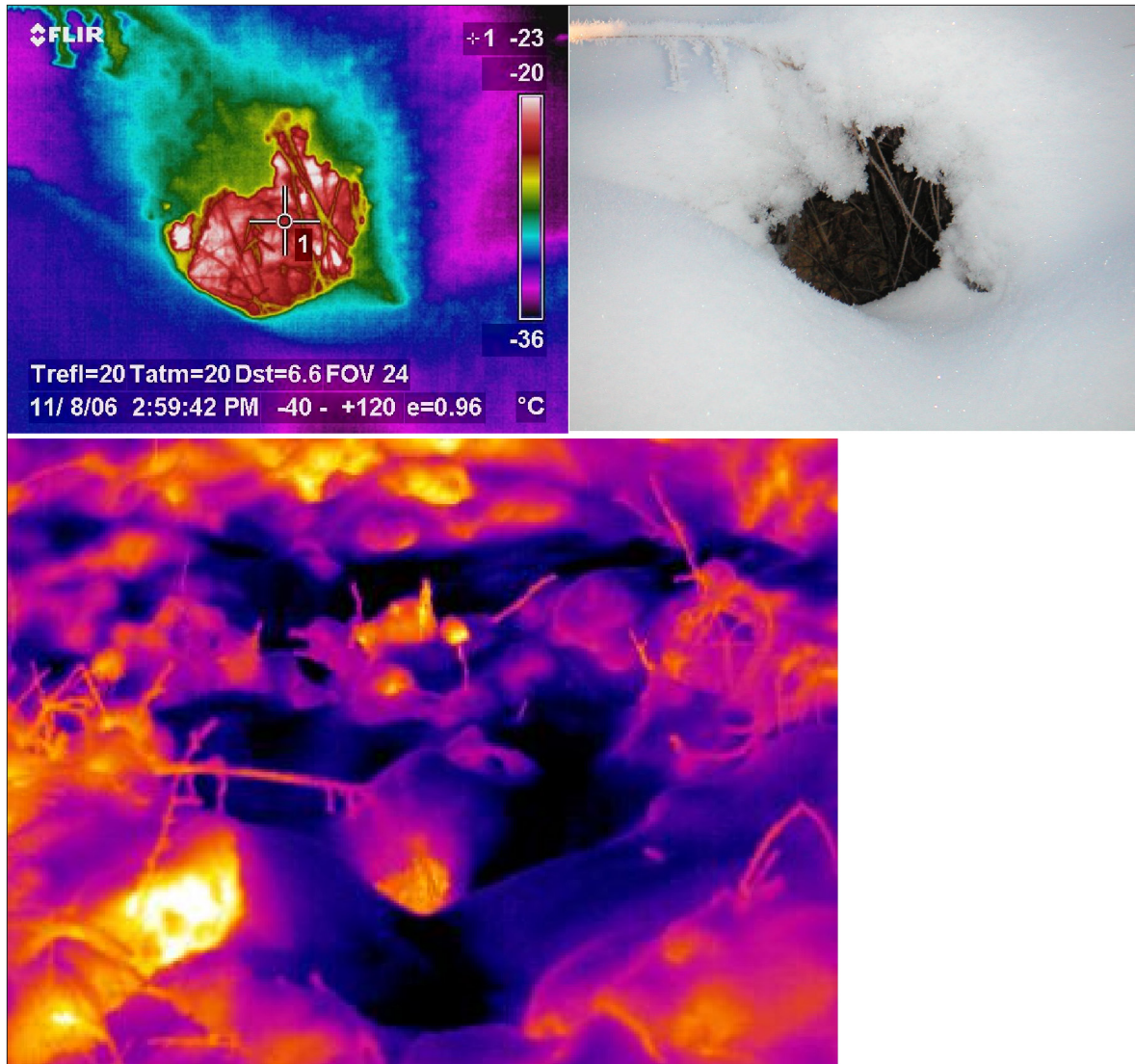
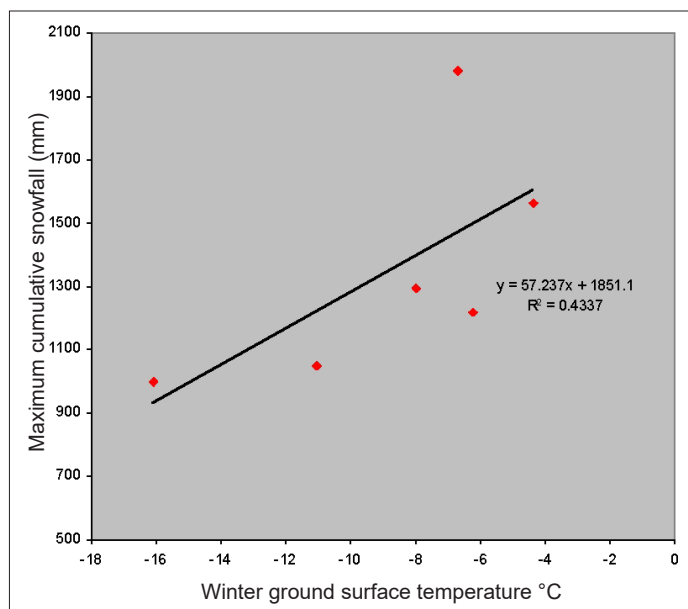


Figure 8 (above). A thermal infrared camera captured an image of the warm sub-snow terrain in early winter (a and c) (November 8, 2006). Condensation was observed at the warm air output (b). This process, which only occurs during low-snow winters, partially exposed the tussocks and enhanced thermal gradients.

Figure 9 (right). Greater snow depths provide more insulation and yield warmer ground temperatures, particularly if snow falls early in the winter. .



### Non-conductive heat transfer in tussock tundra

The stability of regions of discontinuous permafrost is strongly controlled by soil type and the physical and thermal properties of the surface of the active layer. In general, the organic-rich (peat or moss) layer increases the stability of permafrost, perhaps to the extent that the mean annual ground-surface temperature may be positive, from the effect of the thermal offset (Gold and others, 1972). Thermal offset is the process whereby more heat may escape from the active layer in the winter than enters the soil in the summer because of the difference between frozen and unfrozen thermal conductivity of the surface soil. Non-conductive heat transfer is also a very important process that influences permafrost stability.

Most areas in the lower (southern) boundary of mountain permafrost are occupied by rock glaciers or frozen block slopes. Rock glaciers or block slopes have maximum pore space available for convective heat transfer during winter and protection from sun radiation during summer months. Sawada (2003) found permafrost in Hokkaido Island, Japan; the permafrost formed under block slopes as a result of convective heat flow. Woodcock (1974) reported 14 m of permafrost at the summit of Mauna Kea, Hawaii, despite a mean annual ground-surface temperature of +1.2°C. Permafrost or massive ice bodies have been observed in many warm (positive ground-surface temperature) locations due simply to the site-specific heat-transfer process that is enhanced by convection during the winter but diminished during the warmer period. Goering and Kumar (1996) designed a roadbed that promotes winter convection in open, graded embankments for cooling of unstable permafrost. The road embankments are cooler than the surrounding ground during winter periods, driven by convective heat transfer as the cold, dense air circulates in the pore space. During the summer, the surface is warmer and convective heat transfer is minimal as the warmer, less-dense air mass in the pore space does not sink. This structure is commonly used in cold region engineering designs today, such as the Tibet–Qinghai railway.

Tussock tundra is common vegetation observed in interior, western, and northern Alaska. Tussocks develop as earth-hummock mounds (50 cm diameter) with relatively deep (20–50 cm) gaps sometimes filled with standing water. This microtopography produces surfaces that are very difficult for people to traverse. Tussock tundra also experiences cooling by non-conductive heat transfer (table 1). Cooling is enhanced by convective heat transfer during winter months (fig. 8), evapotranspiration during the summer, and blocking of direct solar radiation by the rough surface of the tussock vegetation.

*Table 1. Surface roughness and physical conditions of four study sites*

	Depth (m) of the temperature	Average temperature °C	Minimum temperature °C	Maximum temperature °C	Surface roughness (rms)
Mixed forest	3.00 m	-0.75	-1.59	-0.44	ND
Closed spruce	2.96 m	-1.74	-3.89	-0.79	3.78
Open spruce	3.00 m	-0.39	-0.47	-0.35	4.59
Tussock	2.80 m	-4.11	-9.22	-1.26	8.95

ND = no data

### STOP 3: O'CONNOR CREEK PINGO SITE

Five small, open-system pingos are located near O'Connor Creek, close to the toe of an alluvial fan. These pingos are among the oldest research pingos in Alaska. In the 1950s, Troy Péwé named these pingos, from largest to smallest, as alpha, beta, and gamma (Péwé, 1982).

Alpha pingo is an elliptical mound about 100 m long, 60 m wide, and 10.4 m high. The pingo has a breached crater ~6 m deep in the center. Most of the pingo's overburden is composed of dry silt. Active-layer thickness is 1–3 m. Pingo ice was present from 6 to 10 m below the ground surface, including organic layers (fig. 10). The area surrounding the pingos was originally home to black spruce, muskeg, and bog that were cleared for farming. Ground temperature at Alpha pingo is close to the thawing point (fig. 11).

Beta pingo is about 120 m to the northeast of Alpha pingo, is about half the size, and it has no depression in the center. On the south side, which is steep and slumping, growing trees are deformed and several have split trunks. However, the mounds have been relatively stable for more than 40 years (fig. 12). Some of the old benchmarks that Péwé and a student installed in September 1964 still exist without deformation.

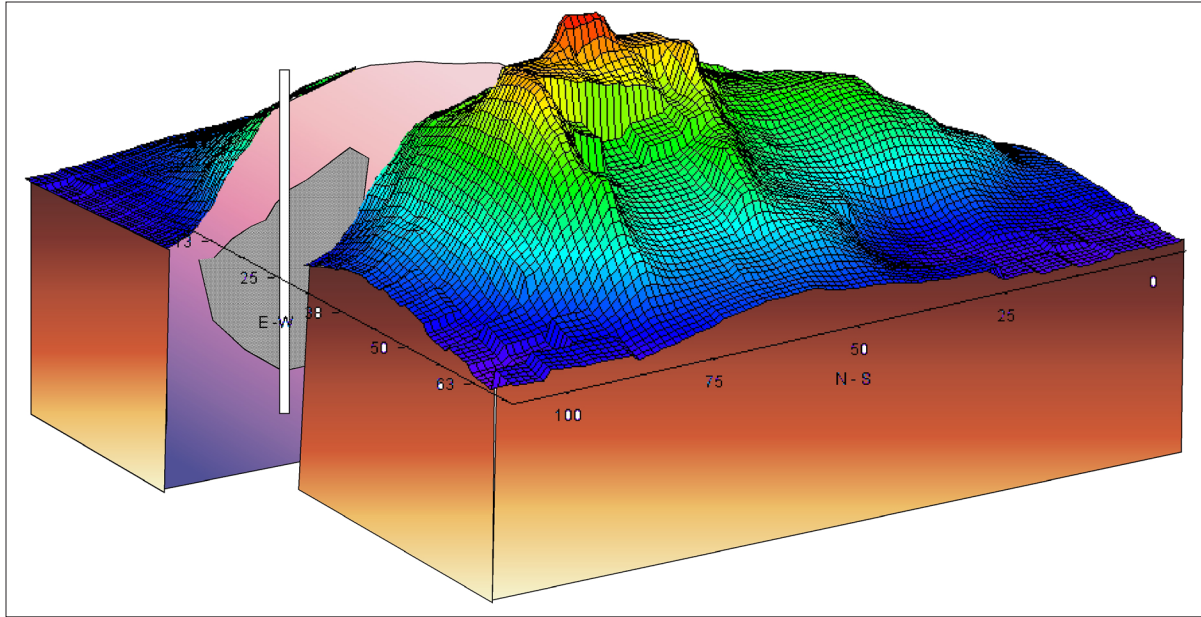


Figure 10. Sketch of Alpha pingo viewed from the northwest side. A massive ice core is present at 6–10 m depth on the north side of the pingo (drilled by Yoshikawa in 2005).

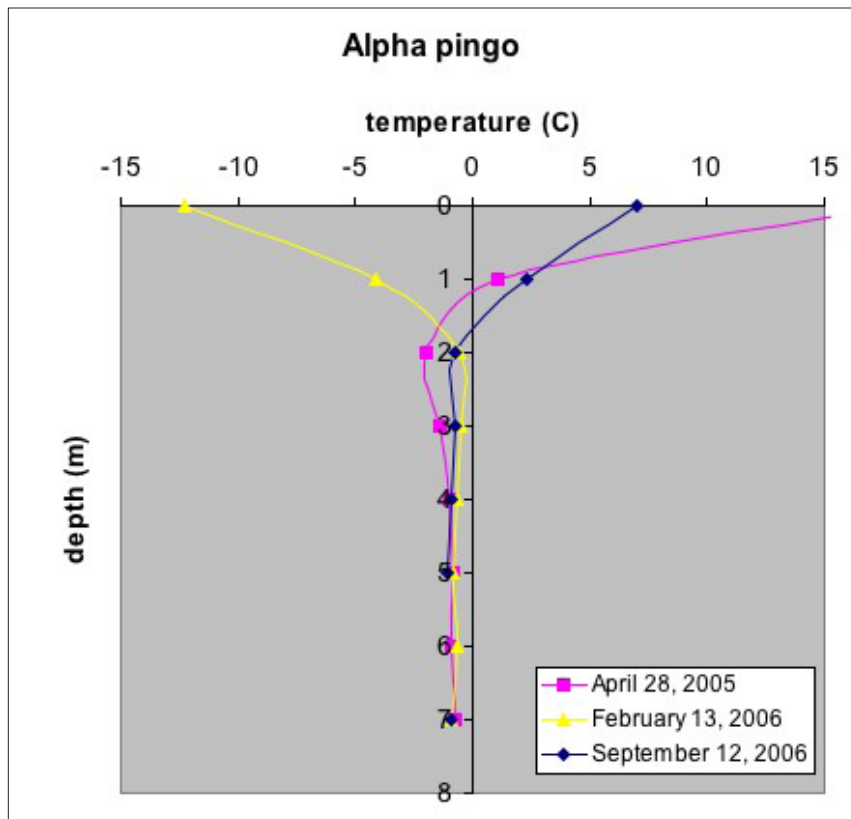


Figure 11. The temperature profile at Alpha pingo displays stable cold temperatures below 2 m. A massive ice core is present between 6 and 10 m depth.



Figure 12. South-facing slope of Beta pingo (but may be palsa near the ice structure drilled by Yoshikawa). Photo at top taken in 1965 by D. Hopkins; photo below taken in 1998 by K. Yoshikawa.

In a nearby drill hole, the silt is 27 m thick and overlies 15 m of creek gravel. The permafrost is 43 m thick. The hydraulic potential of the pingos and the nearby alluvium deposits is high ( $>68\text{kPa}$ ), creating artesian conditions. Most homeowners in the area have installed groundwater wells for domestic use. Heating the well to prevent freezing by the permafrost is critically important and risky work. Permafrost is near the thawing point ( $>-1^\circ\text{C}$ ) and subpermafrost groundwater is close to the freezing point. Groundwater leaking around the outside of the well casing is a typical problem in artesian wells. In some cases the resulting discharge from the wells continues to flow through the winter, creating large masses of aufeis (icings), some of which have destroyed houses and covered roads. In November 2005 serious well leakage occurred near the pingo site. Liquid nitrogen was injected to freeze the seepage around the well in February 2006. The well seepage was completely frozen, stopping the groundwater discharge. We had the opportunity to monitor subpermafrost groundwater potential during and after this event. After the well leakage was stopped, the groundwater hydraulic potential immediately began rising, and in a few weeks it returned to the original pressure (fig. 13).

#### STOP 4: FOX GOLD MINING SITE PERMAFROST OUTCROP

Ice wedges of various ages have been observed in the Fairbanks area associated with gold mining activities. The majority of the ice wedge bodies developed around 30,000–40,000 yr BP (MIS-3). Stable isotope variations in the ice wedges differ according to chronological sequences. Most of the stable isotope distributions (deuterium vs. oxygen 18) fit the present local meteorological water line very well, indicating that the snowmelt was the most consistent source of water filling the frost cracks after the cold winter. The oldest ice wedge group in the Fairbanks region was found about 21 m below the ground surface. A tephra layer from these sediments indicates a possible age of older than 400,000 yr BP (MIS-9–MIS-11) (fig. 14). The stable isotopes of this group ( $\delta^{18}\text{O}$ : $-24\text{‰}$ ,  $\delta^2\text{H}$ : $-170\text{‰}$ ) are heavier than for the late Wisconsinan ice-wedge complex (MIS-3), most of which formed 32,000–39,000 yr BP. The stable isotopes of this major Wisconsinan group ( $\delta^{18}\text{O}$ : $-28\text{‰}$ ,  $\delta^2\text{H}$ : $-210\text{‰}$ ) are lighter numbers than for

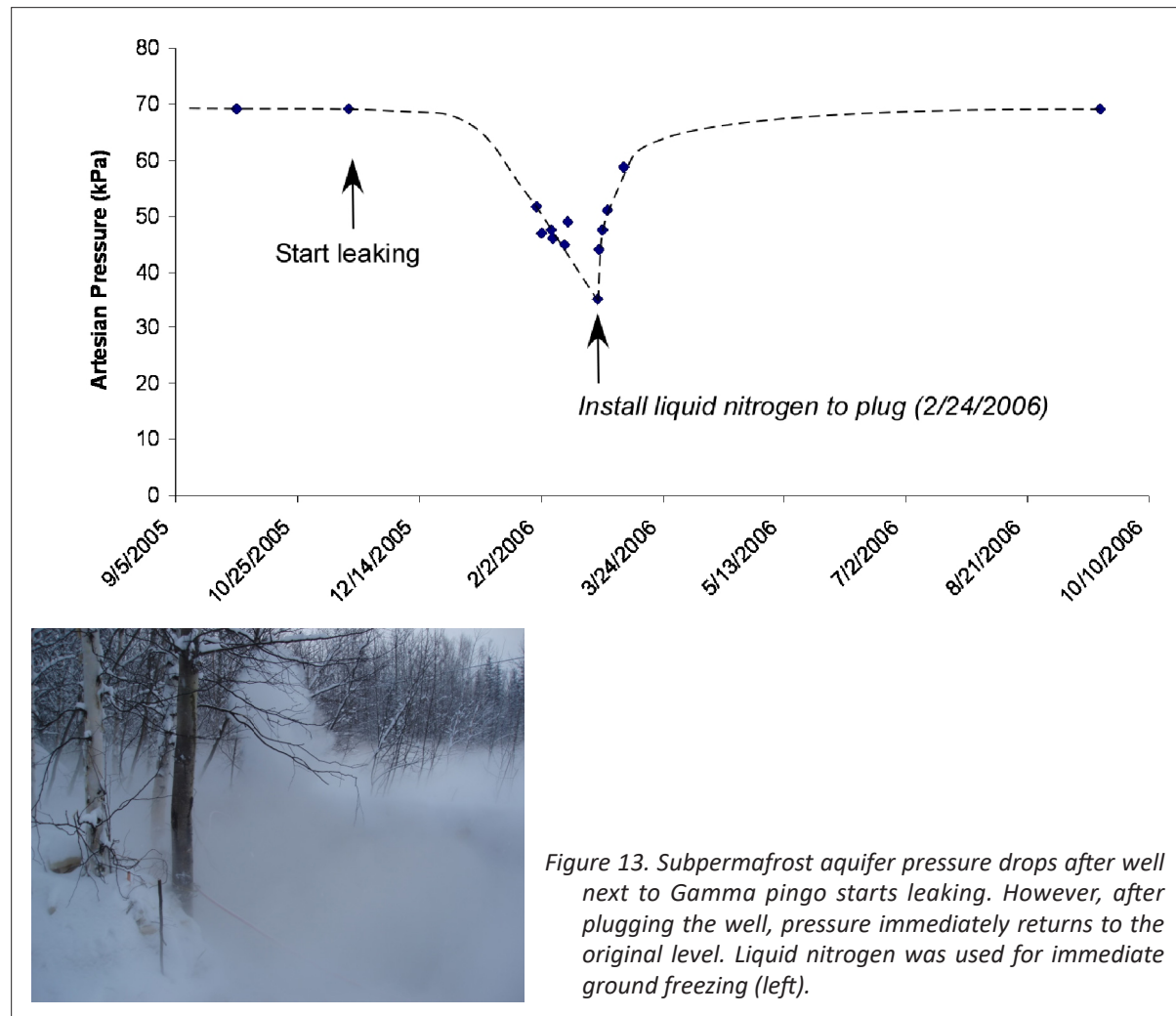


Figure 13. Subpermafrost aquifer pressure drops after well next to Gamma pingo starts leaking. However, after plugging the well, pressure immediately returns to the original level. Liquid nitrogen was used for immediate ground freezing (left).



Figure 14. One of the oldest ice wedges in the mining tunnel (left), and MIS-3 ice wedges exposed by mining activity (right).

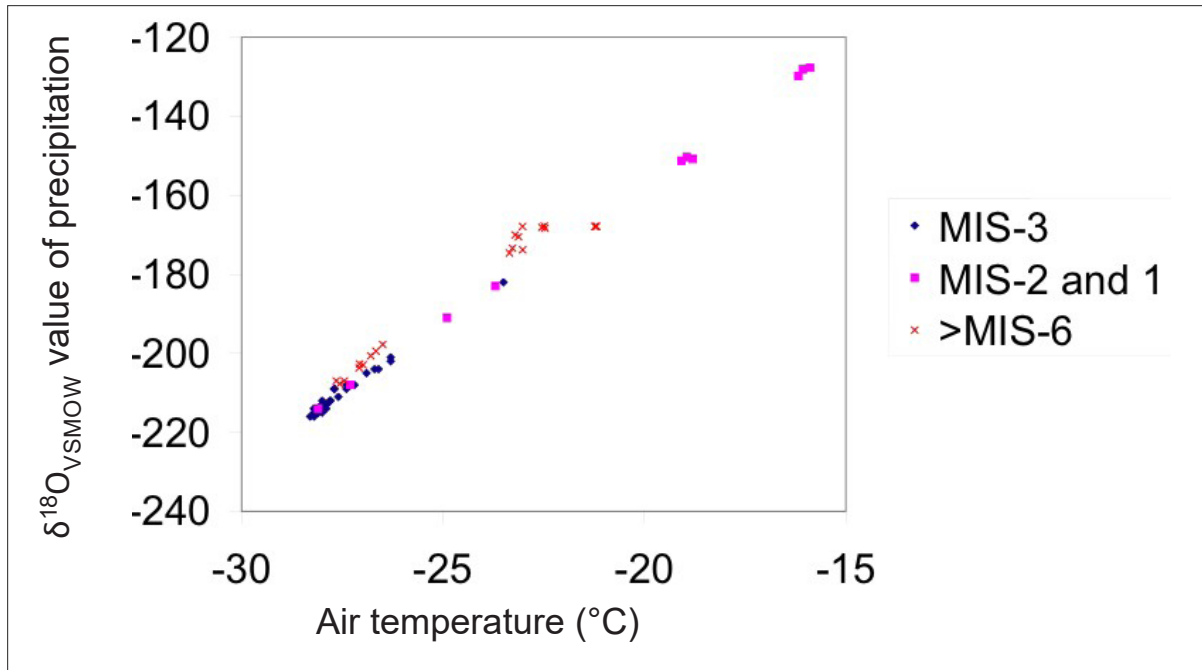


Figure 15. Isotope variations for several ages of wedge ice in the Fairbanks area.

any other ice-wedge group (fig. 15). Not many ice wedges were observed to have formed during the Last Glacial Maximum (MIS-2). Large amounts of loess were deposited here in that period, but the ice wedges are relatively slender, due to less winter precipitation.

The stable isotopes of the Holocene (MIS-1) ice wedges ( $\delta^{18}\text{O}$ : -18‰,  $\delta^2\text{H}$ : -150‰) are heavier than any other ice-wedge group. They are also found at stop 2 (Goldstream Creek valley). The total snow accumulation in Fairbanks had a nearly constant  $\delta^{18}\text{O}$  value between -22 and -23‰ in 2003. The average stable isotopes of snow are slightly lighter than the Holocene ice-wedge group. The heavier infilling water might be coming from soil moisture, or a condensation process, or both (Yoshikawa, 2008).

Between September 1998 and March 2000,  $\delta^{18}\text{O}$  values of precipitation had a strong seasonal signal in the Fairbanks area (fig. 16). Most of the snow precipitation was lighter than -20‰, and rain was heavier than snow. However, there were several strong southern wind events when the jetstream brought large air masses from the Pacific Ocean, carrying  $\delta^{18}\text{O}$  water into the Interior from the Gulf of Alaska (fig. 17).

The spatial distribution of the stable isotopes in Interior Alaska varies between -40‰ and -20‰. Lightest snow values are observed at the summit of Denali (south peak), 6,194 m above sea level. Heaviest snow values (-15‰ or more) were in Fairbanks during the jetstream's irregular cycles (fig. 17). The jetstream flows far south of Alaska almost all winter; however, 2–3 times each winter the circulation patterns of the jetstream break across Alaska, carrying warm, humid air from the Pacific Ocean.

## STOP 5: CHATANIKA

### Gold Mining History

In 1902 a miner named Felice Pedroni (later known as Felix Pedro) located good gold prospects in the Tanana River valley. News of Pedro's gold discovery spread. By September 1902, dozens of prospectors had arrived in the area (fig. 18). A settlement grew around a trading post opened by Elbridge Truman "E.T." Barnette. At the urging of Judge Wickersham, Barnette suggested to the new residents that they name the new community Fairbanks, honoring Indiana Senator Charles Fairbanks, who was chairman of the Joint High Commission charged with settling the Alaska–Canada boundary dispute. Within a year, Fairbanks had attracted 1,200 people.

Near the new community was a better location for sternwheelers to dock. A second town, Chena, developed at this site. Fairbanks promoters, however, successfully waged war with this new competing town. The deciding factor was Judge Wickersham's transfer of the seat of the third judicial district from Eagle to Fairbanks.

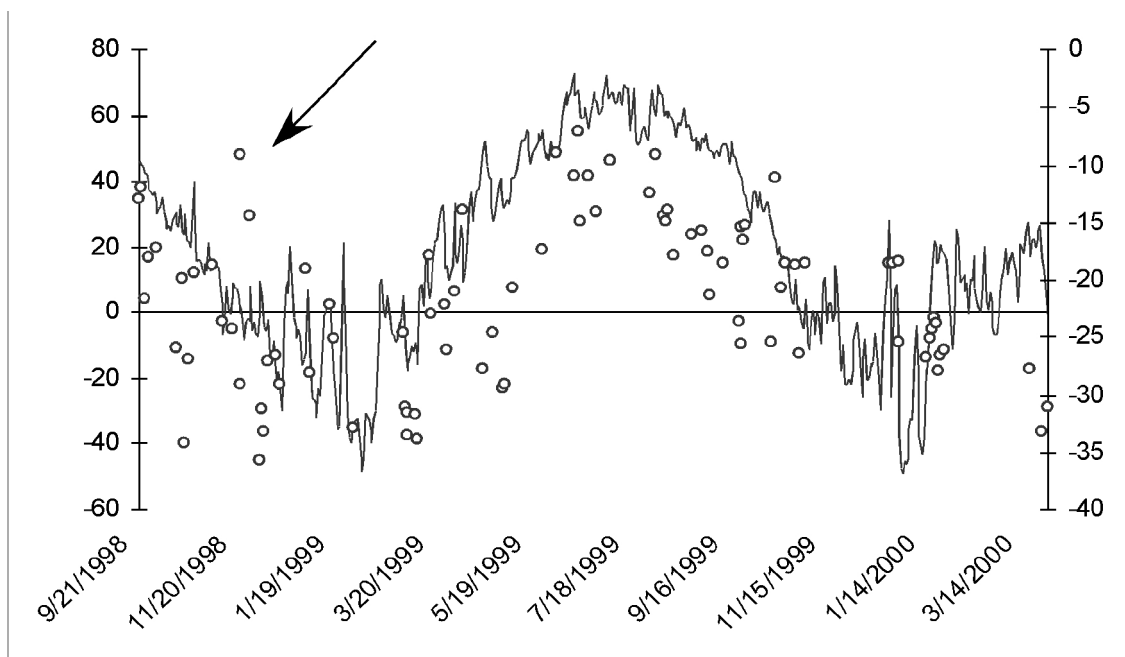
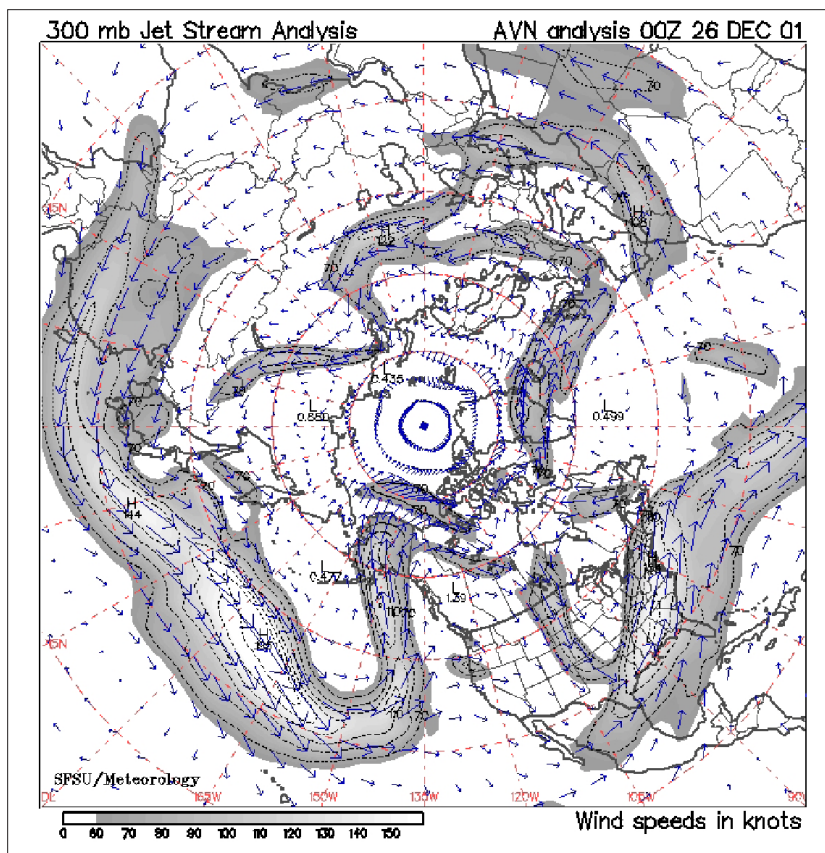
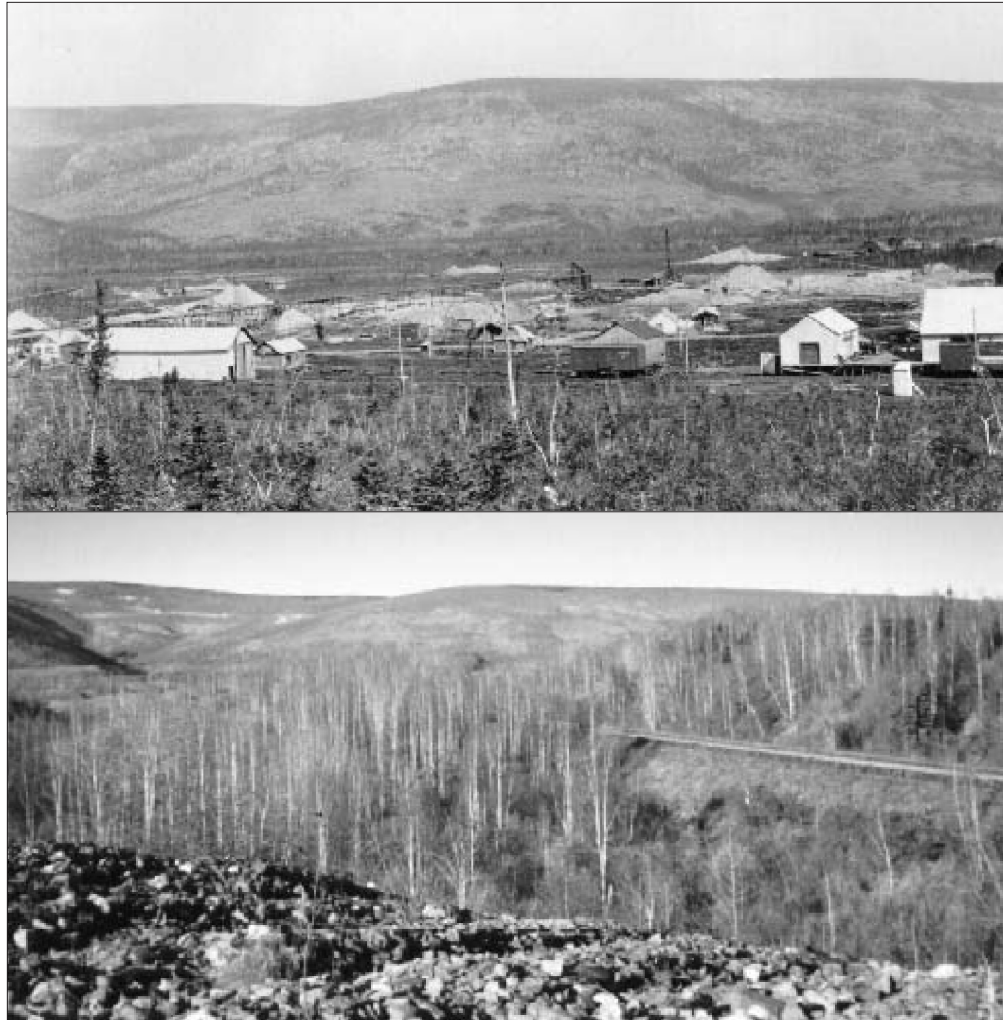


Figure 16.  $\delta^{18}\text{O}_{\text{VSMOW}}$  value of precipitation and air temperature in Fairbanks, Alaska, between September 1998 and March 2000. In general, the isotope value and air temperature have positive correlation, except during 'chinook' storms that occur occasionally in winter (see arrow).

Figure 17. 300 millibar (mb) jetstream distribution during a 'chinook' storm in the northern hemisphere on December 26, 2001 (San Francisco State University; <http://squall.sfsu.edu/crws/jetstream.html>). During this circulation pattern, heavy isotopic snow was observed in interior Alaska.







*Figure 18. The gold rush town of Chatanika in the early 1900s (upper photo) and today (lower photo). These pictures were taken toward the north and show the south-facing slopes; vegetation on the south-facing slopes was shrubs with spruce at the bottom of the valley and the top of the hill.*

Driving north from Fairbanks on the Steese Highway, it is possible to see two pipelines. One is bright and shiny and carries oil; the other is old and rusted and carried water years ago. Both are remarkable examples of engineering for their day. The rusty pipe, almost exactly the same diameter (46–56 inches) as the Trans-Alaska Pipeline (48 inches), represents the remnants of a project undertaken from 1924 to 1929 to bring water to Fairbanks area gold-mining operations. The construction was carried out under the auspices of the Fairbanks Exploration Company (known locally as F.E. Co.), a subsidiary of United States Smelting, Refining and Mining Company (U.S.S.R. & M.). This project, known as the Davidson Ditch, was a 90-mile-long conduit designed to divert water from the Chatanika River at a point below the junction of Faith and McManus creeks to hydraulic sluicing (stripping) operations at Cleary and Goldstream, just north of Fairbanks. The term “ditch” does not do the project justice because, although the open earthwork section comprised most of its length, the course included a 0.7-mile-long tunnel near Fox, and 6.13 miles of inverted siphons along the way. The inverted siphons, which are the pipes visible today, were masterpieces of engineering at the time. There were 15 siphons in all, crossing ridges and the creek beyond. The longest siphon was a 7,961-foot section that crossed the Chatanika River with a head of 544 feet. (The reason that Chatanika water crossed above its source river downstream from the inlet is that the Davidson Ditch had a gradient of only 2.112 feet per mile, whereas the river’s gradient is significantly higher.) (Boswell, 1979)

### Poker Flat Research Range

Poker Flat Research Range (PFRR) is the only non-federal, university owned and operated rocket range in the world and the only high-latitude, auroral-zone rocket-launching facility in the United States. Owned and operated by the University of Alaska Geophysical Institute since 1968, the range primarily has been dedicated to the launch of sounding rockets for auroral and middle- to upper-atmospheric research. Range operations are funded through contracts with NASA, and the range has been operating under a cooperative agreement between NASA and the Geophysical Institute since 1979.

A small group of university employees work year-round at the facility to maintain the physical plant, provide launch support, and obtain the various waivers, approvals, and agreements necessary for operation. Past funding sources include the Defense Nuclear Agency, the U.S. Air Force Geophysics Laboratory, the National Science Foundation, and the National Oceanic and Atmospheric Administration (NOAA).

The 5,132-acre site, located about 30 miles northeast of Fairbanks, Alaska, is the world's largest land-based rocket range and has an established chain of downrange flight and observation facilities from inland Alaska to Spitsbergen, Norway, in the Arctic Ocean, for monitoring and recovery purposes. Data from various scientific instruments are collected by Poker Flat Geospace Environment Data Display System (GEDDS) (<https://www.pfrr.alaska.edu/tour/pfrr/gedds.htm>) and at the Geophysical Institute's Data Analysis Center (<http://www.pfrr.alaska.edu/tour/uaf/dac.htm>).

### STOP 6: CARIBOU-POKER CREEKS RESEARCH WATERSHED (CPCRW)

The Caribou-Poker Creeks Research Watershed (CPCRW) is a 104 km<sup>2</sup> basin near Chatanika reserved for ecological, hydrological, and climatic research (fig. 19). The site is owned jointly by the State of Alaska and the University of Alaska Fairbanks. The entrance to the Research Watershed is on the Steese Highway about 31 miles from Fairbanks (<http://www.lter.alaska.edu/>).



Figure 19. Caribou-Poker Creeks Research Watershed image on 1999 Landsat scene. "Frost fire" experimental burn site (C4 watershed) is indicated by red color.

Following the 1967 Fairbanks flood, hydrologists realized that very little was known about the precipitation and hydrology of upland headwater streams in interior Alaska and that none of the USGS gages on major rivers predicted the 1967 flood. The Inter-Agency Technical Committee for Alaska (IATCA), which had been set up under the President's Water Research Council, had a mandate to "develop a comprehensive plan for use as a general guide by all agencies in establishing hydrologic stations required in connection with developing the water resources of Alaska" (Slaughter and Lotspeich, 1977). A research coordination committee was created to, among other things, identify an upland taiga watershed for designation as a research watershed for "long-term studies of complete catchments in permafrost-dominated uplands" (Slaughter and Lotspeich, 1977). The Caribou and Poker Creek watersheds were identified as the most likely area for study, because they have easy access, are of manageable size, had little human impact, and are owned by state and federal agencies. In 1969, a cooperative agreement between the IATCA and the Alaska Department of Natural Resources (DNR) was written and signed, designating the basin as the Caribou–Poker Creeks Research Watershed for a period of 50 years, and outlining the responsibilities of the signing parties. The document stated that DNR will "recognize research into water- and land/water-related resources . . . as being the presently known highest and best use of these lands, and to permit only compatible uses." The agreement was amended to delegate to the Institute of Northern Forestry (INF), USDA Forest Service, "authority and responsibilities" set forth in the original agreement. INF managed the site from the early 1970s until 1993.

In December 1993, the leadership of the Bonanza Creek Long-Term Ecological Research (BNZ-LTER) program requested of the National Science Foundation that CPCRW be added to the Bonanza Creek Experimental Forest (the main site for BNZ), and that the name and acronym be changed to BNZ-CPW to reflect the additional site. The addition was approved, but the name change was not, so now the BNZ LTER actually includes both the original site at the Bonanza Creek Experimental Forest (BCEF) and the CPCRW site. Prior to 1993, most of the LTER-related research in CPCRW was aquatic, but since then, terrestrial research on the effects of large-scale disturbance, such as climate warming, wildfire, and timber harvest, have been greatly expanded.

Much effort has gone into improving the infrastructure of CPCRW over the years. In the initial years of the early 1970s, access was by foot or helicopter. Various structures and instruments were donated by cooperating agencies, including a laboratory trailer that was airlifted to the site by a Chinook helicopter, and another laboratory trailer donated by the Geophysical Institute and airlifted in with a Sikorsky Skycrane helicopter. Trails were cut during the early 1970s for snowmachine and off-road vehicles, and the primary access was over Haystack Mountain from the Elliott Highway. About 10 miles of gravel roads, including four bridges, passable by four-wheel-drive pickup truck, were constructed in the late 1970s. These roads and one of the bridges are in need of repair. Since the construction of the road "system," the main access to CPCRW has been by fording the Chatanika River at about MP 31 of the Steese Highway. As one might imagine, access was limited or impossible during spring breakup and summer storm events. A steel cable and a basket on pulleys provided limited access in times of high water. In 1995, with cooperation from the U.S. Army and the Cold Regions Research and Engineering Laboratory (CRREL), and funding support from the U.S. Forest Service, a Bailey bridge was constructed across the Chatanika River, immensely improving access to CPCRW.

Since its inception, research at CPCRW has focused on hydrology and climate. Initially, streams were gauged by manual methods on a circum-weekly schedule by personnel who hiked into the watershed. In the mid to late 1970s, fiberglass Parshall flumes with water-level recorders were installed at five sites, and water-level recorders were installed at several other sites with streams too large for flumes. Many of the large-capacity rain gauges were installed by helicopter. Hydrology and climate data have been collected continuously since 1970, although individual sites may not have a complete record. Discharge data for snowmelt runoff are also incomplete because of logistical difficulties.

## Permafrost

The presence of permafrost strongly influences many above- and below-ground processes, including site ecology and hydrology as well as the thermal conductivity of active-layer material. Interior Alaska has very warm, discontinuous permafrost, with temperatures often above  $-1^{\circ}\text{C}$ . Since 1969, many studies have been conducted in the Caribou–Poker Creeks Research Watershed (CPCRW), where permafrost dominates shaded ground or north-facing slopes but is largely absent on south-facing slopes that receive appreciable solar radiation. Permafrost-dominated and permafrost-free slopes support significantly different vegetation types (Haugen and others, 1982). In general, black spruce forest indicates the presence of permafrost. Rieger and others (1972) mapped the soil distribution at CPCRW, on the basis of extensive field surveys and aerial photography. They concluded that a strong relationship exists between permafrost distribution and the type of soil, because the factors that control permafrost formation

also affect soil genesis. Saulich silt loam, Ester silt loam, Karshner silt loam, and Bradway silt loam all have permafrost. Several sharp permafrost boundaries exist along Caribou Creek and Little Poker Creek; they are caused by a geologic boundary between deposits of eolian origin and weathered bedrock. However, soil type alone does not completely explain the permafrost distribution; many other factors also have an influence.

Morrissey, Strong, and Card (1986) mapped permafrost using TM (Thematic Mapper) satellite imagery and a geographic database (vegetation distribution and equivalent latitude). Vegetation is a helpful indicator of ground condition and can be classified on satellite imagery or aerial photography. Their mapping had 78 percent accuracy and compared well with the Rieger and others (1972) classification of permafrost distribution. The analysis of Morrissey and others (1986) indicated that, in general, permafrost is located under the spruce forest at CPRW, but recent field studies have shown there are also many areas free of permafrost under the spruce forest. Koutz and Slaughter (1973), Dingman and Koutz (1974), Jorgenson and Kreig (1988), and Haugen and others (1982) noted a strong correspondence between the presence or absence of permafrost and the equivalent latitude. Equivalent latitude is an index of the long-term potential of direct-beam solar radiation that occurs on a surface and is calculated from the slope and aspect (Frank and Lee, 1966). The equation used to calculate equivalent latitude is:

### Equation 1

$$\phi' = \sin^{-1} (\sin k \cos h \cos \phi + \cos k \sin \phi)$$

where  $k$  = slope of the surface [°]  
 $h$  = aspect of the surface [°]  
 $\phi$  = actual latitude of the area [°]  
 $\phi'$  = equivalent latitude of the area [°]

Approximately 200 temperature probes were installed in 1998 along a transect from the north-facing slope to the south-facing slope. Probes were installed from the ground surface to a depth of 1.5 m below the surface (30, 90, 150 cm). Deep ground temperature profiles were obtained from boreholes drilled by Collins and others (1988) and Yoshikawa and others (2002). Their analysis of the ground thermal regime examined the relationship between mean annual ground-surface temperature ( $T_{mas}$ ) and equivalent latitude. The coefficient of determination ( $r^2$ ) for this relationship is 0.68 ( $T_{mas} = -0.155\phi' + 9.751$ ). The permafrost boundary is predicted at approximately 63° equivalent latitude. Measurement of soil temperature below the depth of significant annual variation is the best indication of permafrost at a single point, but an indirect or modeling method is the better approach to map permafrost distribution over broad areas. However, validation of any new approach and verification of predictive models require intensive measurements of permafrost distribution and condition (fig. 20).

### OIL SPILL AND FROST FIRE EXPERIMENTS

Two large experimental crude-oil spills were conducted in the winter and summer of 1976 at CPRW (fig. 21). The impacts on permafrost and thaw depth were measured for more than 20 years (fig. 22) (White and others, 2004). Even though the volume of oil applied was the same, the effects on the permafrost were far more pronounced on the winter spill site due to a larger surface oiled area. Since the active layer was completely frozen, the oil did not infiltrate, but flowed along the surface for a much greater distance, yielding a much greater impact. The winter spill also had a more drastic effect on the vegetation. Where the asphalt-like surface oil was present, black spruce mortality was 100 percent and there was very little live plant cover except for cottongrass tussocks that recovered in the nearly 30 years following the spill. These sites were burned in a wildfire in 2004. Changes in oil chemistry varied with depth; surface samples had signs of microbiological degradation, whereas some subsurface samples taken just above the permafrost had no evidence of degradation in 1991 and still contained volatile fractions (Collins and others, 1994).

### Fire impact

Wildfires occur commonly throughout most of the boreal forest in Alaska, including CPRW. The fire history of CPRW was studied using fire scars on tree rings (Fastie, 2000). Most of the black spruce were burned and replaced in the 1920s (fig. 23). A particularly severe fire occurred in 1924, killing most of the trees in the watershed, except in some wet areas and valley bottoms. The age of the spruce trees in CPRW today is about 70–80 years. In addition, an experimental, controlled fire burned most of the black spruce forest in the C4 watershed (Hinzman and others, 2003). In 2004, the Boundary wildfire burned most of the Poker Creek watershed.

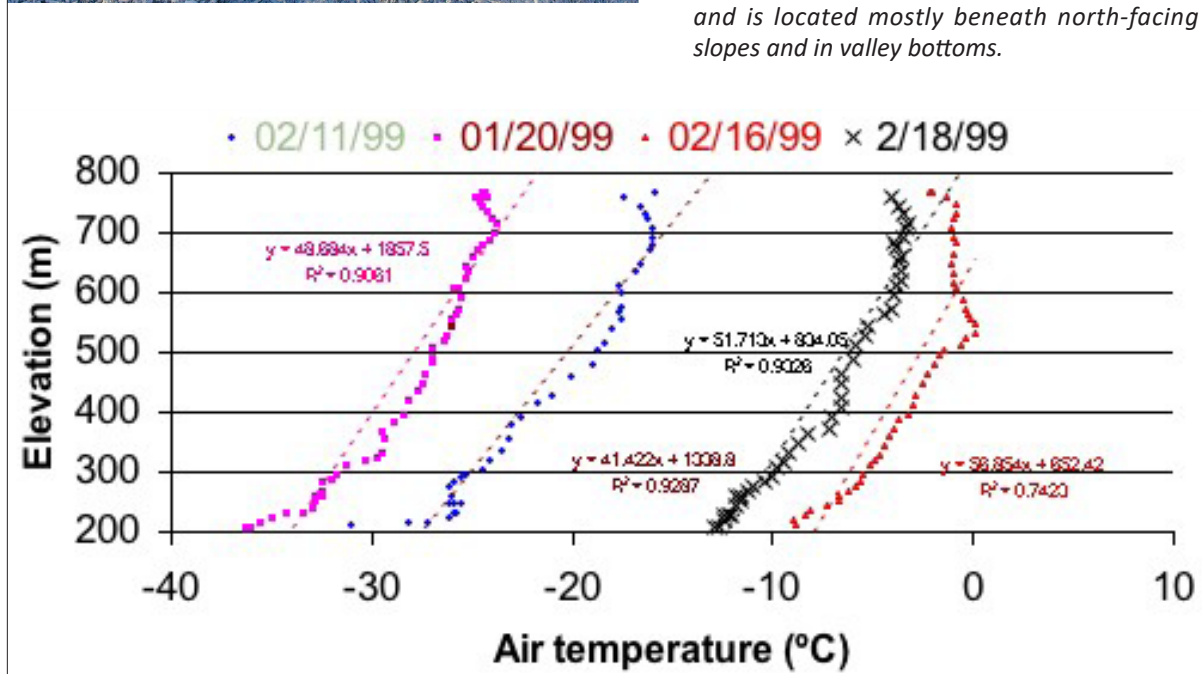
The impact to the permafrost during and after wildfire was studied at CPRW during the “Frost Fire” experiment. Heat transfer by conduction to the permafrost was not significant during fire. Immediately following fire,

the ground thermal conductivity increased to 10 times higher than before and the surface albedo decreased by 50 percent depending upon the severity, which is defined as the extent of burning of the surficial organic soil. The thickness of the remaining organic layer strongly affects permafrost degradation. If the organic layer thickness was not reduced during the burn, then the active layer did not change after the burn despite the decrease in surface albedo. Any significant disturbance to the surface organic layer will increase heat flow through the active layer and into the permafrost. Approximately 3 to 5 years after severe disturbance, depending on site conditions, the active layer will increase to a thickness that does not completely refreeze the following winter. This results in formation of a talik, or unfrozen mass of soil surrounded by permafrost below and seasonally frozen ground above. The thickness (depth) of the talik under the severe burn was 4 m (4.15 m at Rosie Creek Fire in 1983, 3.6 m at Wickersham Fire in 1971). Model studies indicate that if an organic layer of more than 7–12 cm remains following a wildfire, the thermal impact to the permafrost will be minimal in the boreal forests of interior Alaska (Romanovsky and others, 1997; Yoshikawa and others, 2003).

The radiation budget before and after the CPRW controlled burn was measured using short-wave, long-wave, and net radiometers (table 2). Sensors measuring short-wave and long-wave incoming and reflected (emitted) radiation were installed on a 3 m tower (unburned site) and a 1.5 m tower (burned site). Both were higher than the black spruce canopy. The radiation balance ( $Q$ ) is expressed in terms of incoming solar radiation ( $K_{\downarrow}$ ), surface albedo ( $\alpha$ ), incoming long-wave radiation ( $L_{\downarrow}$ ) and emitted long-wave radiation ( $L_{\uparrow}$ ) in the form:



Figure 20. Temperature inversions are very common during winter/spring periods in interior Alaska. The photo (left) displays frost on trees at lower elevations and no frost in higher elevations. In February 1999, stable temperature inversions occurred with similar rates even under different air temperature profiles (graph, below). In CPRW, the difference in air temperature inversion is about 10°C between hilltop and valley bottom. Two major climatic agents control natural formation and degradation of permafrost: (1) solar radiation determines energy input to a site and (2) temperature inversions control the Freezing Degree-Days (FDD). The distribution of permafrost is thus strongly influenced by topography, and is located mostly beneath north-facing slopes and in valley bottoms.



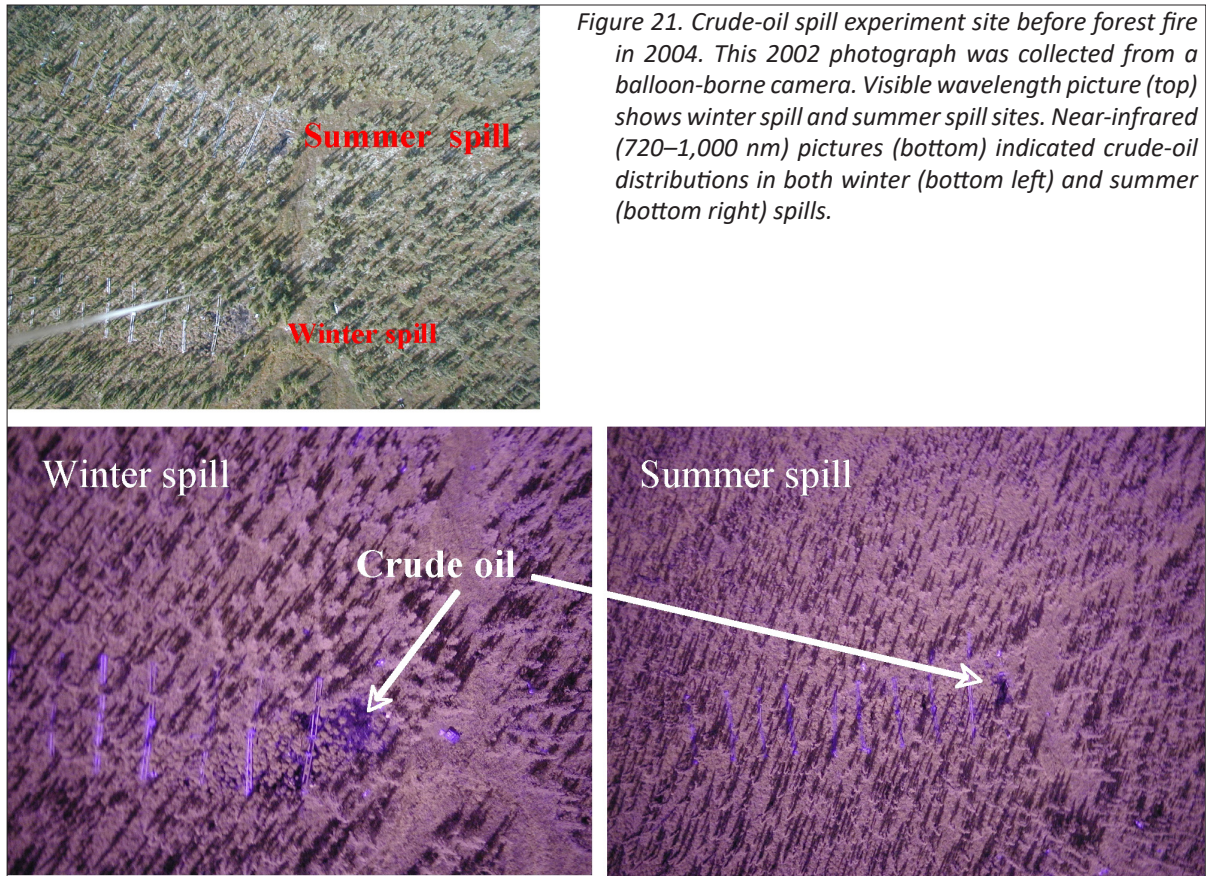


Figure 21. Crude-oil spill experiment site before forest fire in 2004. This 2002 photograph was collected from a balloon-borne camera. Visible wavelength picture (top) shows winter spill and summer spill sites. Near-infrared (720–1,000 nm) pictures (bottom) indicated crude-oil distributions in both winter (bottom left) and summer (bottom right) spills.

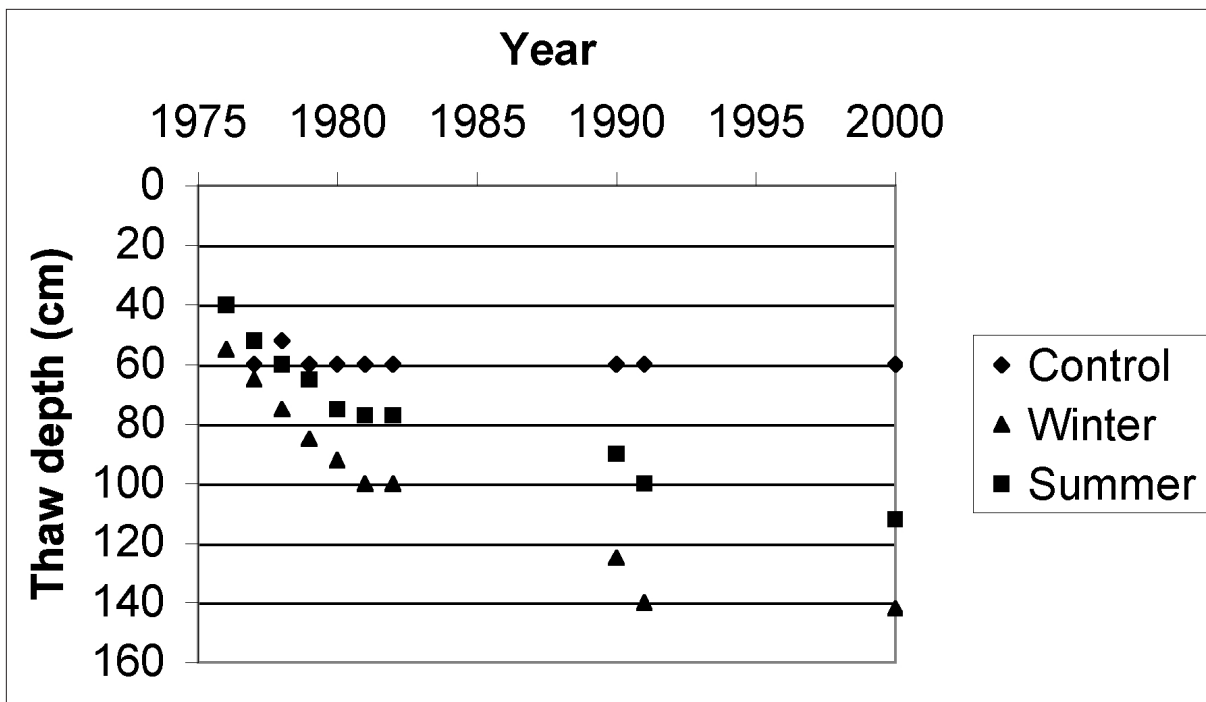


Figure 22. Average thaw depths for each of the oil-spill plots as functions of time (White and others, 2004a).

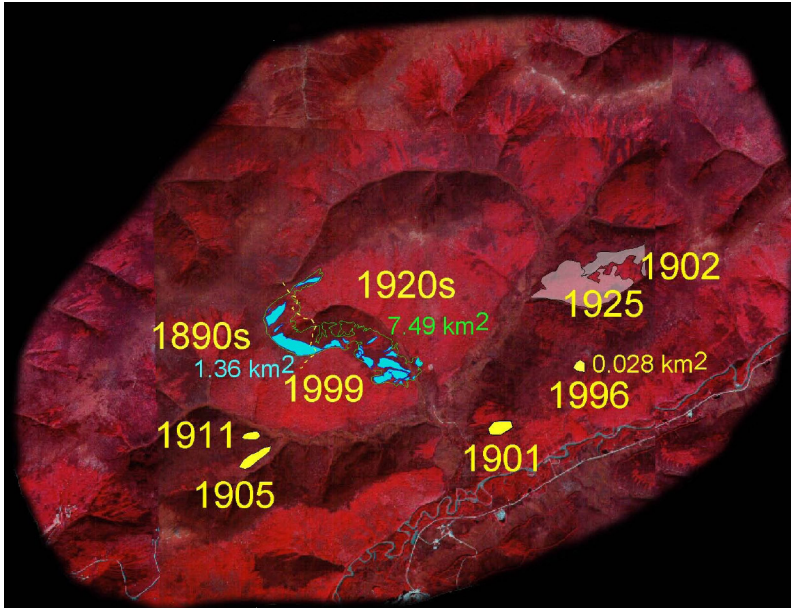


Figure 23. Fire history of CPCRW. This distribution excludes the 2004 Boundary fire (Fastie, 2000).

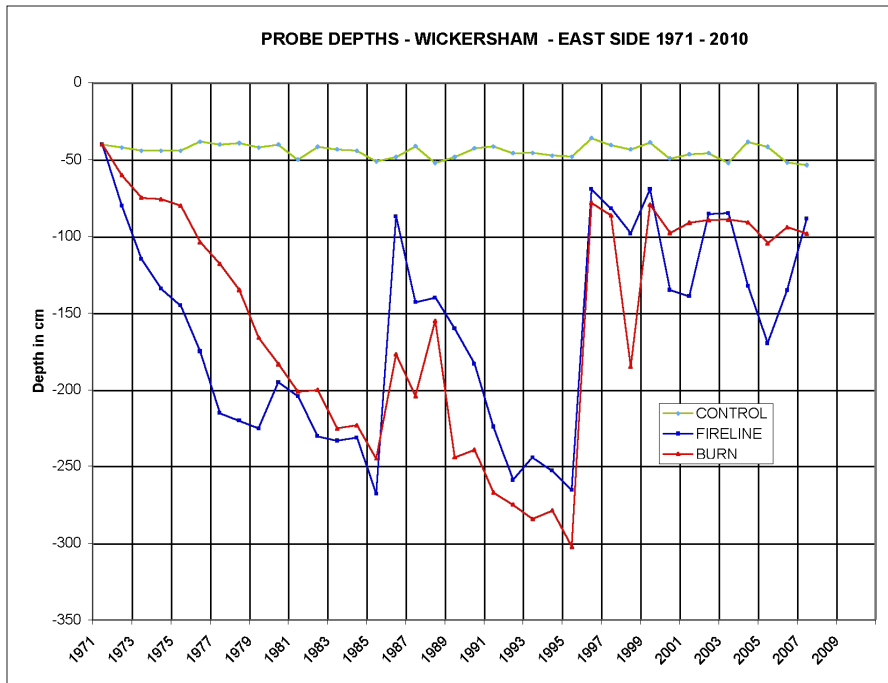


Figure 24. Maximum thaw depth from 1971 to 2007 of an unburned black spruce stand (control), a burned black spruce stand, and a fireline at the east side of the 1971 Wickersham dome fire (Viereck and others, 2008).

Table 2. Radiation balance of burned and control areas at site 1 (net radiation  $Q$ , incoming solar radiation  $K_{\downarrow}$ , reflected short wave radiation  $K_{\uparrow}$ , surface albedo (%)  $\alpha$ , incoming longwave radiation  $L_{\downarrow}$  and emitted longwave radiation  $L_{\uparrow}$ , Radiation efficiency  $Re$ , Total net radiation  $\Sigma Q$ ) (after Yoshikawa and others, 2002).

Radiation	$K_{\downarrow}$	$K_{\uparrow}$	$\alpha$ (%)	$L_{\downarrow}$	$L_{\uparrow}$	$Re$	$Q$	$\Sigma Q$ (MJ/m <sup>2</sup> )	Max. (W/m <sup>2</sup> )	Min. (W/m <sup>2</sup> )
Burn (site 1)	100	4.6	0.05	105	122	0.47	47.43	97.7	458	-37.6
Unburned (site 1)	100	13.5	0.14	105	118	0.74	73.59	160.2	537	-48.7

From July 23, 1999, to August 10, 1999 (sensor height 1 m at burn, 1.5 m at unburned)

**Equation 2**

$$Q = K\downarrow (1 - \alpha) + L\downarrow - L\uparrow$$

**Succession change in active layer**

Long-term observations such as those made on the active layer and vegetation changes over the last 36 years at the 1971 Wickersham Fire site are extremely valuable for developing an understanding of the effects of fire and fireline construction in the taiga of Alaska.

At the Wickersham fire site, a layer of seasonal frost formed that eventually remained frozen throughout the entire year and continued to remain frozen for the next 10 years. Permafrost is recovering at the Wickersham fire site in the burned stand, however, it is not recovering on the fireline. The increased maximum thaw depth pattern for the two sites is similar, with a maximum thaw of ~266 cm for the fireline and ~302 cm for the burn (fig. 24). Also, the development of an upper frozen zone was similar in 1986 and 1996. The difference between the fire site and the fire line is that the upper zone for the fire site has remained frozen but on the fireline it has become intermittent. The fireline's upper zone may be rejuvenated by another cold, snowless winter.

A temperature profile from the borehole at the Wickersham fire site during the period of maximum thaw in September 2002 (fig. 25) shows an active layer of 1.4 m. The new frozen layer was approximately 50 cm thick and extended from 1.4 to 1.9 m below the current active layer. This new permafrost layer divided the active layer and the talik underlying. The talik temperatures were very close to 0°C. Below 3.4 m the temperatures of the permafrost layer decreased to -0.09°C at the bottom of the borehole (6.5 m). The lower permafrost depth stabilized at 3.5–4.0 m and an unfrozen soil (talik) remained between the two frozen layers. However, in September 2006,

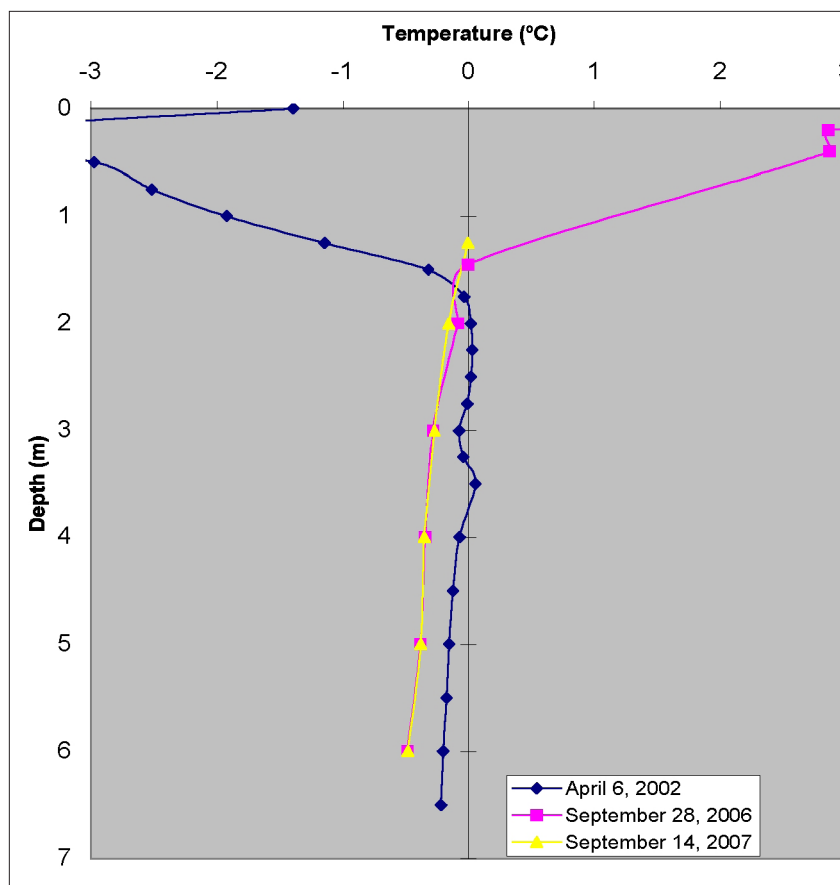


Figure 25. Ground temperature profiles (6.5 m deep) from borehole to the Wickersham dome fire site. In 2002 the profile showed a new frozen layer approximately 50 cm thick extending from 1.4 to 1.9 m below the active layer. Profiles in 2006 and 2007 show complete freezing of the talik.



the temperature profile (fig. 25) shows the disappearing talik layer. The permafrost temperature at 6 m depth is more than 0.3°C colder after 3 years. Permafrost development since 1996 accelerated the refreezing of the talik layer. As a result of the three years of permafrost aggradations, the ground temperature profile is approaching a “normal” gradient (0.1°C/m).

Figure 26 illustrates what actually happened at the burned site after the Wickersham Fire. The active layer did increase for the first 25 years following the fire. However, an upper layer of seasonal frost remained frozen 17 years after the fire and then became discontinuous for the next ten years. Since 1996 the seasonal frost layer has remained frozen. This created a new permafrost layer with an active layer of 90 cm and an unfrozen talik between the upper layer and the lower frozen layer. This new permafrost layer has accelerated the refreezing of the talik layer, and by 2006 the talik layer disappeared and the permafrost has returned to the pre-fire thermal conditions.

## STOP 7: AUFEIS (ICING) AND PERMAFROST HYDROLOGY

Research studies conducted in CPRW include studies of groundwater source, pathway, residence time, and relation of aufeis and open-system pingos. Figure 27 displays the aufeis distribution, springs, and major fault system at CPRW. The annual mean ground-temperature of CPRW varies between -3 and 0.5°C in permafrost areas and up to 2.5°C on south-facing slopes. The thermal and hydraulic properties of the soil are strongly affected by the absence or presence of permafrost. These hydrologic and thermal regimes directly control aufeis or pingo (fig. 28). There are 463 open-system pingos reported in interior Alaska, including the Brooks Range (Holmes and others, 1968; Hamilton and Obi, 1982; Slaughter and Hartzmann, 1993). Many of the open-system pingos in other areas have a different type of groundwater system and genesis, such as glacier fed and near-shore type (Yoshikawa and Harada, 1995).

The type of aufeis (icing) and the source of water were classified using the winter dissolved organic carbon (DOC) and inorganic carbon (IC) concentrations in the ice and water. The three types of aufeis—spring aufeis, stream aufeis, and ground aufeis—are distinguished by DOC and IC ratios. Ground aufeis had the highest DOC content (8–9 mg/l in ice, 35–40 mg/l in water). The source of this water is believed to be of shallow origin. Permafrost was distributed throughout most of the valley bottom and on the north-facing slopes in the research watershed. The active layer was usually completely frozen between January and early February. After February, almost all of the stream base flow came from natural groundwater springs, which had high concentrations of IC and low concentrations of DOC. The ground aufeis volume was less than 1 percent of total aufeis volume. The

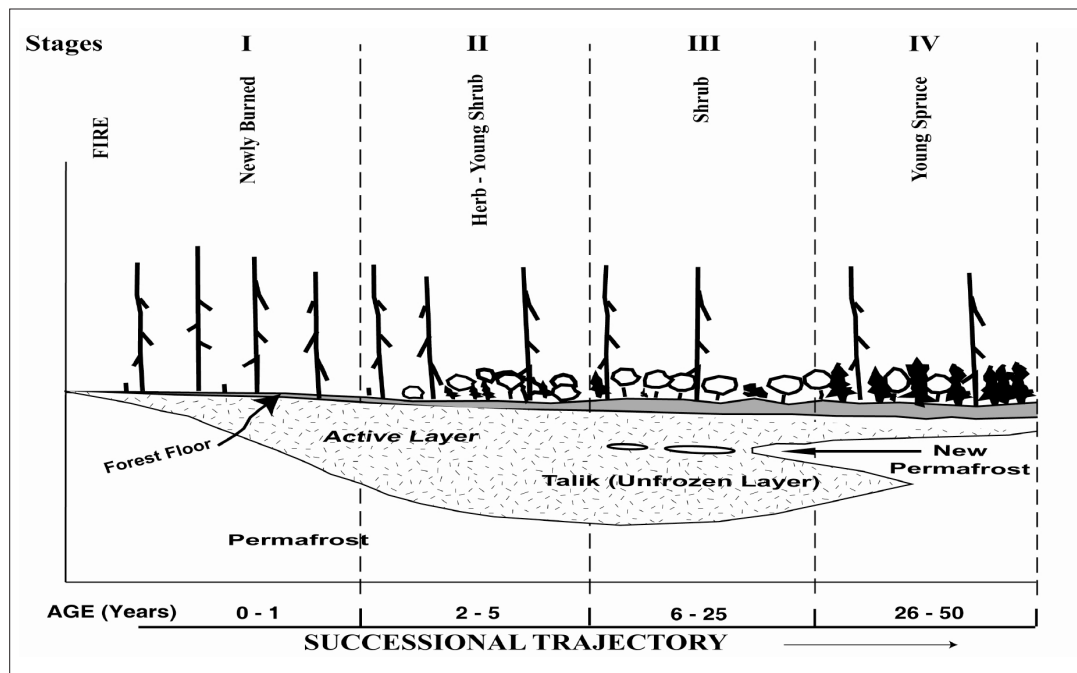


Figure 26. Successional changes observed in vegetation and the active layer at the Wickersham fire site following the 1971 burn (Vierrick and others, 2008).

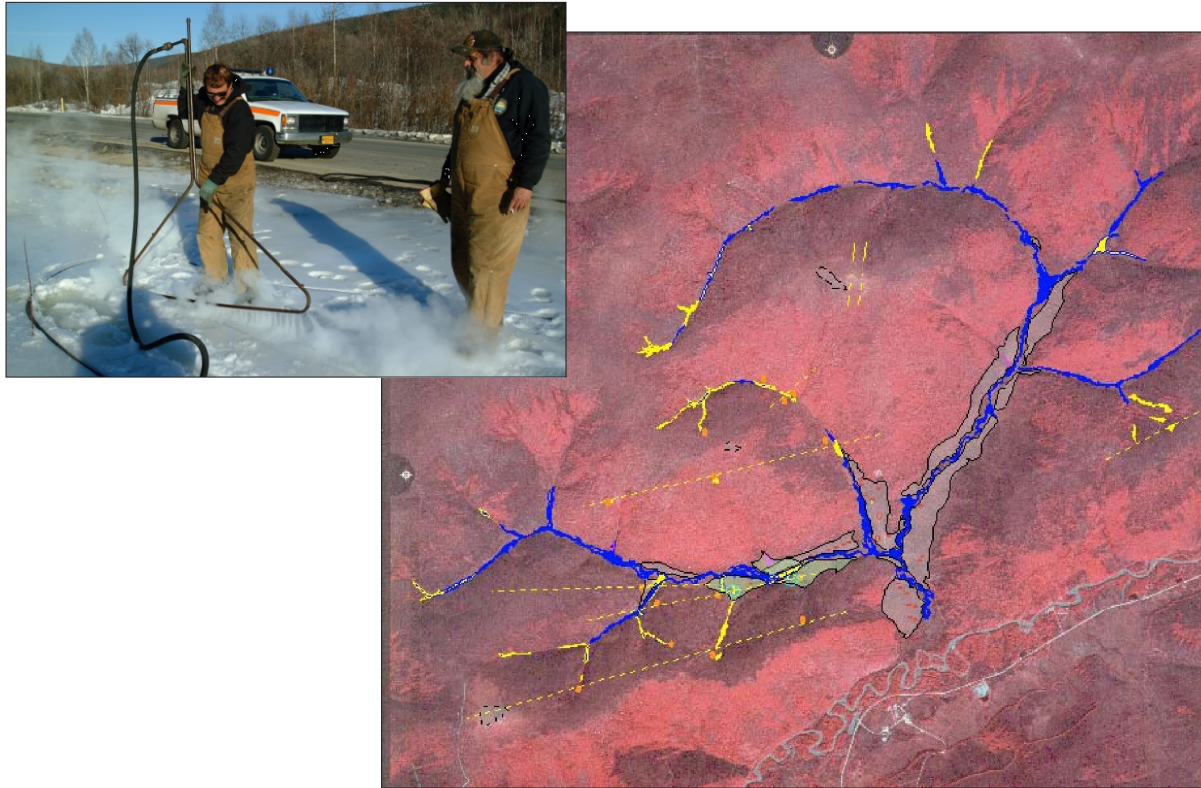
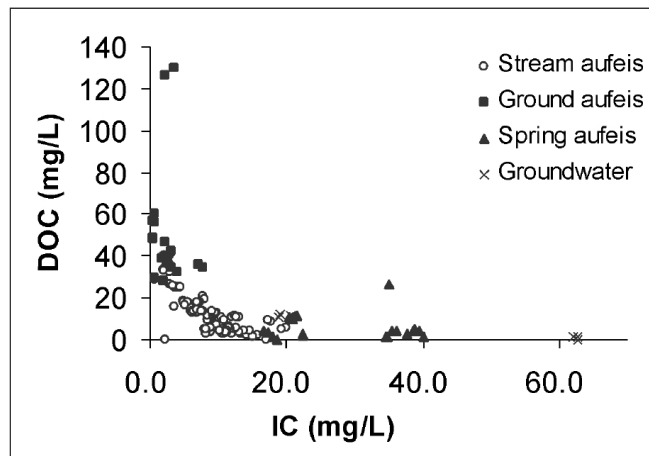


Figure 27. Aufeis distribution. Springs shown in dark yellow and major fault systems shown in dashed yellow. Blue indicates stream aufeis, yellow marks spring aufeis. Aufeis is one of the major winter hazards of Alaska's road system.

Figure 28. The relation between dissolved organic carbon (DOC) and inorganic carbon (IC) from different sources of aufeis water (Yoshikawa and others, 2003).



source of the water for ground aufeis is the seasonal active frozen layer (2.2–3 m thickness) on the permafrost-free south-facing slopes. Most of the south-facing slopes have thin surface sediments. Ground aufeis develops at the interface of the permafrost boundary near the base of the south-facing slope, usually beginning in late February. On the other hand, spring aufeis began forming in late October or November and melted in May, yielding the longest lasting and thickest ice formation in the watershed. Spring aufeis is characterized by the high IC content (30 mg/l). Water from springs on north- and south-facing slopes had similar DOC/IC ratios, demonstrating that permafrost is not a controlling factor of the spring water DOC/IC ratio. Most of the spring water came from a deep geologic feature, such as a fault. Spring locations were generally linear and found along the major faults. The DOC/IC ratio of the stream aufeis fell between spring aufeis and ground aufeis, indicating both sources provide water. Stream aufeis starts developing in late December to January and the dissolved organic content decreases until mid winter and increases from early March until spring melt. Over the last 30 years, the aufeis records at the watershed demonstrate that up to 40 percent of stream base flow may be stored in aufeis. However, during heavy snow years such as 1971, 1972, and 1995, aufeis does not develop or is minimal.

### Infiltration processes

Summer evapotranspiration creates relatively dry soil conditions in the root zone. Minor summer precipitation events are offset by evapotranspiration (Kane, 1980). The snowmelt and summer heavy storm events were the most reliable sources of groundwater recharge. The  $\delta^{18}\text{O}$  value of the precipitation has strong seasonal signals in Fairbanks area. The groundwater mixing ratio from the snowmelt and summer storm water was distinguished using a two-member mixing model (Rantz and others, 1982).

### Equation 3

$$Q = \frac{Q_a (I_s - I_{gw})}{(I_{gw} - I_r)}$$

where Q = discharge of spring  
 Q<sub>s</sub> = infiltration volume of snowmelt water  
 I<sub>s</sub> =  $\delta^{18}\text{O}$  value of the snowmelt water  
 I<sub>gw</sub> =  $\delta^{18}\text{O}$  value of the groundwater  
 I<sub>r</sub> =  $\delta^{18}\text{O}$  value of the summer storm water

The springs and base flow at CPRW had a nearly constant value of  $\delta^{18}\text{O}$  value between -17 and -18.5‰ (Caribou Creek,  $\sigma = 0.12$ ; pingo spring,  $\sigma = 0.89$ ), which indicates 33–40 percent of the groundwater was derived from snowmelt infiltration. The infiltration process during snowmelt through the seasonally frozen dry materials mainly occurs near the upper part of the hill. The infiltration rate is reduced to about one-half that for the unfrozen condition (Kane, 1980).

Table 3. Characteristics of major spring flow (sampled March 2000). From White and others, 2002.

	Sr µg/L	Na mg/L	Mg mg/L	SO <sub>4</sub> mg/L	K mg/L	Ca mg/L	U µg/L	Conductivity µS/cm	$\delta^{18}\text{O}$	$\delta^2\text{H}$	Temperature °C
C3	105	1.55	3.48	37	0.98	34	0.96	113	-18.68	-149.0	0.00
Pingo	345	2.43	11.7	52	2.1	54.4	3.71	380	-19.80	-147.0	-0.01
TR6	ND	ND	ND	ND	ND	ND	ND	113	ND	-125.9	0.10
MD	87.6	0.96	2.66	8	0.78	13.3	0.05	97	-18.25	-154.0	0.96
SS	41.5	1.62	1.8	<2	1.2	15	.009	74	-18.56	ND	2.40
SB	ND	ND	ND	ND	ND	ND	ND	155	-18.34	-125.4	0.43
DG	65.6	1.53	2.9	4	0.7	12	0.01	75	-20.60	-154.0	1.10
CB	68.9	1.91	3.06	12	0.81	17.2	0.01	118	-20.30	-152.0	0.12
Cabin Well	524	3.33	14.1	56	7	94.2	3.65	524	-16.52	ND	ND
MD Well	53.7	9.63	4.55	11	1.2	16.7	0.17	201	-17.93	ND	2.60
Haystack	119.8	1.63	2.96	ND	0.35	15.2	0	120	-18.40	-141.9	ND

ND = no data

### Water–Rock (permafrost) interactions

There were no isotope-exchange processes observed in the water from spring sites, such as exchange with CO<sub>2</sub> or hydration of silicates. The ratio between δ18O and δ2H of the groundwater is aligned with the local meteoric waterline (δ2H = 6.7469 δ18O – 21.589) (table 3). Pingo spring and cabin well water (schist bedrock aquifer 18 m below surface) at the base of the south-facing slope also had higher Ca concentrations. The source of the Ca (limestone bedrock) is possibly located in these areas.

The strontium isotope (<sup>87</sup>Sr/<sup>86</sup>Sr) data also indicate pingo spring water passed through highly weathered, fractured Birch Creek Schist formation (0.74071 ± 1 ppb) (Farmer and others, 1998). Current seasonal variation of the tritium value was 4.96 (summer) and 10.96 (winter) TU. The time (t) is calculated following an equation using the Anchorage, Alaska, tritium database (IAEA/WMO, 2001).

#### Equation 4

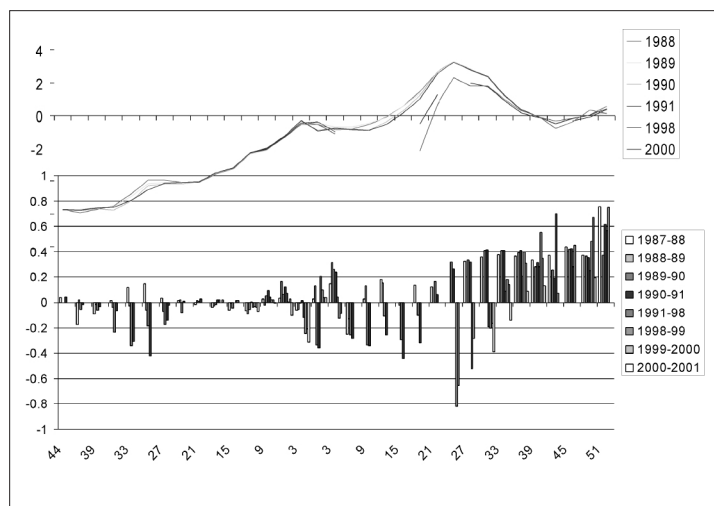
$$t = -17.93 \ln \frac{a_t^{3\text{H}}}{a_0^{3\text{H}}}$$

where  $a_t^{3\text{H}}$  is the tritium value of sample water (TU)  
 $a_0^{3\text{H}}$  is the tritium value of infiltration water  
 (Neary, 1997).

Table 4. Correlation coefficients between spring water and forest floor leachates.

	Birch	Feathermoss	Spruce fiberic NOM	Organic silt
Haystack	0.142	0.483	0.775	0.782
C3	0.139	0.453	0.687	0.702
CB	0.391	0.644	0.793	0.800
SB	0.200	0.334	0.405	0.434
SF	0.238	0.367	0.426	0.426
DG	0.206	0.449	0.611	0.618
MD	0.279	0.422	0.445	0.453
Pingo	0.777	0.672	0.399	0.427
TR-1	0.944	0.805	0.536	0.528

Figure 29. Ground shifting (heaving and collapsing) around pingo. A new pingo (or frost blister) developed on the upper slope of the collapsed pingo. The benchmarks were installed at 3 m intervals in 1987. The x-axis indicates position of benchmark south (center to the right: 0 to 54 m) and north (center to the left: 0 to 44 m). The dramatic collapsing was observed after the 1990s around benchmark south 27–30 m. New upheaving has occurred around benchmark south 30 to 54 m.



## Discharge process

Three different types of aufeis are classified by the discharge process: Spring aufeis, ground aufeis, and stream aufeis. Many of the springs are associated with a local fault system (east-northeast–west-southwest) (fig. 27). Most of the springs develop aufeis starting in October. The shape of the aufeis varies depending on water temperature and discharge volume as well as freezing conditions of each year. Aufeis never developed at one of the south facing slope springs, where the water temperature was  $0.43^{\circ}\text{C}$  and discharge was  $0.8\text{ l/sec}$ . During relatively cold winters (such as 1999 and 2002) impressive ground aufeis, caused by subsurface seeping water, was observed. Ground aufeis frequently forms by the freezing of intra-permafrost water. Intra-permafrost water flow is observed near the silt and bedrock interface. The source of this interface water, the upper part of permafrost-free slopes, is also connected with a fractured bedrock groundwater system (table 4). This groundwater level has annually fluctuated 2 m (maximum, September–October; minimum, just before snowmelt). The bedrock groundwater level also displays similar trends at one of the valley bottom wells: 18 m below the bedrock aquifer).

The genesis of the pingo is also related to the thermal processes of the groundwater system. There has been no remarkable uplift or subsidence of crater pingos (fig. 30) since observations began in 1987. Figure 29 displays topographic changes detected at the collapsed pingo site over 15 years. The inner wall of the pingo crater rim is the only place of major changes from mass movements. Since 1999, icing blisters have developed on the upper



Figure 30. Winter view of Corn pingo, which contained 16 m of massive ice core.

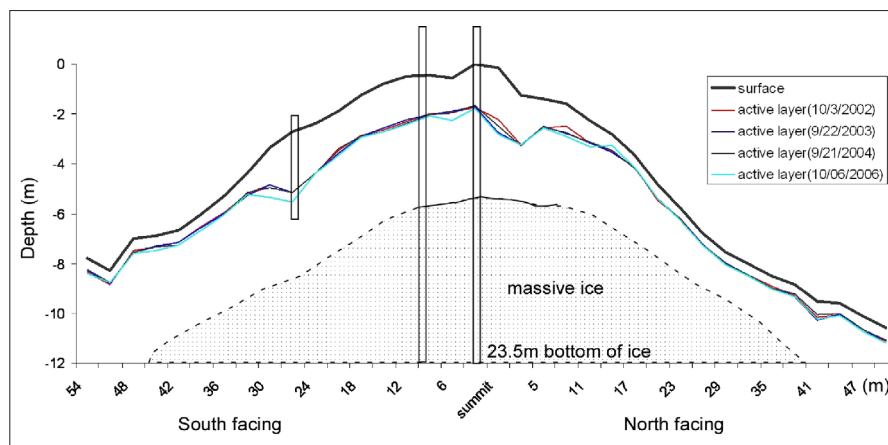


Figure 31. Active-layer measurements at Corn Pingo site. Active layer is thinner on north-facing slope of pingo (30–60 cm), and deeper on south-facing slope (>2.5m).

hillslope of the pingo, where the spring emerged. The artesian pressure (50kPa) was measured and calculated based on the winter of 2001–2002. The pingo ice still existed 5.6 m below the pond in 2002. The melting rate of pingo ice was 2.1 cm/yr since it was first drilled in 1995.

CPCRW contains two pingos along Caribou Creek at the base of north-facing slopes. The thickness of the permafrost is about 120 m and the annual mean upper-permafrost temperature is  $-0.7^{\circ}\text{C}$ . The Caribou Creek Corn pingo has a 60–80 m base diameter, and is more than 10 m tall (fig. 30). The massive ice core starts 7.35 m below the ground surface and extends down to 23.5 m depth. Several segregated and inclusive ice layers a few centimeters to 30 cm thick are present in the silty overburden permafrost. This pingo survived several wildfires. A charcoal layer is present 15 cm below the surface ( $820 \pm 40$  yr BP [GX-28572]). Active-layer thickness fluctuated between 1 m (present) and 2 m (post fire disturbance) during the Holocene. The increases in active-layer thickness during the climatic optimum or post wildfire disturbance, or both, decreased the ice content of the upper permafrost (fig. 31). Schist bedrock is present just below the lower contact of the massive ice.

### STOP 8: ISABELLA CREEK

One of the features characteristic of mature thaw lakes is a floating mat covering. Floating mats greater than 1 m in thickness can be traversed year round. This Isabella Creek bog lake is 7 m deep and has an open talik underneath. Discharge from the lake of 5 l/sec was measured in 2003. This area has permafrost with artesian conditions, which means that groundwater recharges the lake water year round. Kane and Slaughter (1973) studied this lake to estimate discharge and hydrological conductivity using piezometric measurement at different depths in the middle of lake. They determined the silt permeability and discharge using Darcy's equation. The hydraulic gradients are 0.2–0.5 m/min. The rate of discharge ( $Q$ ) is calculated, based on the talik area ( $A$ ), hydraulic conductivity ( $k$ ) and groundwater gradient ( $dx/dz$ ). The piezometric pressure was obtained at four depths in piezometric-pressure monitoring wells. A positive vertical gradient was measured year round (1969–1970), allowing these ponds to recharge via the taliks throughout the year.

#### Equation 5

$$Q = k \times A \times dx/d$$

where  $Q$  = discharge

$k$  = hydraulic conductivity;

$A$  = cross-sectional area of thaw

$dx/dz$  = hydraulic gradient.

Hydraulic conductivities of the materials beneath the lakes were estimated based on unfrozen silt. Field observations in 2003 support the discharge rate determined by earlier work (fig. 32).

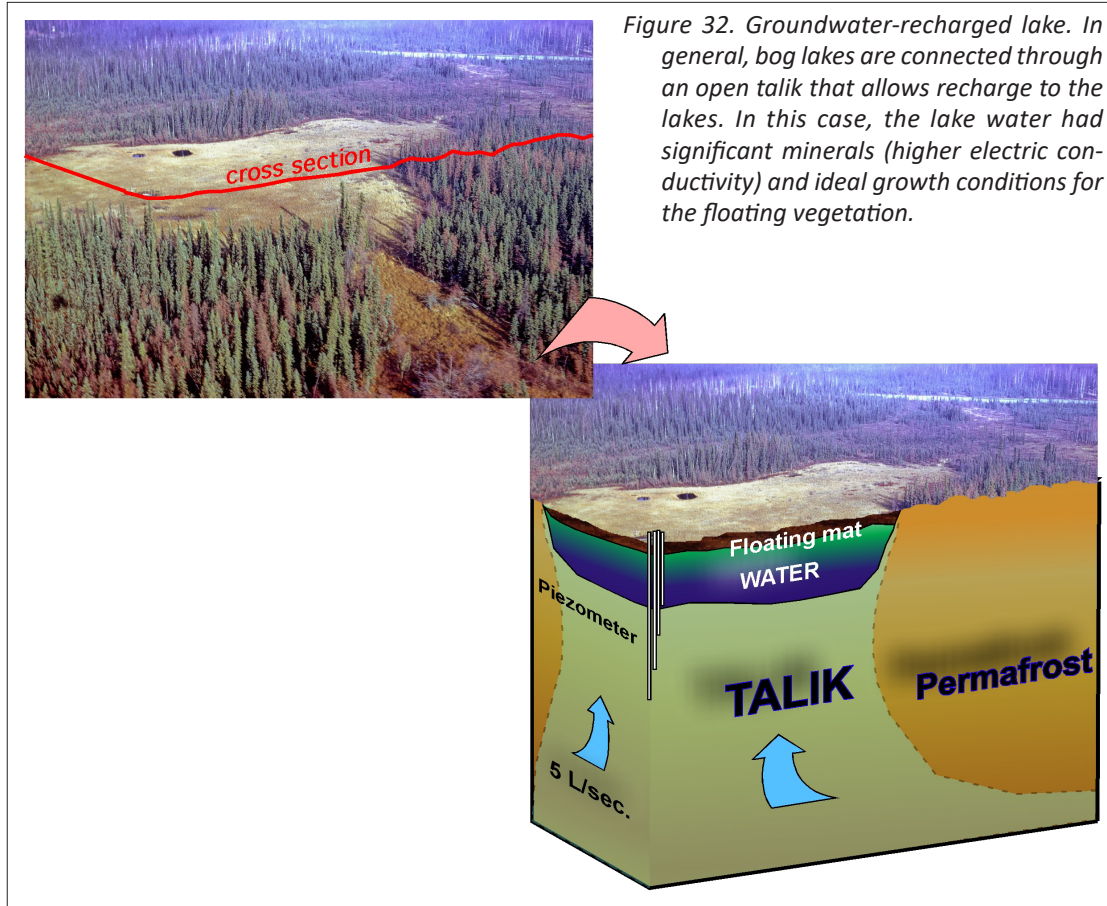


Figure 32. Groundwater-recharged lake. In general, bog lakes are connected through an open talik that allows recharge to the lakes. In this case, the lake water had significant minerals (higher electric conductivity) and ideal growth conditions for the floating vegetation.

## REFERENCES

- Boike, Julia, and Yoshikawa, Kenji, 2003, Mapping of periglacial geomorphology using kite/balloon aerial photography: *Permafrost and Periglacial Processes*, v. 14, no. 1, p. 81–85.
- Boswell, J.C., 1979, History of Alaskan operations of United States Smelting, Refining, and Mining Company: Fairbanks, University of Alaska, Mineral Industry Research Laboratory Special Publication, 126 p.
- Brown, Jerry, Ferrians, O.J., Jr., Heginbottom, J.A., and Melnikov, E.S., 1997, Circum-Arctic map of permafrost and ground-ice conditions: U.S. Geological Survey Circum-Pacific Map 45, 1 plate, scale 1:10,000,000.
- Collins, C.M., Haugen, R.K., and Kreig, R.A., 1988, Natural ground temperatures in upland bedrock terrain, interior Alaska, *in* Senneset, Kaare, ed., *Permafrost*, Fifth International Conference: Tapir, Trondheim, Norway, Proceedings, International Conference on Permafrost, v. 5, no. 1, p. 56–60.
- Collins, C.M.; Racine, C.H., and Walsh, M.E., 1994, The physical, chemical, and biological effects of crude oil spills after 15 years in a black spruce forest, interior Alaska: *Arctic*, v. 47, no. 2, p. 164–175.
- Dingman, S.L., and Koutz, F.R., 1974, Relations among vegetation, permafrost, and potential insolation in central Alaska: *Arctic and Alpine Research*, v. 6, no. 1, p. 37–42.
- Farmer, G.L., Goldfarb, R.J., Lilly, M.R., Bolton, W., Meier, A.L., and Sanzolone, R.F., 1998, The chemical characteristics of ground water near Fairbanks, Alaska: U.S. Geological Survey Professional Paper 1615, p. 167–178.
- Fastie, C.L., 2000, Fire history of the C4 and P6 basins of the Caribou–Poker Creeks Research Watershed, Alaska; The role of fire in the boreal forest and its impacts on climatic processes, FROSTFIRE Synthesis Workshop, March 21–23, 2000: Fairbanks, Alaska, University of Alaska Fairbanks, 45 p.
- Frank, E.C. and Lee, R., 1966, Potential solar beam irradiation on slopes: Fort Collins, Colorado, U.S. Forest Service Research Paper RM-18, 116 p.

- Goering D.J., and Kumar P., 1996, Winter-time convection in open-graded embankments: *Cold Regions Science and Technology*, v. 24, no. 1, p. 57–74.
- Gold, L.W., Johnston, G.H., Slusarchuk, W.A., and Goodrich, L.E., 1972, Thermal effects in permafrost, *Proceedings of the February 2–4, 1972, Canadian Northern Pipeline Conference: Ottawa, Ontario, Canada, National Research Council, Associate Committee for Geotechnical Research Technical Memorandum*, v. 104, p. 25–36.
- Hamilton, T.D., and Obi, C.M., 1982, Pingos in Brooks Range, northern Alaska, USA: *Arctic and Alpine Research*, v. 14, p. 13–20.
- Haugen, R.K., Greeley, N.H., and Collins, C.M., 1993, Permafrost mapping using GRASS, *in Proceedings of the Sixth International Conference on Permafrost, Beijing, China: Guangzhou, South China University of Technology Press, CRREL report MP 3460*, v. 2, p. 1,128–1,131.
- Haugen, R.K., Slaughter, C.W., Howe, K.E., and Dingman, S.L., 1982, Hydrology and climatology of the Caribou–Poker Creeks Research Watershed, Alaska: *Cold Regions Research and Engineering Laboratory Report 82–26*, 34 p.
- Hinzman, L.D., Fukuda, M., Sandberg, D.V., Chapin, F.S., III, and Dash, D., 2003, FROSTFIRE—An experimental approach to predicting the climate feedbacks from the changing boreal fire regime: *Journal of Geophysical Research*, v. 108, no. D1, p. 8153, doi:[10.1029/2001JD000415](https://doi.org/10.1029/2001JD000415).
- Holmes, G.W., Hopkins, D.M., and Foster, H.L., 1968, Pingos in central Alaska: *U.S. Geological Survey Bulletin* 1241-H, 40 p.
- IAEA/WMO, 2001, Global Network for Isotopes in Precipitation, The GNIP Database: Accessible at: [http://www-naweb.iaea.org/napc/ih/GNIP/IHS\\_GNIP.html](http://www-naweb.iaea.org/napc/ih/GNIP/IHS_GNIP.html), accessed 2/1/2010.
- Jorgenson, M.T., and Kreig, R.A., 1988, A model for mapping permafrost distribution based on landscape component maps and climatic variable, *in Senneset, K., ed., Proceedings of the Fifth International Conference on Permafrost: Trondheim, Norway, Tapir Publishers*, v. 1, p. 176–182.
- Kane, D.L., 1980, Snowmelt infiltration into seasonally frozen soils: *Cold Regions Science and Technology*, v. 3, no. 2, p. 153–161.
- Kane, D.L., and Slaughter, C.W., 1973, Recharge of a central Alaska lake by subpermafrost groundwater, *in Permafrost—The North American Contribution to the Second International Conference; Groundwater in permafrost areas: Washington, D.C., National Academy of Sciences*, p. 458–462.
- Koutz, F.R., Slaughter, C.W., 1973, Equivalent latitude (potential insolation) and a permafrost environment: Caribou–Poker Creeks Research Watershed, Interior Alaska, *Technical Note: Hanover, NH, U.S. Army Cold Regions Research Engineering Laboratory*, 33 p.
- Morrissey, L.A., Strong, L.L., and Card, D.H., 1986, Mapping permafrost in the boreal forest with Thematic Mapper satellite data: *Photogrammetric Engineering and Remote Sensing*, v. 52, no. 5, p. 1,513–1,520.
- Neary, M.P., 1997, Tritium enrichment—To enrich or not to enrich?: *Radioactivity and Radiochemistry*, v. 8, n. 4, p. 23–35.
- Osterkamp, T.E., and Romanovsky, V.E., 1999, Evidence for warming and thawing of discontinuous permafrost in Alaska: *Permafrost and Periglacial Processes*, v. 10, p. 17–37.
- Péwé, T.L., 1982, Geologic hazards of the Fairbanks area, Alaska: *Alaska Division of Geological & Geophysical Surveys Special Report 15*, 119 p.
- Rantz, S.E., compiler, 1982, Measurement and computation of streamflow; Volume 1, Measurement of stage and discharge; Volume 2, Computation of discharge: *U.S. Geological Survey Water Supply Paper 2175*, <http://pubs.usgs.gov/wsp/wsp2175/>, accessed 2/1/2010.
- Rieger, S., Furbush, C.E., Schoephorster, D.B., Summerfield, H., Jr., and Geiger, L.G., 1972, Soils of the Caribou–Poker Creeks Research Watershed: Hanover, NH, U.S. Army Cold Regions Research and Engineering Laboratory, *Technical Report 236*, 14 p.
- Romanovsky, V.E., and Osterkamp, T. E., 1995, Interannual variations of the thermal regime of the active layer and near-surface permafrost in northern Alaska: *Permafrost and Periglacial Processes*, v. 6, no. 4, p. 313–335.
- Romanovsky, V.E., Osterkamp, T.E., and Duxbury, N., 1997, An evaluation of three numerical models used in simulations of the active layer and permafrost temperature regimes: *Cold Regions Science and Technology*, v. 26 no. 3, p. 195–203.
- Sawada, Y., 2003, Monitoring of ground-ice formation in a block slope at Mt. Nishi-Nupukaushinupuri, Hokkaido, Japan, *in Phillips, Marcia, Springman, S.M., and Arenson, L.U., eds., Proceedings of the eighth international conference on Permafrost: Zurich, Switzerland, International Conference on Permafrost, Proceedings*, v. 8, no. 2, p. 1,001–1,005.



- Slaughter, C.W., and Hartzmann, R.J., 1993, Hydrologic and water quality characteristics of a degrading open-system pingo, *in* Cheng Guodong, chairperson, Permafrost; sixth international conference proceedings: Beijing, China, International Conference on Permafrost, Proceedings, v. 6, no. 1, p. 574–579.
- Slaughter, C.W., and Lotspeich, F.B., 1977, Caribou–Poker Creeks Research Watershed: Arctic Bulletin, v. 2, no. 10, p. 182–188.
- Viereck, L.A., Werdin-Pfisterer, N.R., Adams, P.C., and Yoshikawa, K., 2008, Effect of wildfire and fireline construction on the annual depth of thaw in a black spruce permafrost forest in interior Alaska—a 36-year record of recovery, *in* Kane, D.L., and Hinkel, K.M., eds., Proceedings, 9th International Conference on Permafrost, Fairbanks, Alaska, June–July 2008: Fairbanks, Alaska, International Conference on Permafrost, v. 9, p. 1,845–1,850.
- White, D.M., Collins, C.M., Barnes, D.L., and Byard, Helena, 2004, Effects of a crude oil spill on permafrost after 24 years in interior Alaska, *in* Smith, D.W., Sego, D.C., and Lenzion, C.A., eds., It's a cool world; Proceedings of the 2004 Cold Regions Engineering and Construction Conference, 2004, Edmonton, AB, Canada: Reston, VA, American Society of Civil Engineers, v. 12.
- White, D.M., Yoshikawa, Kenji, and Garland, D.S., 2002, Use of dissolved organic matter to support hydrologic investigations in a permafrost-dominated watershed: Cold Regions Science and Technology, v. 35, no. 1, p. 27–33.
- Woodcock, A.H., 1974, Permafrost and climatology of a Hawaii volcano crater: Arctic and Alpine Research, v. 6, no. 1, p. 49–62.
- Yoshikawa, K., 2008, Stable isotope composition of ice in seasonally and perennially frozen mounds, *in* Kane, D.L., and Hinkel, K.M., eds., Proceedings, Ninth International Conference on Permafrost, June 28–July 2, 2008, Fairbanks Alaska: International Conference on Permafrost, v. 9, p. 1997–2002.
- Yoshikawa, K., and Harada, K., 1995, Observations on nearshore pingo growth, Adventdalen, Spitsbergen: Permafrost and Periglacial Processes, v. 6, no. 4, p. 361–372.
- Yoshikawa, K., Bolton, W.R., Romanovsky, V.E., Fukuda, Masami, and Hinzman, L.D., 2003, Impacts of wildfire on the permafrost in the boreal forests of Interior Alaska: Journal of Geophysical Research, v. 108, no. D1, 14 p. doi:[10.1029/2001JD000438](https://doi.org/10.1029/2001JD000438), 2002. [printed 108(D1), 2003]
- Yoshikawa, Kenji, Hinzman, L.D., and Gogineni, Prasad, 2002, Ground temperature and permafrost mapping using an equivalent latitude/elevation model: Journal of Glaciology and Geocryology, v. 24, no. 5, p. 526–531.
- Yoshikawa, Kenji, White, D.M., Hinzman, L.D., Goering, D., Petrone, K., Bolton, W., and Ishikawa, N., 2003, Water in permafrost; case study of aufeis and pingo hydrology in discontinuous permafrost, *in* Phillips, Marcia, Springman, S.M., and Arenson, L.U., eds., Proceedings of the 8th International Conference on Permafrost, Zurich, Switzerland, July 12–25, 2003: International Conference on Permafrost, v. 8, no. 2, p. 1,259–1,264.